SYNTHESIS AND CHARACTERISATION OF SOME MOLYBDENUM COMPLEXES AND THEIR USE AS EPOXIDATION CATALYSTS

ANIL THOMAS ANTHONY FERNANDEZ

This Thesis is submitted in candidature for the degree of Doctor of Philosophy of the University of London

Bourne Laboratory
Royal Holloway and Bedford New College

September, 1986

ABSTRACT

With the aim of inducing asymmetric epoxidation, the metal catalysed epoxidation of alkenes and substituted alkenes using tert-butyl hydroperoxide and various molybdenum catalysts have been studied.

In Chapter I, the synthesis of various cis dioxomolybdenum complexes from 2,4-pentanedione dioxomolybdenum(VI) by reaction with various racemic and chiral diol ligands and amino alcohols is described. Under more vigorous reaction conditions, cis dioxomolybdenum(VI) complexes were dimerised giving complexes with a $O_tMoO_bMoO_t$ core. The reactions of L-histidine with molybdenum hexacarbonyl and molybdenum(VI) oxide afforded the potassium salts of tricarbonyl-L-histinato and histidinatotrioxomolybdate(VI) respectively. The complexes were characterised by ^1H and ^{13}C nmr spectroscopy.

In Chapter II, kinetic data is presented for the metal catalysed epoxidation of 1-decene and 1-dodecene at 70^o using various molybdenum catalysts and tert-butyl hydroperoxide. Reactions with equimolar concentrations and a ten-fold excess of olefin to tert-butyl hydroperoxide were carried out. A possible mechanism is proposed.

Chapter III deals with the asymmetric epoxidation experiments carried out using the molybdenum catalysts synthesised from chiral ligands. Geraniol, 3-methyl-2-butene-1-ol and 1-methyl cyclohexene were epoxidised with varying degrees of success. The highest enantiomeric excess achieved was 85% for 3-methyl-2-butene-1-ol oxide using cis-Bis(phenyl ethane-1,2-diolato) dioxomolybdenum(VI). Epoxy alcohols were reacted with (-)-α-methoxy-α-trifluoromethyl phenyl acetyl chloride to give the corresponding esters, enabling enantiomeric excess to be calculated by ^{19}F nmr. Reactions carried out at different temperatures showed variations in enantiomeric excess - a higher enantiomeric excess being obtained at lower temperature.

ACKNOWLEDGEMENTS

For this thesis, there are several people to whom I owe a considerable debt. Foremost is my supervisor Dr Paul Powell, for his encouragement and support of the research.

I thank Dr Paul Finch for his helpful advice during the experimental part of the research.

The preliminary nmr work was run by Mr Don Parkinson. The high field spectra were run by Mr Peter Haycock at the ULIRS (400 MHz NMR Service at Queen Mary College). I am grateful for the help both of them provided.

I thank Mr Bill Gunn and Mr Andy Cakebread of the ULIRS GC/MS Unit at Queen Elizabeth College.

I would like to thank the departmental technical services at Royal Holloway and Bedford New College and in particular Mr John Turner who so skillfully made some of the glassware.

I thank the Royal Holloway and Bedford New College Council for financial support.

Finally, my sincere thanks to Mrs Eileen Kearsey and Mrs Jackie Evans for transforming those 'rough drafts' of paper to this final copy.

I dedicate this thesis to

my parents Thomas and Edna Fernandez

and my brother Dilip

CONTENTS

CONTENTS (contd.)

CONTENTS (contd.)

CONTENTS (contd.) Page No.

LIST OF TABLES

Page No.

List of abbreviations

o	Unless stated, all temperatures are referred to in degrees centigrade.
b	broad
d	doublet
d,d	doublet of doublets
e.e.	enantiomeric excess
$MoO_2(acac)_2$	2,4-pentanedione dioxomolybdenum (VI)
MoO_3	molybdenum trioxide
nmr	nuclear magnetic resonance
o	octet
P.P.M.	parts per million
s	singlet
S	solvent peak
TBHP	tert-butyl hydroperoxide
THF	tetrahydrofuran

Chapter I

SYNTHESIS AND CHARACTERISATION OF MOLYBDENUM COMPLEXES

CHAPTER I SECTION 1

I.1 INTRODUCTION

The interest in molybdenum centres in the oxomolybdoenzymes has been covered by various reviews[1-6], their interest in this work stems from the success of molybdenum as an epoxidising catalyst[7,8].

The structural chemistry of Mo (VI) is dominated by the presence of oxo groups bound to molybdenum. These oxygen atoms utilise sigma and pi donation to produce a strong (multiple) Mo-O bond. Many compounds of Molybdenum -(V) and -(VI) are derived from oxo species $Mo_xO_y^{n+}$ with one or more oxygen atoms as bridging ligands (i.e. bonded to two molybdenum atoms)[9,10]. An essential feature is multiple bonding between the oxygen atom and the metal atom. A detailed review by Mitchell catalogues various structural and physical measurements of oxo species of molybdenum V and VI.[11]

Vibrational spectroscopic information on the oxomolybdenum complexes showed the strong metal oxygen absorptions standing out from the ligand bands, the type of metal-oxygen core being identifiable from the spectral features. The cis-dioxo MoO_2 group gives two strong bands at 900-950 cm^{-1}, the cis-trioxo MoO_3 gives two bands in the range 800-900 cm^{-1} and Mo-O-Mo bridge vibrations at 700-800 cm^{-1}[12].

Mo-O and O-Mo-O bond distance values were catalogued from relevant crystal structure determinations[13]. Most of the compounds dealt with involved molybdenum in the oxidation state +6 or +5.

Schroder et al[14] characterised cis-Bis(2-hydroxyethyl-1-oxo) dioxomolybdenum (VI), the first known alkoxide of Mo(VI) without a halogen atom. The structure of this is shown in Fig. I.1(1).

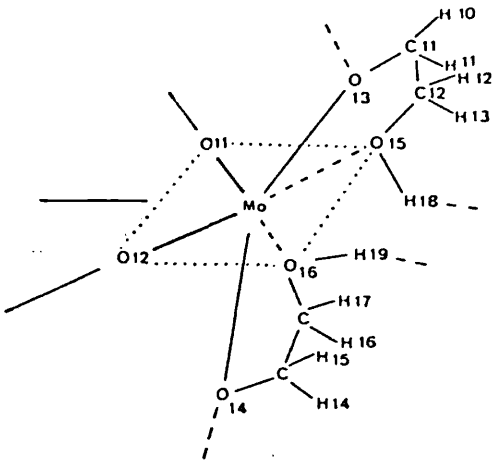

Fig. I.1(1)

Fig. I.1(2) shows the molecular packing in the unit cell of cis-Bis (butane-2,3-diolato)dioxomolybdenum VI-Butane 2,3diol(1:2)[15]. The crystal structure consists of molecules of $(MoO_2[OCH(CH_3)CH(CH_3)OH]_2)$ each surrounded by two molecules of 2,3-butane diol which are attached by hydrogen bonds to the molybdenum complex and also linked by hydrogen bonds to the neighbouring 2,3-butane diol molecule, the extensive hydrogen bonding resulting in a layered structure.

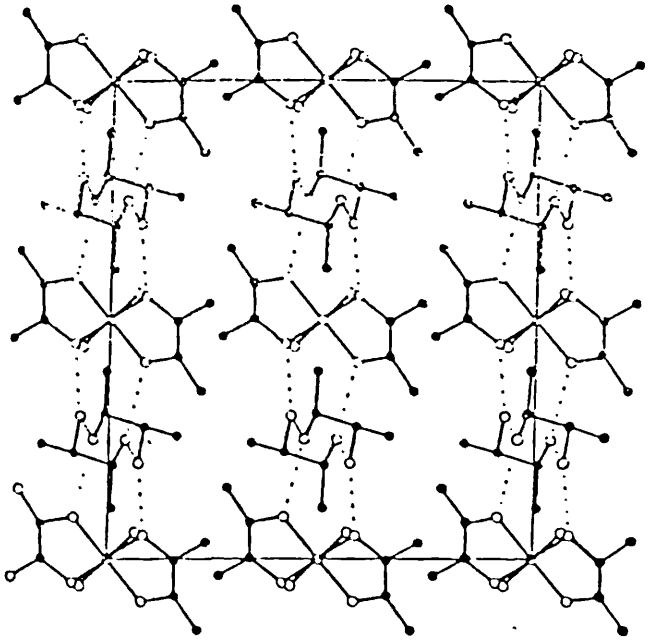

Fig. I.1(2)

A crystal structure determination of μ-Oxo-Bis([2,3-dimethyl-2,3-butane diolato(1-)] [2,3-dimethyl-2,3-butane diolato(2-)])oxo-molybdenum (VI) , Fig. I.1(3), has established that each molybdenum atom is coordinated to two bidentate ligands, one of which is singly deprotonated and the other doubly deprotonated; two intramolecular hydrogen bonds link the ligands attached to the different molybdenum atoms[16].

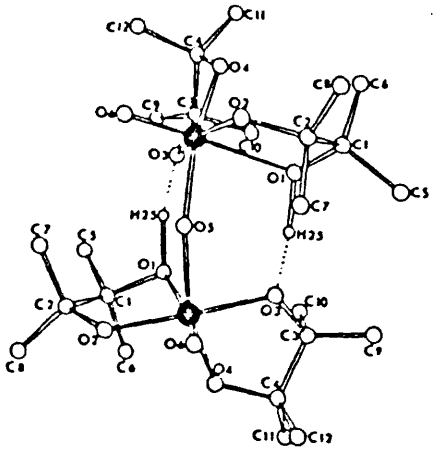

Fig. I.1(3)

While the structural data on Mo^{VI} and Mo^{V} complexes using infra-red and X-ray is quite wide-spread, the characterisation by nuclear magnetic resonance spectroscopy is limited. Wise et al[17] studied the non-equivalence of the methyl groups in cis-Bis(2,4-pentanedionato) dioxomolybdenum (VI) by following the variable temperature nmr spectra. They found that at low temperature two methyl resonances appeared whereas increasing the temperature led to coalesence. They attributed this to rapid configurational changes which exchanges the methyl group between the non-equivalent sites. From the data they observed, they calculated the activation energy, the enthalpy and entropy of activation.

The (acetylacetanato) (-)-N alkylephedrinato dioxomolybdenum (VI) complex which successfully asymmetrically epoxidised various allylic

alcohols was characterised by nmr [18,19].

Garner et al[20] reported that the structure of cis-Bis (L-cysOR)$_2$ dioxomolybdenum (VI) was Λ in the solid state, while in the solution state, two isomers were observed in ca. 5:1 ratio by nmr spectroscopy. These isomers were assigned to the the Λ and Δ diastereoisomers of the complex. The same group of workers[21] characterised cis-Bis(O-methyl (S)-penicillaminato)dioxomolybdenum (VI). X-ray data gave the Λ isomer while liquid nmr gave the diastereoisomers in 2:1 ratio (Λ:Δ), the reverse being the case for the (R)- ligand complex. The two diastereoisomers are in dynamic equilibrium and the ^{1}H nmr data collected over the temperature range 297-285K gives activation parameters for the Λ→Δ interconversion. The mechanism for the inversion of configuration at molybdenum is considered to proceed by an intramolecular process, involving Mo-N bond rupture followed by rotation of the ligand atoms of the subsequent intermediate and ring closure (Scheme I).

Scheme I

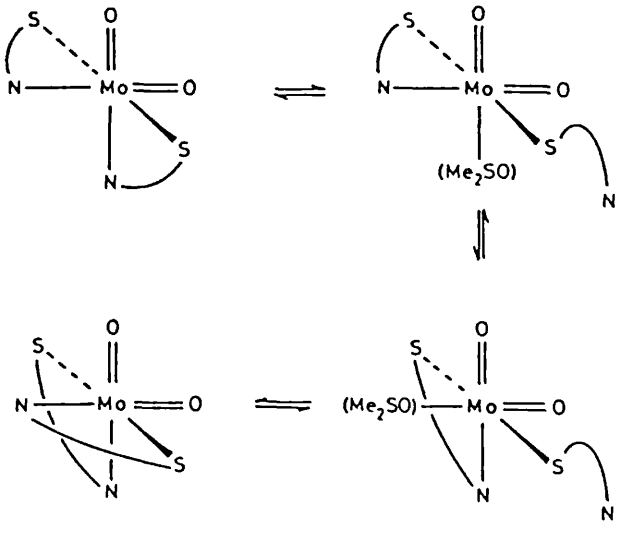

CHAPTER I SECTION 2

I.2 RESULTS and DISCUSSION

I.2.1a 400.13 MHz ^{1}H nmr of cis-Bis(D(-)butane-2,3-diolato) dioxomolybdenum (VI)-D(-) Butane 2,3 diol (1:1)

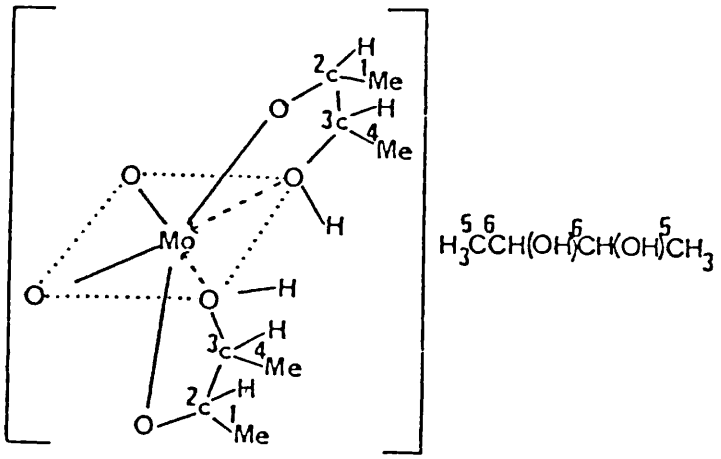

Fig. I.2.1(1)

Table I.2.1a 400.13 MHz ^{1}H nmr spectra data of $\left(MoO_2\left[^{2}OCH(^{1}CH_3)^{3}CH(^{4}CH_3)OH\right]_2\right)\left(H_3^{5}C^{5}CH(OH)^{6}CH(OH)^{5}CH_3\right)$

	$^1CH_3$	^2CH	^3CH	$^4CH_3$	$^5CH_3$	^6CH	-OH
307K							
Chemical shift/ppm	1.38,d	4.32,b	3.84,b	1.48,d	1.33,b	3.73,b	5.06,s
Coupling const./Hz	6			6			
257K							
Chemical shift/ppm	1.38,d	4.31,o	3.83,o	1.49,d	1.32,d	3.73,o	5.53,o
Coupling const./Hz	6	9.8	9.8	6	6	9.8	

Sample run in CD_3OD.

The non-equivalence of the methyl and methine protons of the free and complexed ligand are shown by the spectra in Fig. I.2.1(2) and Fig. I.2.1(3). This non-equivalence is due to the deshielding of the protons by the molybdenum atom.

In the case of the complexed ligand, from selective decoupling the doublet at 1.38 ppm, $^{1}CH_3$ (J_{CH_3-H} 6 Hz) is coupled to ^{2}CH at 4.32 ppm giving an octet (J_{H-H} 9.8 Hz). Similarly, the broader methyl group $^{4}CH_3$ at 1.48 ppm (J_{CH_3-H} 6 Hz) is coupled to ^{3}CH, giving a broad octet at 3.84 ppm.

The free ligand, not having the constraints of the five ring system, is more clearly defined. Both the methyls are chemically equivalent, giving a doublet at 1.32 ppm (J_{CH_3-H} 6 Hz). The methine protons, ^{6}CH, are equivalent giving an octet at 3.73 ppm (J_{H-H} 9.8 Hz). The hydroxyl peak from the free and complexed ligands average out to a singlet. Its resonating frequency, being temperature dependent, moves to higher field as the temperature increases due to the hydrogen bonds dissociating (at 307 K, 5.06 ppm and at 257 K, 5.53 ppm).

The spectra, do contain three other small peaks at 1.42, 3.82 and 4.19 ppm. This could be the Δ diastereoisomer; if so, the ratio of Λ to Δ is 7:1.

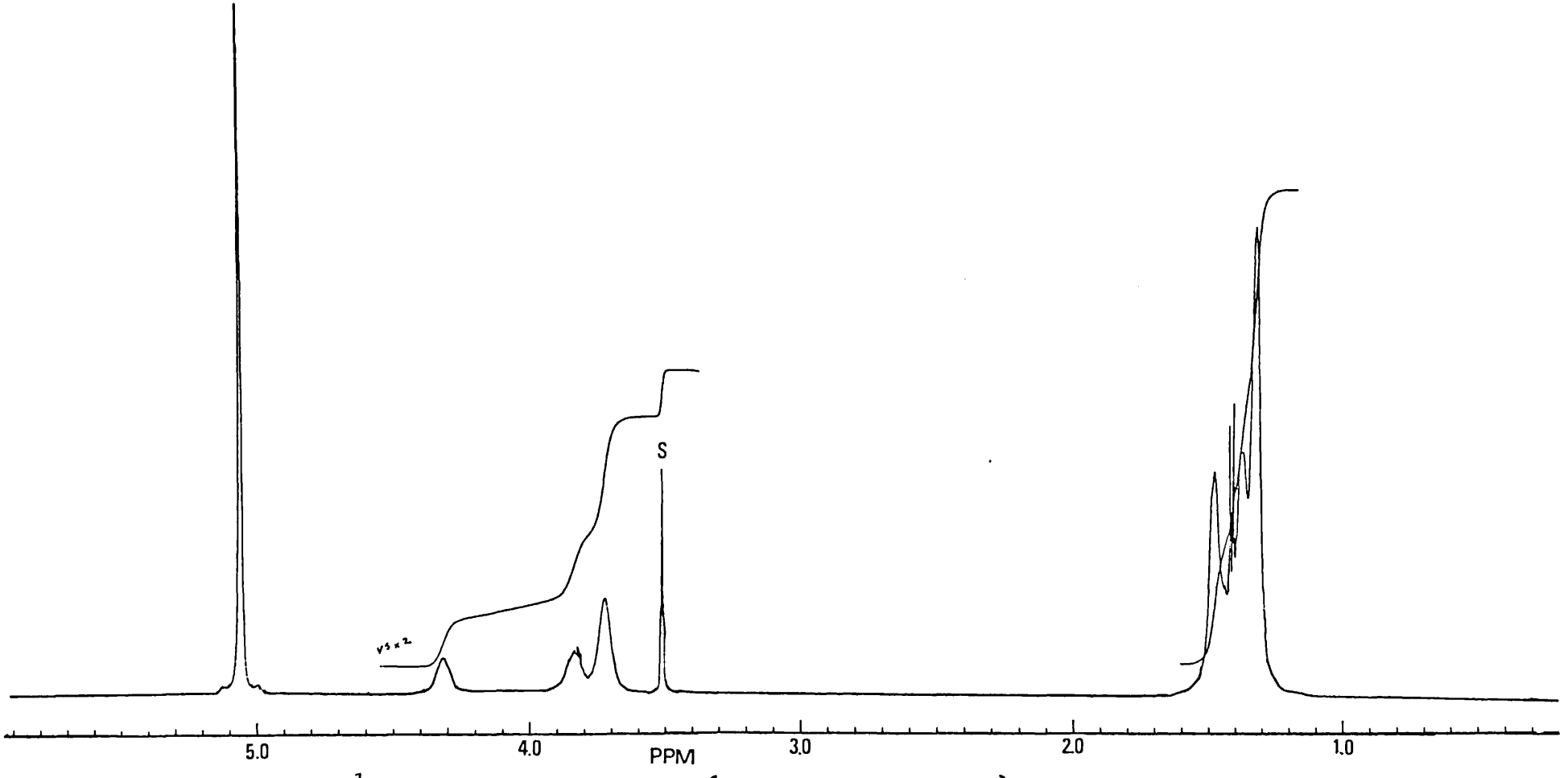

Fig. I.2.1(2) 400.13 MHz ^{1}H nmr spectrum of cis-Bis(D(-)butane-2,3-diolato)dioxomolybdenum VI-D(-)Butane 2,3 diol (1:1) at 307 K in CD_3OD.

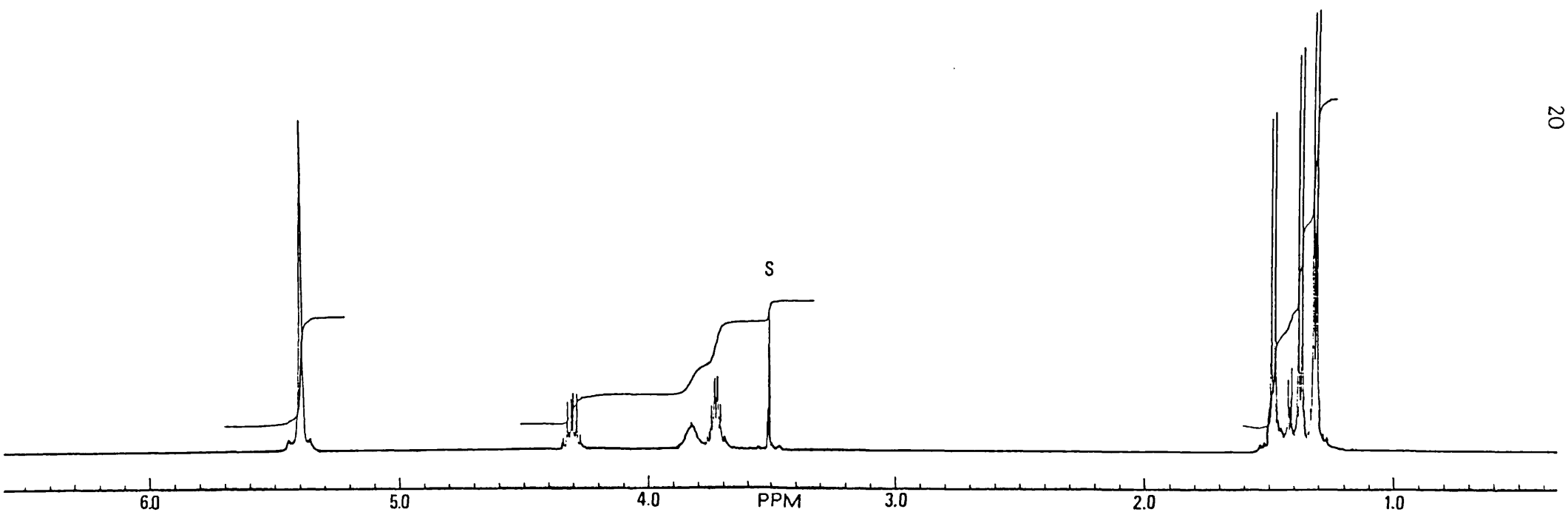

Fig. I.2.1(3) 400.13 MHz ^{1}H nmr spectrum of cis-Bis(D(-)butane-2,3-diolato)dioxomolybdenum VI-D(-)Butane 2,3-diol (1:1) at 257 K in CD_3OD.

I.2.1b 100.62 MHz ^{13}C nmr of cis-Bis(D(-)butane-2,3-diolato) dioxomolybdenum (VI)-D(-)Butane 2,3 diol (1:1)

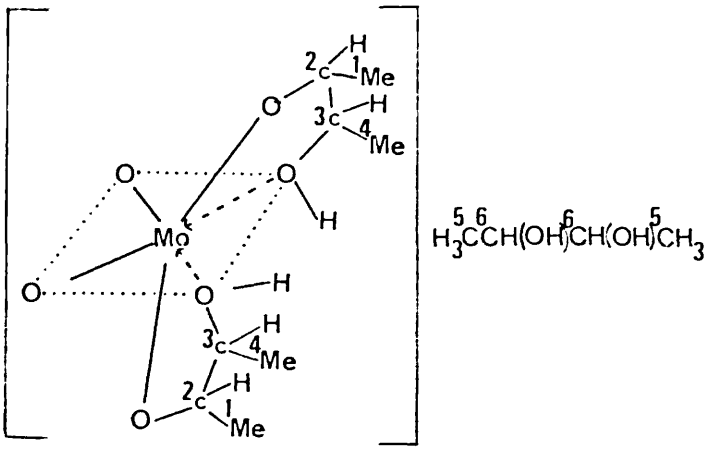

Fig. I.2.1(4)

The nmr spectrum of the complex Fig. I.2.1(4) at 217 K is shown in Fig. I.2.1(5). Three highfield methyl resonances at 18.66 ppm, 18.93 ppm and 20.11 ppm along with three lowfield methine resonances at 72.70 ppm, 76.27 ppm and 87.15 ppm are present. Selective decoupling along with off-resonance decoupling Fig. I.2.1(6) was carried out to assign the spectrum completely.

The assignment of the spectrum is as follows:-

	Chemical shift/ppm
C-1	20.11,s
C-2	87.15,s
C-3	76.27,s
C-4	18.66,s
C-5	18.93,s
C-6	72.70,s

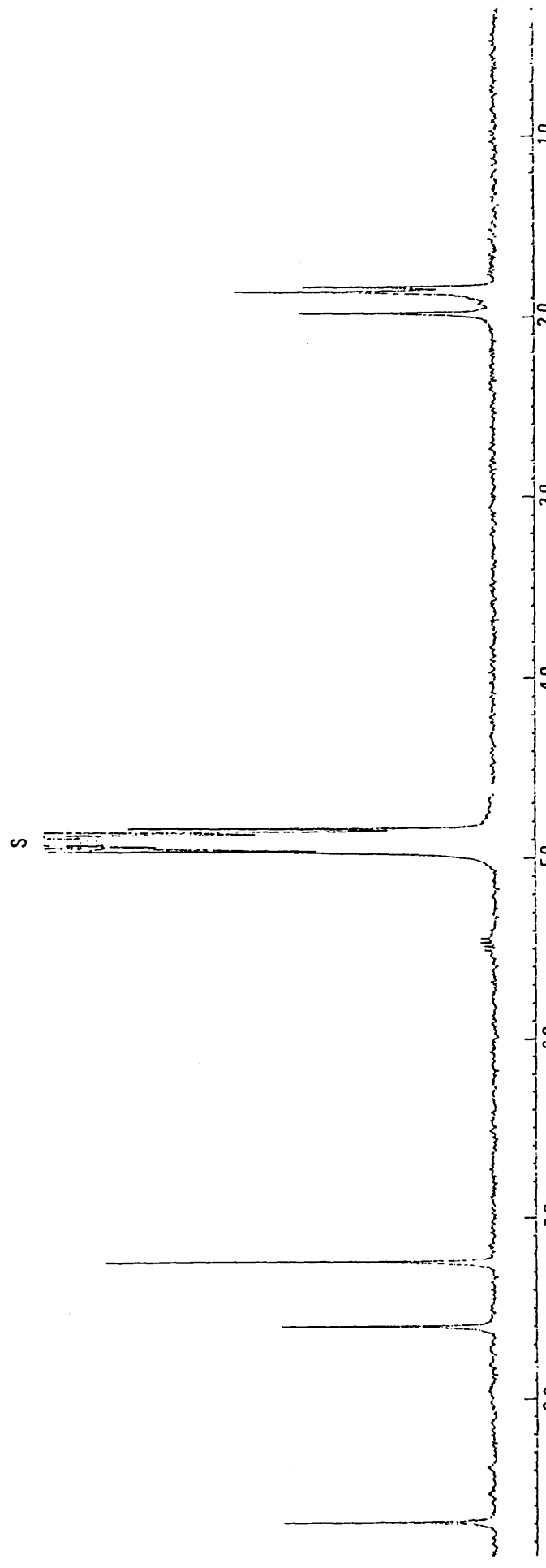

Fig. I.2.1(5) 100.62 MHz $^{13}C\{^{1}H\}$ spectrum of cis-Bis(D(-)butane-2,3-diolato)dioxomolybdenum (VI)-D(-)Butane 2,3-diol (1:1) at 217 K in CD_3OD.

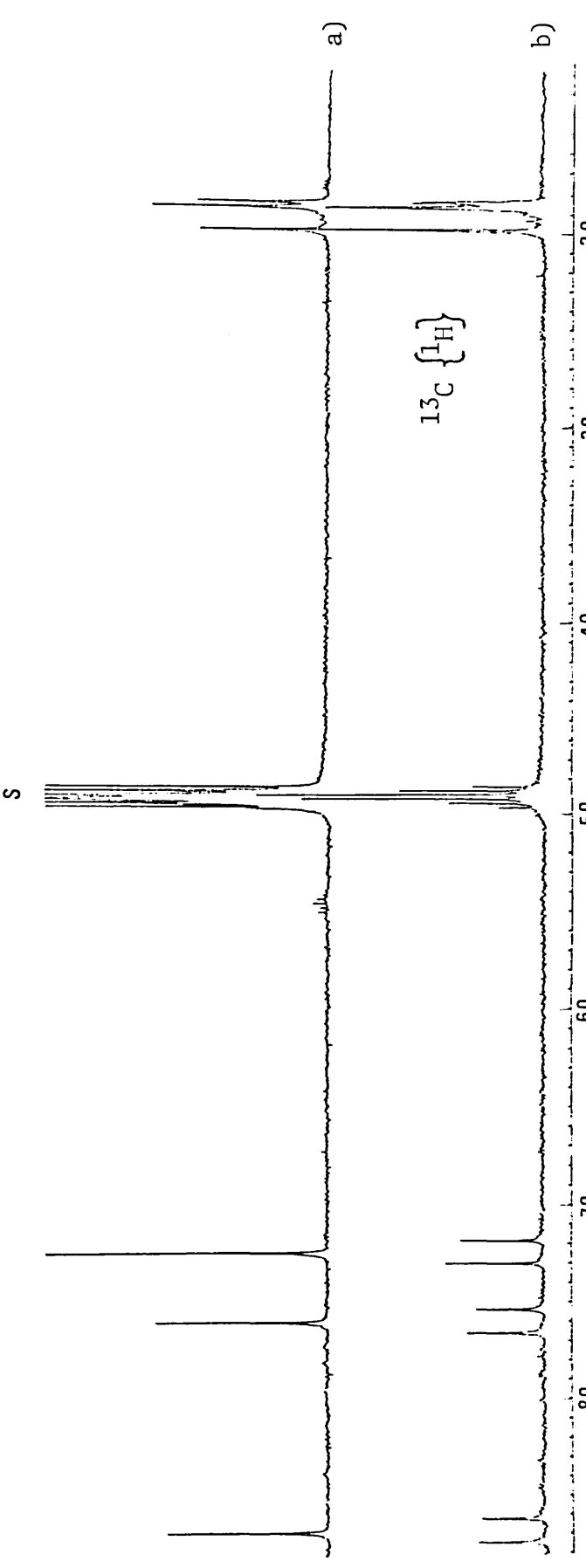

Fig. I.2.1(6) a) 100.62 MHz $^{13}C\{^{1}H\}$ spectrum of cis-Bis(D(-)butane-2,3-diolato)dioxomolybdenum VI-D(-) Butane 2,3-diol (1:1) at 217 K in CD_3OD.

b) 100.62 MHz Offresonance $^{13}C\ ^{1}H$ spectrum of cis-Bis(D(-)butane-2,3-diolato) dioxomolybdenum VI-D(-) Butane 2,3-diol (1:1) at 217 K in CD_3OD.

I.2.2a 400.13 MHz ^{1}H nmr of cis-Bis(butane-2,3-diolato) dioxomolybdenum (VI)-Butane 2,3 diol (1:2)

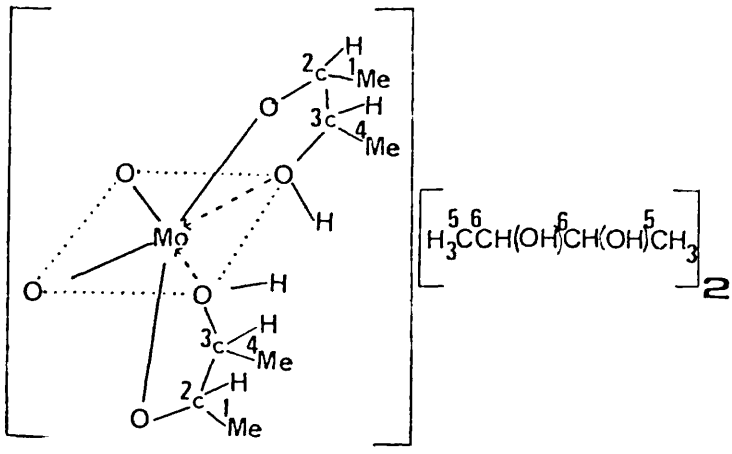

Fig. I.2.2(1)

The spectrum, when analysed in conjunction with that of cis-Bis(D(-)butane-2,3-diolato)dioxomolybdenum (VI)-D(-)Butane-2,3 diol (1:1) (Section I.2.1a) confirms the structure (Fig. I.2.2(1)) but ascertaining detailed data was difficult.

The predominant component in the spectrum, Fig. I.2.2(2) in CD_3OD is the free ligand. When CD_3CN was used as solvent, more complex is present (c.f. CD_3OD) - but the free ligand is still dominant. This is due to the solubility problems posed by the complex - in this case, acetonitrile is more favourable than methanol.

The multiplet at 3.73 is the methine proton from the free ligand, H^6. When decoupled, it collapses the doublet of doublets at 1.32 ppm and 1.35 ppm which arise from the methyl group $^5CH_3$, to singlets. As the starting material consists of D-/L- form and the meso-form - both of which can be discriminated by nmr, from Section I.2.1a, the

methyl group from the free ligand is at 1.32 ppm. From this, one can conclude that the peak at 1.32 ppm has to be $^{5}CH_3$ arising from the D-form and the peak at 1.35 ppm is that of the meso-form (J values in both cases, $^{2}J_{CH_3\text{-}H}$ ~6 Hz; $^{3}J_{CH_3\text{-}H}$ ~2 Hz).

On account of the small amount of complex present, the assignment of the methyl groups are not possible. However, with the aid of Section I.2.1a, H^3 gives a very broad peak at 3.85 ppm, H^2, the characteristic ABX_3 octet ($J_{Me\text{-}H}$ ~6 Hz; $J_{H^2\text{-}H^4}$ ~9.8 Hz) at 4.30 ppm and the hydroxyl group, a singlet at 5.36 ppm.

	$^{1}CH_3$	H^2	H^3	$^{4}CH_3$	$^{5}CH_3$	H_6	-OH
Chemical shift/ppm	*	4.30, o	3.85, b	*	(1.32, d.d; D-form)	3.73,m	5.36,s
					(1.35, d.d; meso-form)		
Coupling const./Hz		$J_{Me\text{-}H}$ ~6			$^{2}J_{Me\text{-}H}$ ~6		
					$^{3}J_{Me\text{-}H}$ ~2		
		$J_{H^2\text{-}H^4}$ ~9.8					

* not assignable

Spectrum run at 257 K in CD_3OD.

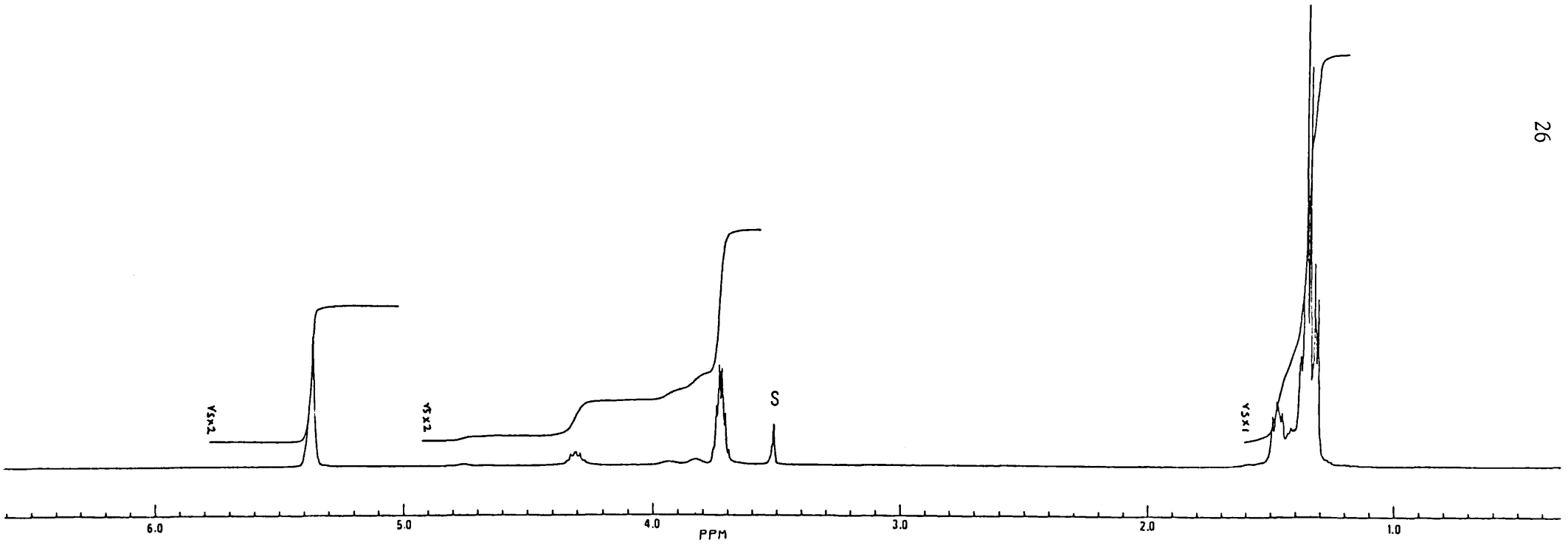

Fig. I.2.2(2) 400.13 MHz ^{1}H nmr spectrum of cis-Bis(butane-2,3-diolato)dioxomolybdenum (VI)-Butane 2,3-diol (1:2) at 257 K in CD_3OD.

I.2.2b 100.62 MHz ^{13}C nmr of cis-Bis(butane-2,3-diolato) dioxomolybdenum (VI)-Butane2,3diol (1:2)

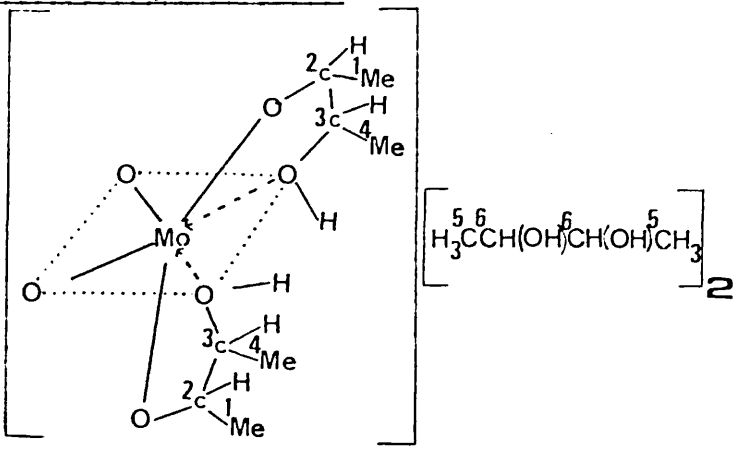

Fig. I.2.2(3)

	chemical shift/ppm
C-1	20.1
C-2	87.23
C-3	76.31
C-4	18.64
C-5	19.10;mesoform 18.92;D-/L-form
C-6	72.74

Spectrum run at 237K in CD_3OD.

Selective decoupling was used to assign C-1, C-4 and C-5 and off-resonance decoupling to assign C-2, C-3 and C-6. As in the proton spectrum, Fig. I.2.2(2), the meso and D-/L- enantiomers were distinguishable Fig.I.2.2(3) along with the large excess of free ligand.

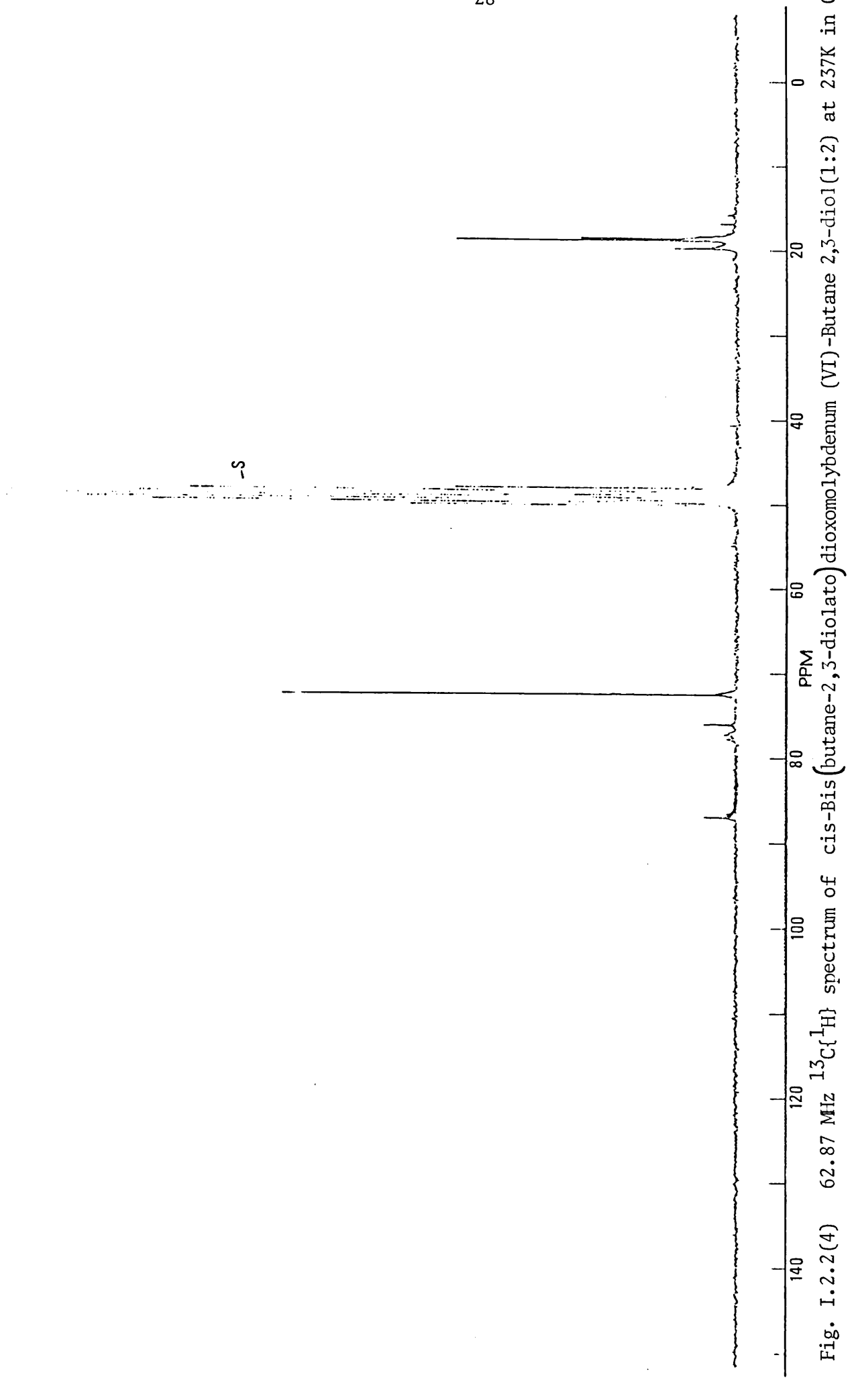

Fig. I.2.2(4) 62.87 MHz $^{13}C\{^1H\}$ spectrum of cis-Bis(butane-2,3-diolato)dioxomolybdenum (VI)-Butane 2,3-diol(1:2) at 237K in CD_3OD

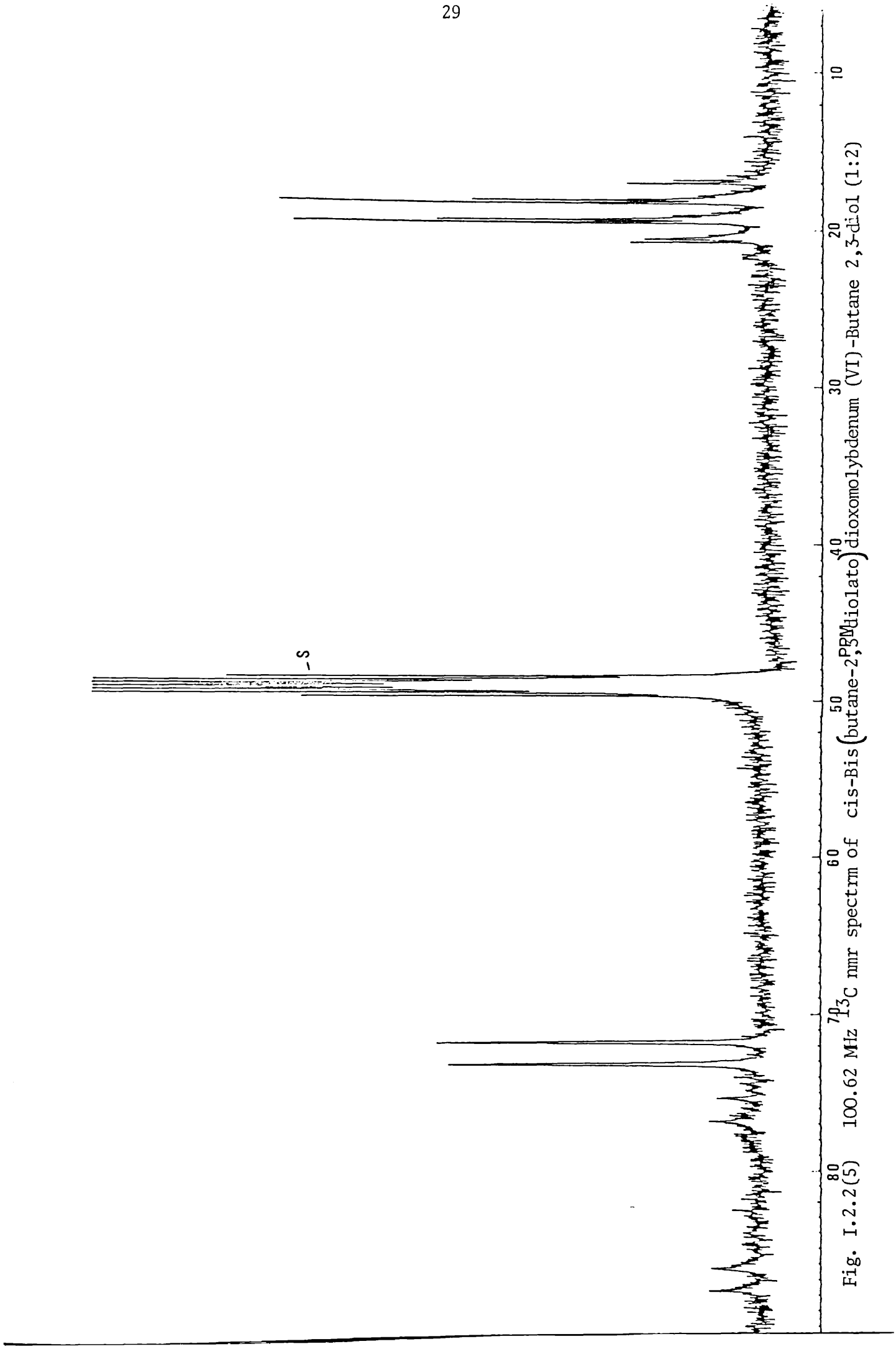

Fig. I.2.2(5) 100.62 MHz ^{13}C nmr spectrm of cis-Bis(butane-2,3-diolato)dioxomolybdenum (VI)-Butane 2,3-diol (1:2)

I.2.3a 400.13 MHz ^{1}H nmr of μ-Oxo-Bis(oxo [2,3-dimethyl-2,3-D(-) butane-2,3-diolato (1-)] [2,3-dimethyl-2,3-D(-)butane-2,3-diolato (2-)]) molybdenum (VI).

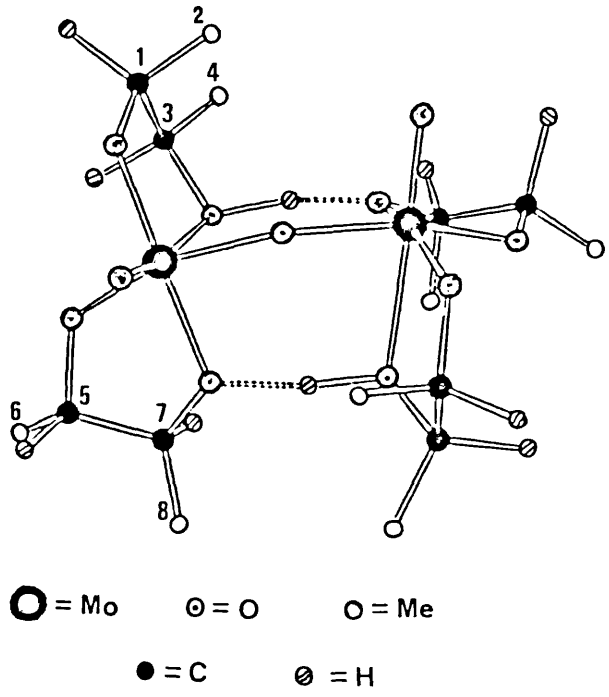

Fig. I.2.3(1)

Table I.2.3a 400.13 MHz ^{1}H nmr spectrum data of $(Mo_2O_3[^1OCH(^2CH_3)^3CH(^4CH_3)OH]_2[^5OCH(^6CH_3)^7CH(^8CH_3)O]_2)$

	Chemical shift (ppm)	Coupling const. (J/Hz)	Integral Height
^{1}CH	4.84;m		1
^{2}CH	1.30;d	4	3
^{3}CH	3.88;m		1
^{4}CH$_3$	1.28;d	4	3
^{5}CH	4.76;m		1
^{6}CH$_3$	1.27;d	4	3
^{7}CH	4.67;m		1
^{8}CH$_3$	1.31;d	4	3
-OH	1.60;s		2

Spectrum run at 297K in $CDCl_3$.

Broad impurity consisting of an octet at 3.55ppm coupled to the doublet at 1.20ppm has been assigned to the free diol.

The assignment of each bidentate ligand was made possible by selective decoupling - the results of which are summarised below:-

i) Decoupling at 4.84ppm collapses the doublet at 1.30ppm to a singlet, and the octet at 3.88ppm to a quartet.

ii) Decoupling at 4.76ppm collapses the doublet at 1.27ppm to a singlet, and the octet at 4.67ppm to a quartet.

iii) Decoupling at 4.67ppm collapses the doublet at 1.31ppm to a singlet, and the octet at 4.76ppm to a quartet.

iv) Decoupling at 3.88ppm collapses the doublet at 1.28ppm to a singlet, and the octet at 4.84ppm to a quartet.

v) Decoupling at 3.55ppm collapses the doublet at 1.20ppm to a singlet. These two peaks were assigned as impurities arising from free butane 2,3 diol.

The characterisitc ABX_3 peak patterns of the methine protons was similar to those found in the spectrum of the monomer, discussed in I.2.1a. Amongst our earlier findings in the case of the monomer, the methine proton adjacent to the hydroxyl group was found upfield compared with the methine proton adjacent to the oxygen bonded to the metal. Therefore the proton at 3.88ppm is ^3CH. From the selective decoupling results summarised in (i) and (iv) the proton at 4.84ppm must be that of ^1CH.

Similarly, in the case of the other bidentate ligand, ^{7}CH, is hydrogen bonded to the -OH. This could in effect increase the electron density and with it the shielding at the proton due to the interaction of the free electron pair of the oxygen atom. Using the same rationale as above, ^{7}CH is the proton at 4.67ppm and the decoupling results summarised in (ii) and (iii) infer that the proton at 4.76ppm is ^{5}CH.

Finally, the assignment of the methyl groups follows directly from the selective decoupling experiments.

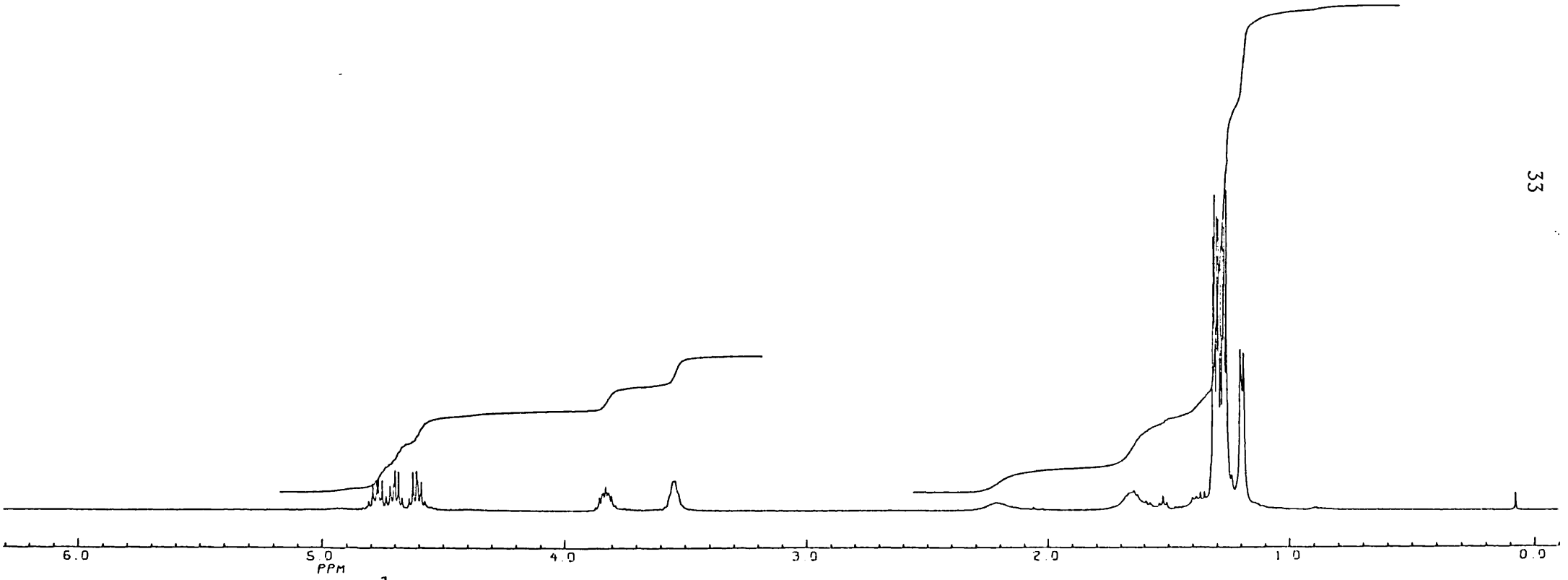

Fig. I.2.3(2) 400.13 MHz ^{1}H nmr spectrum of μ-Oxo-Bis (oxo [2,3-dimethyl-2,3-D(-)butane-2,3-diolato(1-)] [2,3-dimethyl-2,3-D(-) butane-2,3-diolato(2-)] molybdenum (VI) in $CDCl_3$.

I.2.3b 100.62 MHz ^{13}C nmr of μ-Oxo-Bis (oxo[2,3-dimethyl-2,3-D(-) butane-2,3-diolato(1-)] [2,3-dimethyl-2,3-D(-)butane-2,3-diolato (2-)] molybdenum (VI).

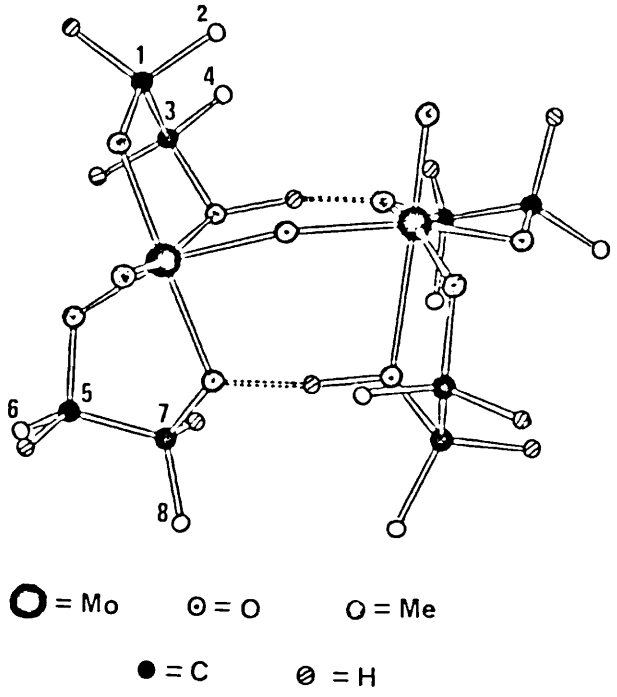

Fig. I.2.3(3)

The ^{13}C spectrum of Fig. I.2.3(3) shown in Fig. I.2.3(4) has five highfield methyl peaks along with five lowfield methine peaks. The free diol impurity found in the ^{1}H spectrum is apparent in the ^{13}C spectrum (CH_3, 19.35ppm; CH 72.50ppm). However, to assign the C atoms, a 2D heteronuclear ^{1}H-^{13}C nmr spectrum is necessary and the rationale used in the assignment of the ^{1}H spectrum (section I.2.3a) applied. Fig. I.2.3(5) shows the ^{1}H-^{13}C correlations of the methyl region and Fig. I.2.3(6) shows the ^{1}H-^{13}C correlations of the methine region. What does not show up in these two spectra Figs. I.2.3(5) and

Fig. I.2.3(6) is the diol impurity found in ^{13}C and ^{1}H spectra of this complex.

The assignment of the spectrum is as follows:-

	chemical shift/ppm
C-1	88.46
C-2	18.14
C-3	74.20
C-4	19.10
C-5	93.90
C-6	20.53
C-7	92.49
C-8	19.90

Spectrum run at 297K in $CDCl_3$.

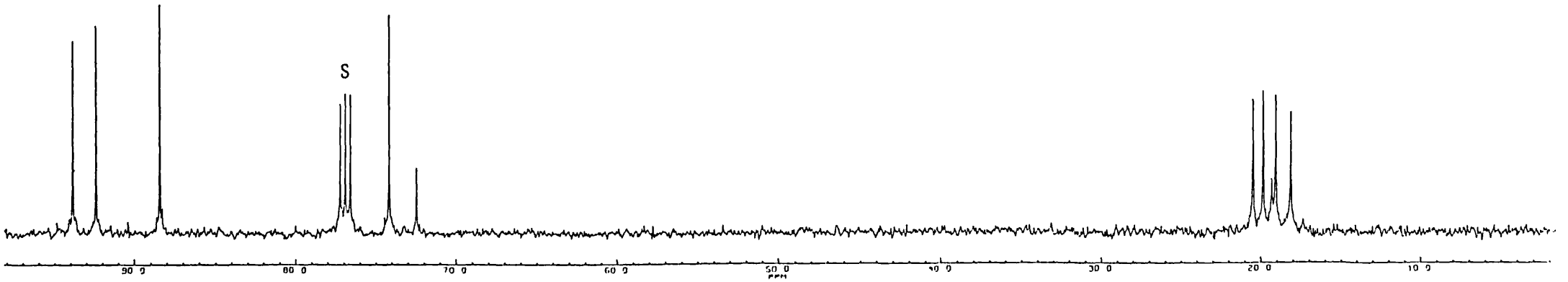

Fig. I.2.3(4) 100.62 MHz $^{13}C\{^{1}H\}$ nmr spectrum of μ-Oxo-Bis(oxo[2,3-dimethyl-2,3-D(-)butane-2,3-diolato(1-)] [2,3-dimethyl 2,3-D(-)butane-2,3-diolato(2-)] molybdenum (VI) .

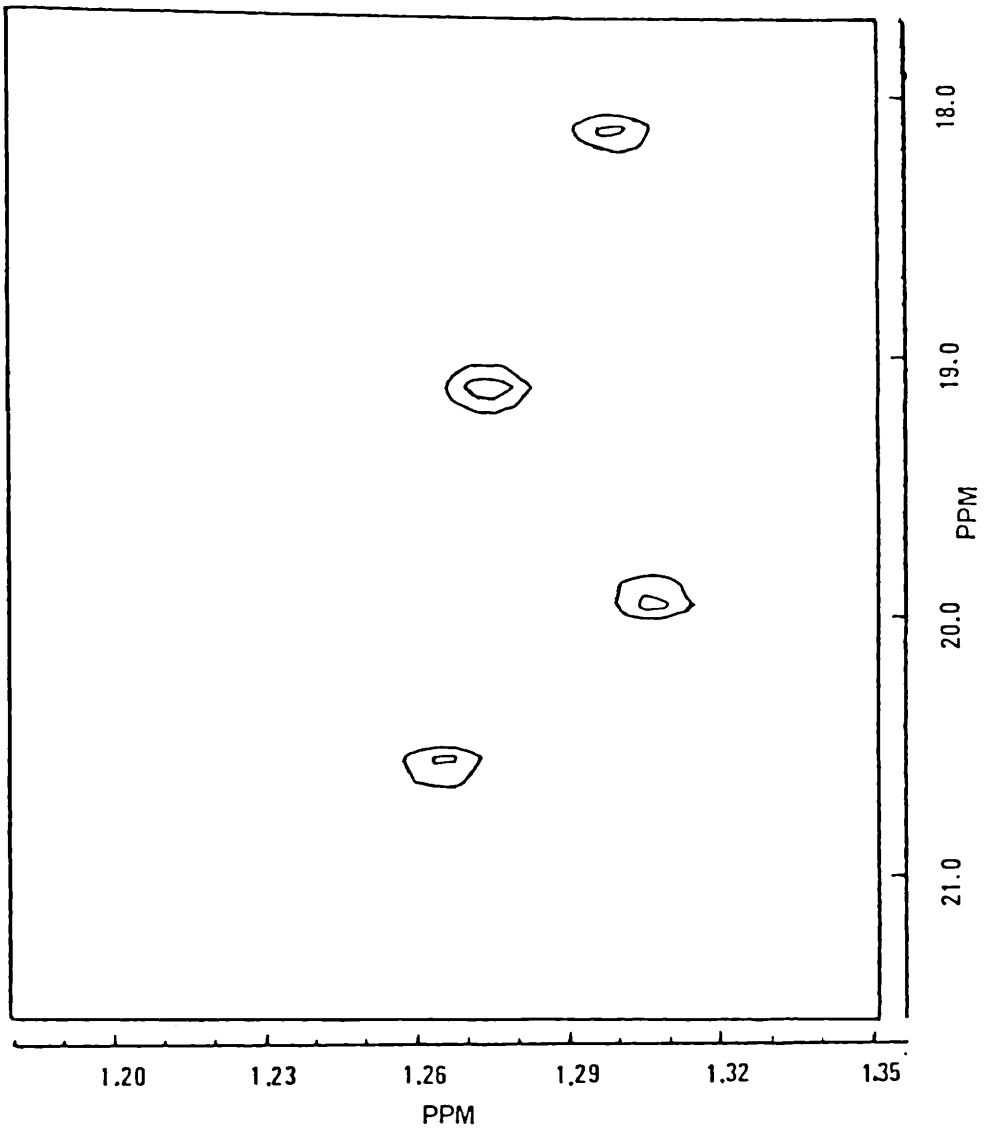

Fig. I.2.3(5) 2D Heteronuclear ^{1}H-^{13}C nmr spectrum of μ-Oxo-Bis(oxo [2,3-dimethyl-2,3-D(-)-2,3-diolato(1-)] [2,3-dimethyl-2,3-D(-)butane-2,3 diolato(2-)] molybdenum (VI) showing the methyl region.

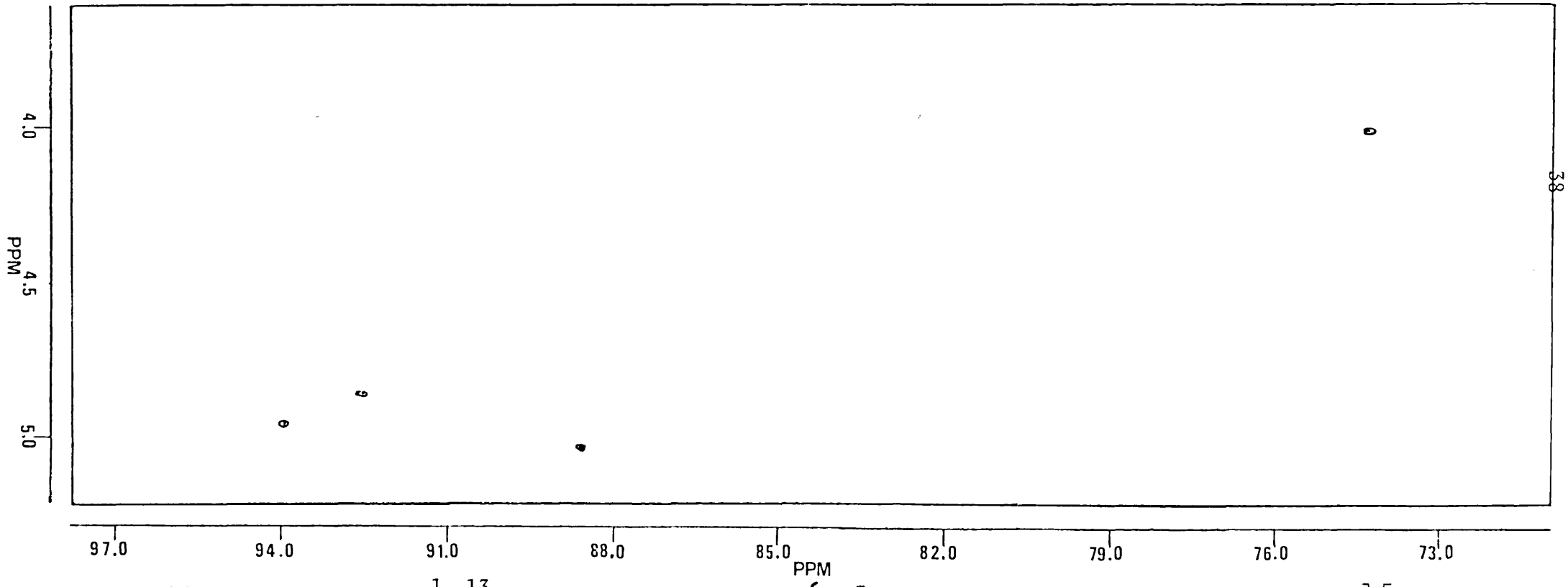

Fig. I.2.3(6) 2D Heteronuclear ^{1}H-^{13}C nmr spectrum of μ-Oxo-Bis(oxo[2,3-dimethyl-2,3-D(-)butane-2,3-diolato(1-)][2,3-dimethyl-2,3-D(-)butane-2,3diolato(2-)]molybdenum (VI) showing the methine region.

I.2.4 400.13 MHz ^{1}H nmr of μ-Oxo-Bis(oxo [2,3-dimethyl-2,3-butane -2,3diolato(1-)] [2,3-dimethyl-2,3-butane-2,3-diolato(2-)] molybdenum (VI) .

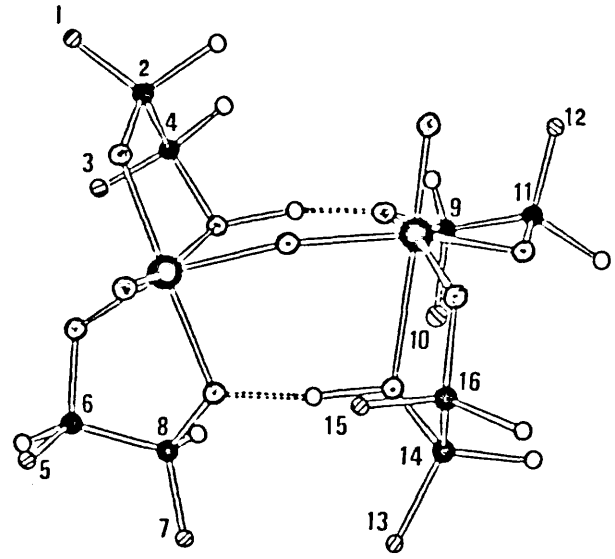

Fig. I.2.4(1)

From section I.2.3a, the methine protons consisted of four different chemical environments with each site having an integral of two. This is due to the configuration of all the bidentate ligands being the same - the molecule having a rotational symmetry along the bridged oxygen. However, using the racemic diol as ligand changes the configuration of the ligands. From the crystal structure of μ-Oxo-Bis ([2,3-dimethyl-butane-2,3diolato(1-)] [2,3-dimethyl-butane-2,3-diolato(2-)] molybdenum (VI) [16,22], one ligand is assigned to the bis (RR) or Δ absolute configuration while the other ligand is assigned to the bis (SS) (Λ configuration). The hydrogen-bonded solvate diol molecules are

entirely of the meso (RS) type.

Considering Fig. I.2.4(2), the solvate diol molecules are assigned RS - this means that one of the bidentate ligands has to be bis (RR) and the other bis (SS). Arbitarily assigning ring 1 as RR, ring 2 and 3 as RS and ring 4 as SS, from the spectrum of the complex (Fig.I.2.4(3)) the

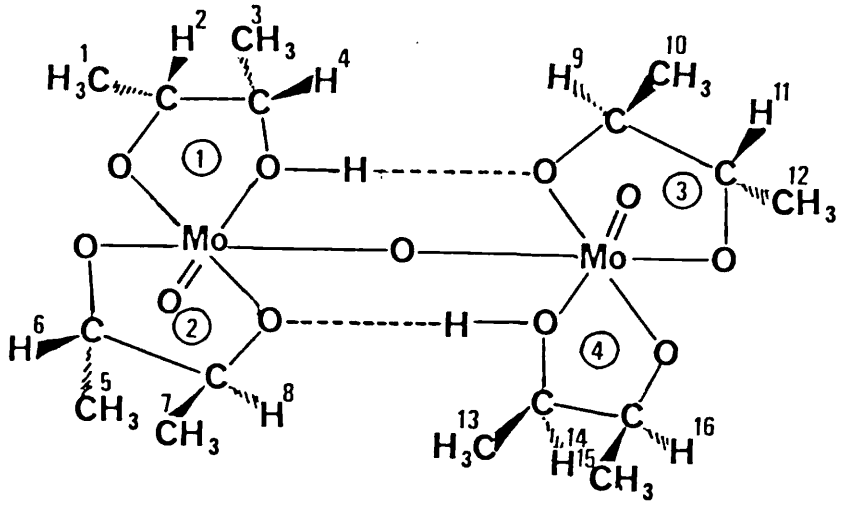

Fig. I.2.4(2)

peak patterns of the methine protons at 5.51ppm and 4.93ppm are similar, hence these are assigned as the meso (RS) type. It is not possible to specifically assign either of the meso bidentate ligands. From the model of the structure and Fig. I.2.4(2) , the methyl groups in the bis (RR) configurations, ring 1, are more shielded when compared to the methyl groups in the bis (SS) configuration - hence, the methine peak at 3.82ppm is that of the bis (RR) configuration. This leaves the doublet of quartets at 5.19ppm (J_{H-H} 5Hz) coupled to the doublet of quartets at 4.61ppm which have to be the bis (SS) configuration (or Λ absolute configuration).

The assignment of the methyl groups was made possible by selective decoupling - the results of which are summarised below:-

i) Decoupling at 5.51ppm collapses the doublets at 1.51ppm and 1.34ppm to a singlet.

ii) Decoupling at 5.19ppm collapses the doublet at 1.34ppm to a singlet and the doublet of quartets at 4.61ppm to a quartet.

iii) Decoupling at 4.93ppm collapses the doublets at 1.47ppm and 1.43ppm to a singlet.

iv) Decoupling at 4.61ppm collapses the doublet at 1.39ppm and the doublet of quartets at 5.19ppm to a quartet.

v) Decoupling at 3.82ppm collapses the doublet at 1.16ppm to a singlet.

From Section I.2.1a, it can be infered that the Mo-O-CH(Me) group is less shielded than Mo ← OHCH(Me). This, along with the data obtained by selective decoupling experiments leads to the direct assignment of the methyl groups (J_{Me-H}6Hz for all) as shown below:-

Assignment of spectrum:-

Spectrum run at 297K in $CDCl_3$.

bis(RR), Δ configuration

C^1H_3, C^3H_3	1.16ppm,	6 protons, J(6.5Hz).
H^2, H^4	3.82ppm,	2 protons.

meso(RS)

As said earlier, it is not possible specifically to assign ring 2 or 3. The assignments of ring 2 and 3 could possibly be the other way round i.e. C^5H_3 could be $C^{12}H_3$, C^7H_3 could be $C^{10}H_3$ and H^6, H^8 could be H^{11}, H^9 respectively.

Ring 2:-

C^5H_3	1.51ppm,	3 protons, J(6.5Hz).
C^7H_3	1.34ppm,	3 protons, J(6.5Hz).
H^6,H^8	5.51ppm,	2 protons.

Ring 3:-

$C^{12}H_3$	1.47ppm,	3 protons,	J(6.5Hz)
$C^{10}H_3$	1.43ppm,	3 protons,	J(6.5Hz)
H^{11},H^{9}	4.93ppm,	2 protons.	

Bis(SS), Λ Configuration

$C^{13}H_3$	1.34ppm,	3 protons,	J(6.5Hz)
$C^{15}H_3$	1.39ppm,	3 protons,	J(6.5Hz)
H^{14}	5.19ppm,	1 proton,	J(5Hz)
H^{16}	4.61ppm,	1 proton,	J(5Hz)

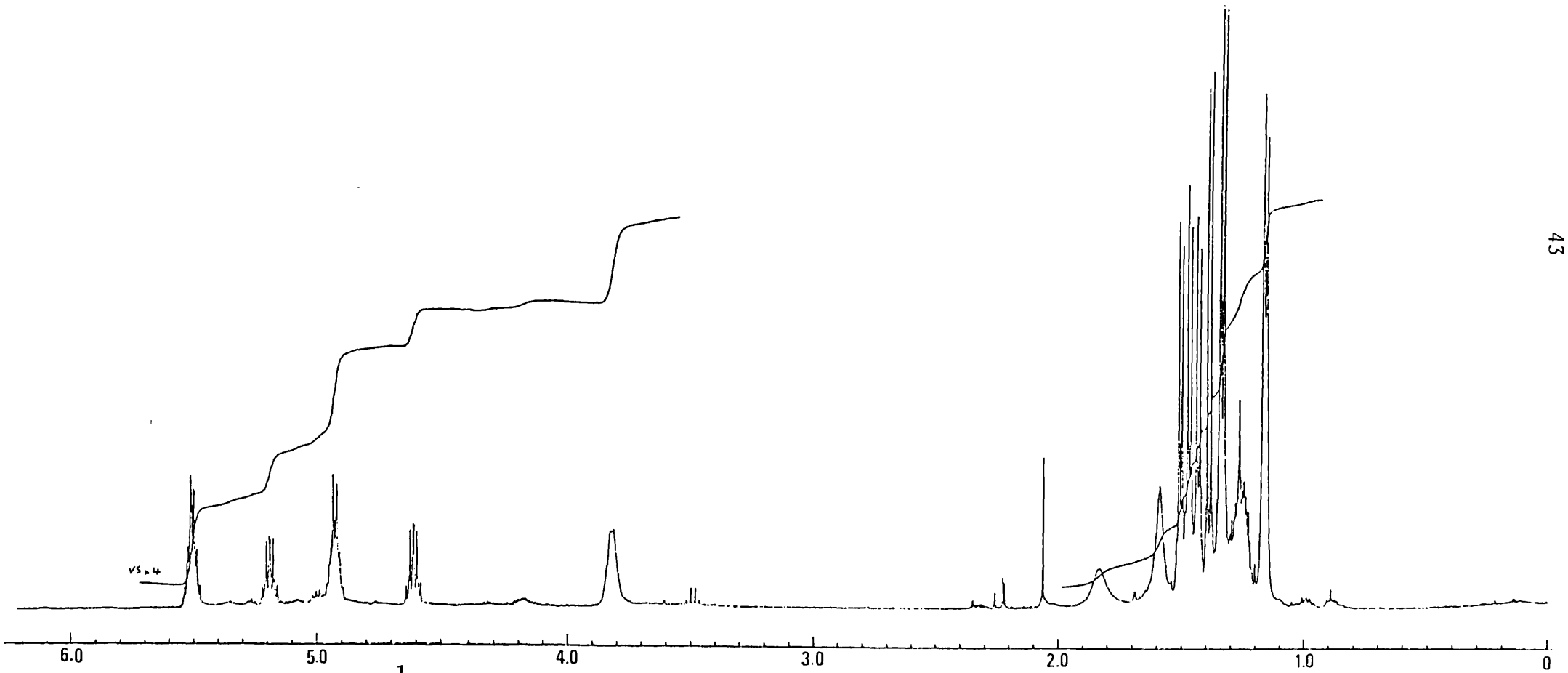

Fig. I.2.4(3) 400.13 MHz ^{1}H nmr spectrum of μ-Oxo-Bis (oxo [2,3-dimethyl-2,3-butane-2,3-diolato(1-)] [2,3-dimethyl-2,3-butane -2,3-diolato(2-)] molybdenum (VI) in $CDCl_3$

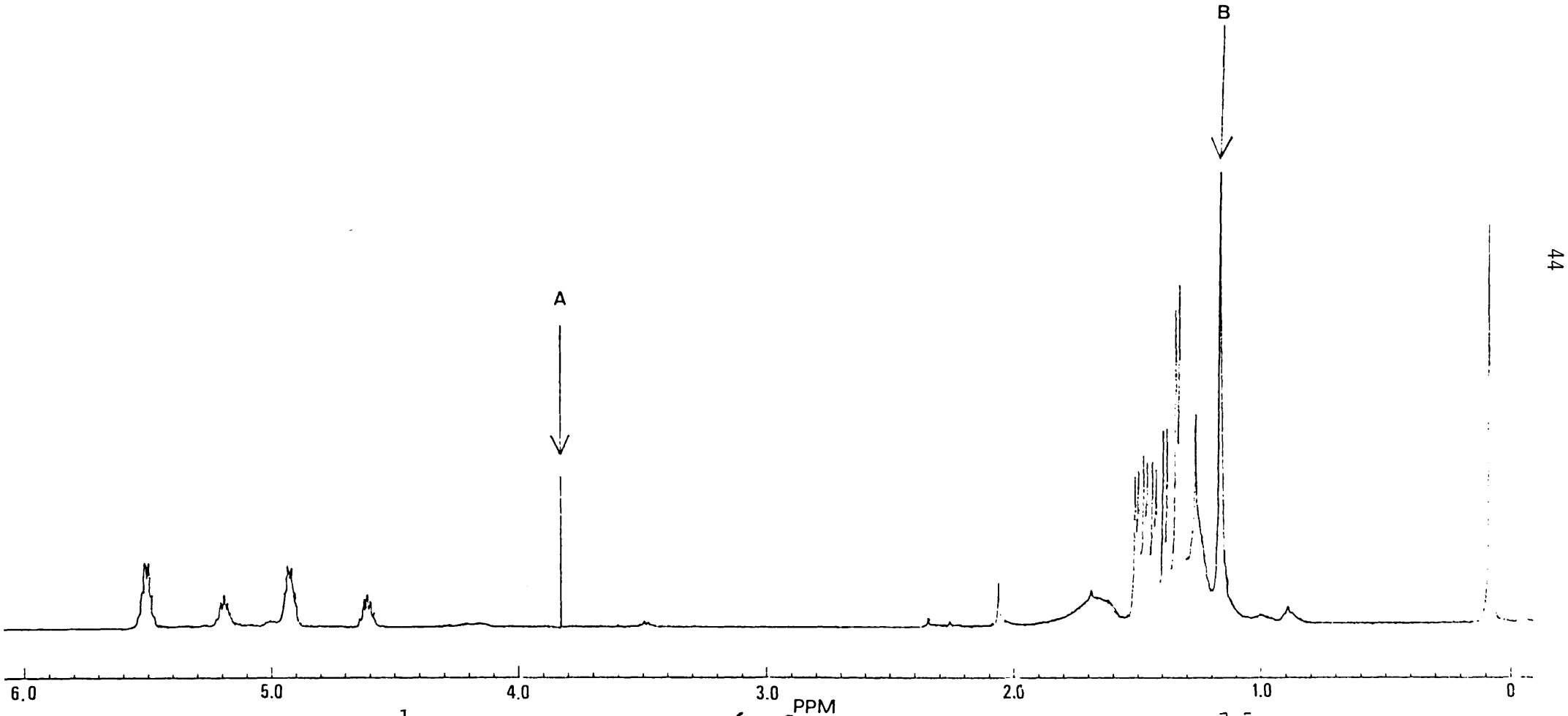

Fig. I.2.4(4) 400.13 MHz ^{1}H nmr spectrum of μ-Oxo-Bis(oxo [2,3-dimethyl-2,3butane-2,3diolato(1-)] [2,3-dimethyl-2,3-butane-2,3-diolato(2-)]) molybdenum (VI) selectively decoupled at A, collapsing signal at B to a singlet (cf Fig. I.2.4(3)).

I.2.5a 400.13 MHz ^{1}H nmr of S(+)Propane 1,2 -diol

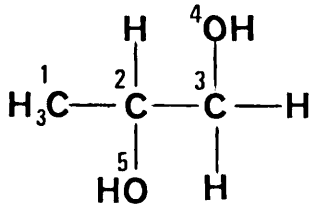

Fig. I.2.5(1)

	$^{1}CH_3$	^{2}CH	$^{3}CH_2$	^{4}OH	^{5}OH
chemical shift/ ppm	0.93,d	3.65,m	3.18,m; 3.34,m	4.67,t	4.59,d
coupling const. Hz.	6.5				2.5
Integral Ht/Units	3	1	1 1	1	1

Spectrum run at 297K in $CDCl_3$.

The broadening of the spectrum at room temperature is due to the viscosity of the diol. The line width could be improved if the sample were either heated or diluted. The asymmetric carbon atom makes the diastereotopic protons non-equivalent. The purity of the synthesized compound is shown up by the hydroxyl peaks; instead of a singlet, there is a triplet (possibly a doublet of doublet?) resonating at 4.67ppm arising from coupling to $^{3}CH_2$ and a doublet arising from coupling to ^{2}CH at 4.59ppm.

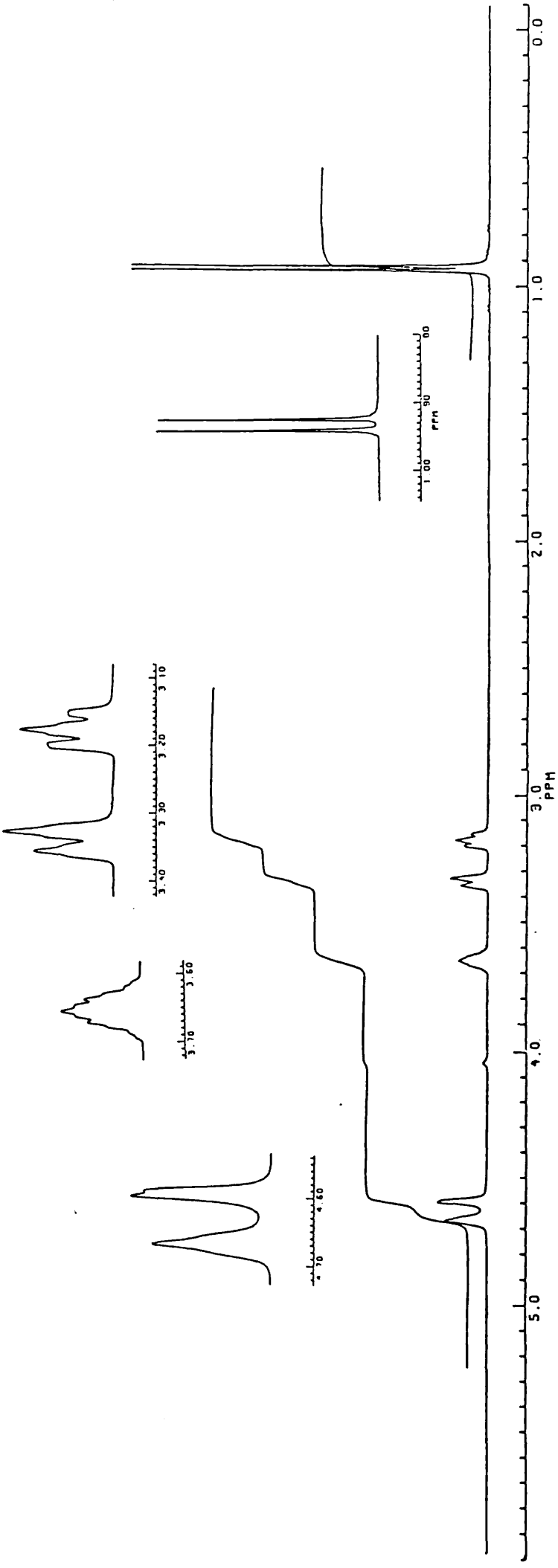

Fig. I.2.5(2) 400.13 MHz ^{1}H nmr spectrum of S(+)propane 1,2-diol in $CDCl_3$.

I.2.5b 400.13 Mlz ^{1}Hnmr of cis-Bis(S(+)propane-1,2-diolato) dioxomolybdenum(VI)

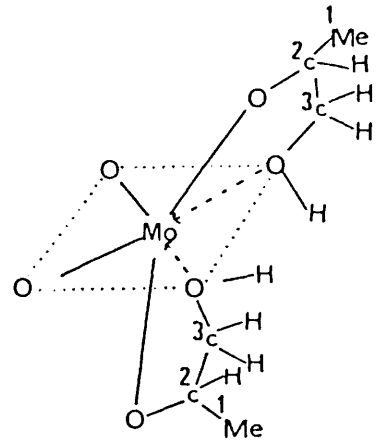

Fig. I.2.5(3)

	$^1CH_3$	^2CH	$^3CH_2$	-OH
chemical shift/ppm	1.31,d	3.93,m	3.50,d	5.55
coupling coust./Hz	6.3		6.4	

Spectrum run at 257K in CD_3OD.

The methyl group gives the expected doublet with a coupling of 6.3 Hz. As the ligand contains an asymmetric carbon atom, the magnetic equivalence of neighbouring protons can be destroyed by its presence. This can be explained by considering the conformations I - III that are represented as Newman projections in Fig. I.2.5(4):-

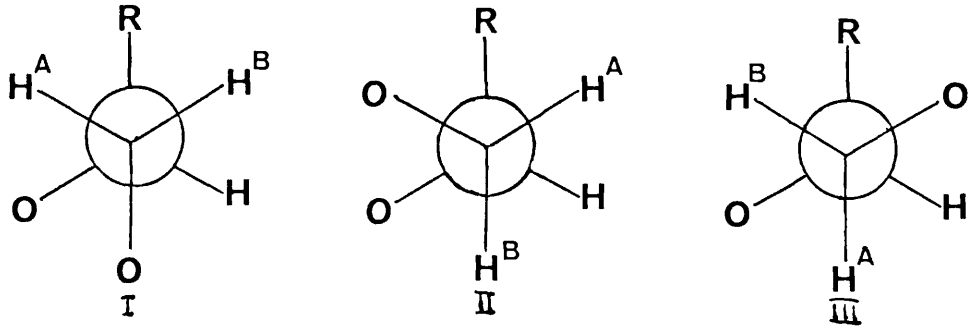

Fig. I.2.5(4)

From Fig. I.2.5(4), it can be seen that H^A and H^B are always located in different chemical environments. Even if the populations of the three rotamers I, II and III are equal, which is generally not the case, the non-equivalence between H^A and H^B remains, because of the presence of the group O, the resonance frequencies $\nu_A(I) \neq \nu_B(III)$, $\nu_B(I) \neq \nu_A(II)$ and $\nu_B(II) \neq \nu_A(III)$.

The non-equivalent or diastereotopic protons H^A, H^B would be expected to give a doublet of doublets. Instead, we have a doublet (6.4 Hz). The reason for this could be due to the shift difference not being great enough - hence what we have is an overlap of the two doublets.

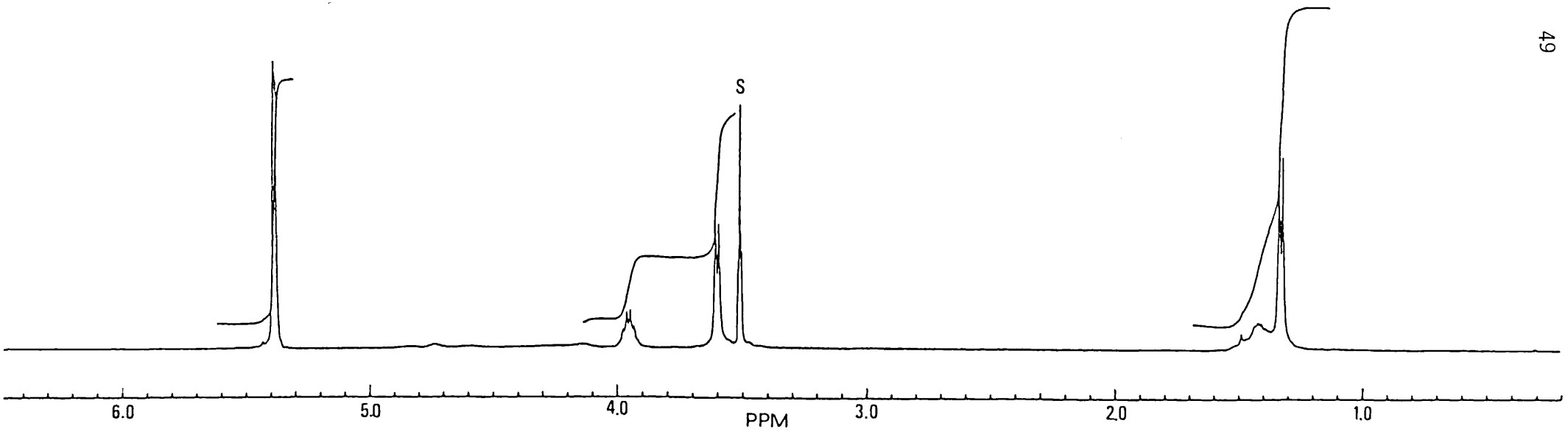

Fig. I.2.5(5) 400.13 MHz ^{1}Hnmr spectrum of cis-Bis(S(+)propane-1,2-diolato) dioxomolybdenum (VI) in CD_3OD run at 257K.

I.2.5c 400.13 MHz ^{1}Hnmr of cis-Bis(propane-1,2-diolato) dioxomolybdenum (VI)

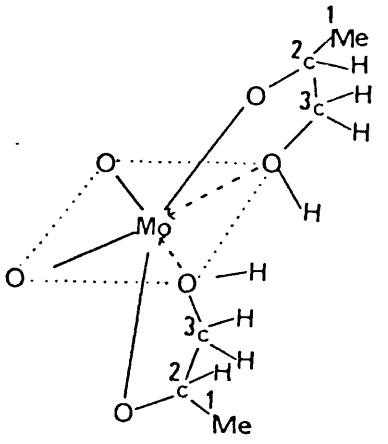

Fig. I.2.5(6)

	$^1CH_3$	^2CH	$^3CH_2$	-OH
Chemical shift/ppm	1.31,d	3.93,m	3.50,d	5.55
Coupling const. Hz	6.3		6.4	

Spectrum run at 257K in CD_3OD.

Since racemic propane 1,2-diol was used as the ligand, complexing on to the metal could be of the RR, SS, RS or SR configuration. RR and SS would not be distinguished by nmr spectroscopy however, RS (or SR) would be distinguished from RR and SS.

The nmr spectrum for Fig. I.2.5(6) was similar to cis-Bis(S(+) propane-1,2,diolato)dioxomolybdenum (VI), Fig. I.2.5.(5). From this, we can infer that the ligand complexed in the RR or SS configuration.

The chemical shift for the hydroxyl proton varies with the value obtained in Section L.2.5b because of intermolecular hydrogen bonding.

I.2.5d 100.62 MHz ^{13}C nmr of cis-Bis(S(+)propane 1,2-dialato) dioxomolybdenum (VI).

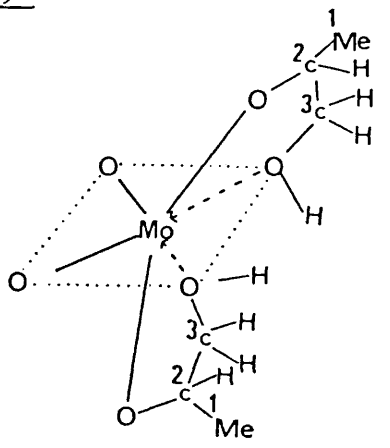

Fig. I.2.5(7)

	Chemical shift/ppm
C-1	19.81
C-2	69.41
C-3	68.64

Spectrum run at 237K in CD_3OD.

At room temperature, C-2 and C-3 are unresolvable. Lowering the temperature, sharpens the peaks; the assignments of the methine and methylene carbons are confirmed by the distortionless enhancement by polarization transfer (DEPT) pulse sequence (see Fig. I.2.5(9))

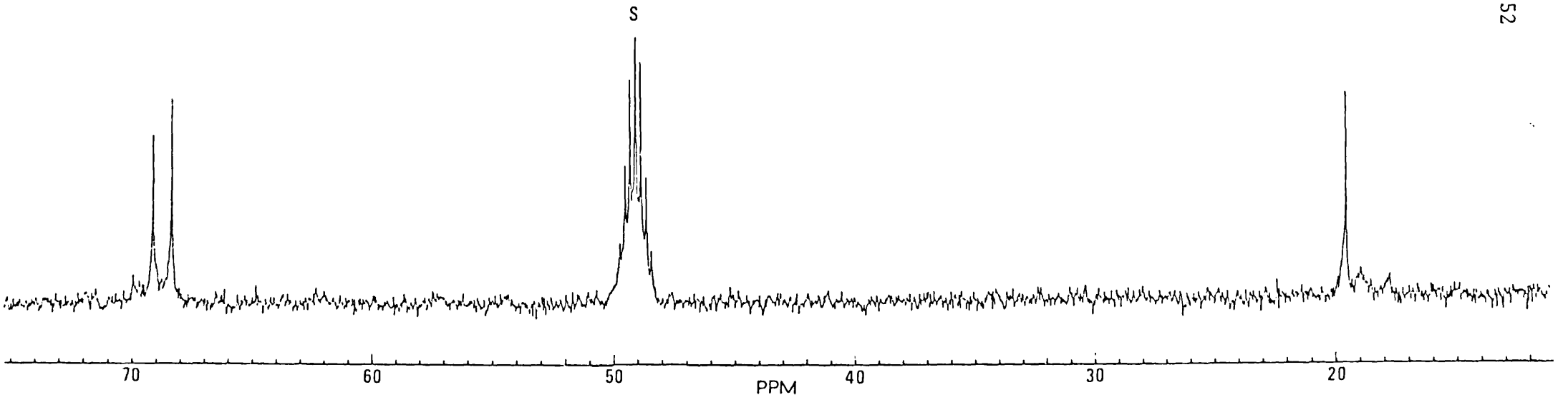

Fig. I.2.5(8) 100.62 MHz ^{13}C $\{^{1}H\}$ nmr spectrum of cis-Bis(S(+)propane-1,2-diolato)dioxomolybdenum (VI) in CD_3OD run at 257K.

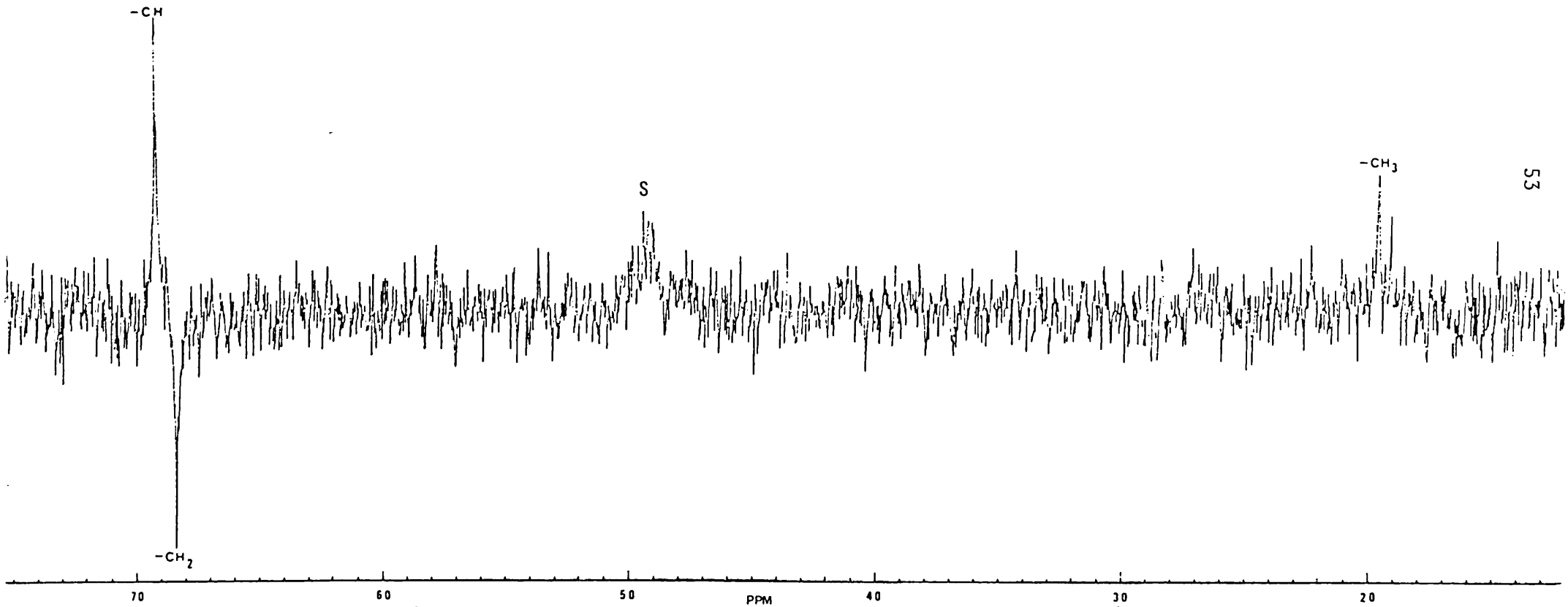

Fig. I.2.5(9) 100.62 MHz ^{13}C $\{^{1}H\}$ nmr spectrim showing the DEPT pulse sequence of cis-Bis (S(+)propane-1,2-diolato) dioxomolybdenum (VI) in CD_3OD at 257K.

I.2.5e 100.62 MHz ^{13}C nmr of cis-Bis(propane-1,2-diolato)dioxomolybdenum (VI).

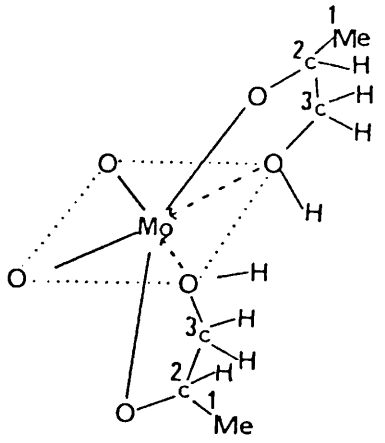

Fig. I.2.5(10).

	Chemical shift/ppm
C-1	19.80
C-2	69.39
C-3	68.63

Spectrum run at 237K in CD_3OD.

The chemical shifts are in agreement with those obtained using the chiral ligand (see Section I.2.5d). The reason as to why this is the case has been stated in Section I.2.5c.

I.2.6a 400.13 MHz ^{1}H nmr of cis-Bis(butane-1,3-diolato)dioxomolybdenum (VI).

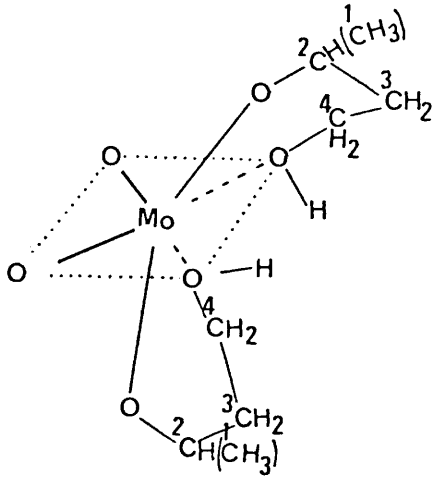

Fig. I.2.6(1)

	$^1CH_3$	^2CH	$^3CH_2$	$^4CH_2$	-OH
Chemical shift/ppm	1.36,d	4.08,m	1.85,m	3.86,m	5.07,s
Coupling const. Hz	6.2				

The spectrum confirms the suggested structure in Fig. I.2.6(1) but in order to get accurate chemical shift and coupling constant values, computer simulation is needed. The complications arise due to the large number of nuclei present which lead to complex spin systems, making the first order analysis difficult.

Due to the chiral centre at C-2, the diastereotopic protons are non-equivalent. The expected six spin system (A_3BB^1C) ought to be split into sixteen lines; instead, there is a very broad multiplet.

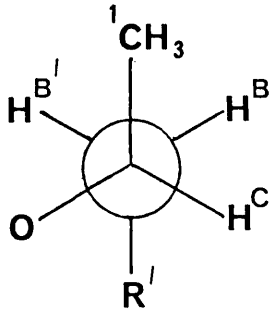

Fig. I.2.6(2)

Fig. I.2.6(2) is probably the most favourable projection. From the spectrum Fig. I.2.6.(5), the major coupling is from the methyl group (J = 6.2 Hz). The different dihedral angles, ϕ, between H^C,H^B and $H^C,H^{B'}$ are bound to make the vicinal couplings, ^3J, between $^3J_{HCHB}$ and $^3J_{HCHB'}$, different[23,24]. Approximate values from the spectrum make $^3J_{HCHB} \sim 2$ Hz and $^3J_{HCHB} \sim 10$ Hz.

The diastereotopic protons have different chemical shifts, this is seen on the spectrum Fig. I.2.6(5) which has an asymmetric pattern. The characterisitc AA' BB' system, showing the 'roof effect' and symmetry about the centre is seen in the $^4CH_2O$ case. This implies that the trans conformation Fig. I.2.6(3) is favoured. The gauche conformation Fig. I.2.6(4), is less stable and is more likely to conform to the ABCD system.

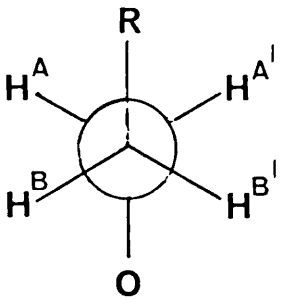

Fig. I.2.6(3)

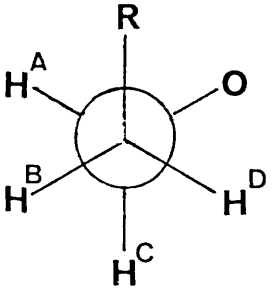

Fig. I.2.6(4)

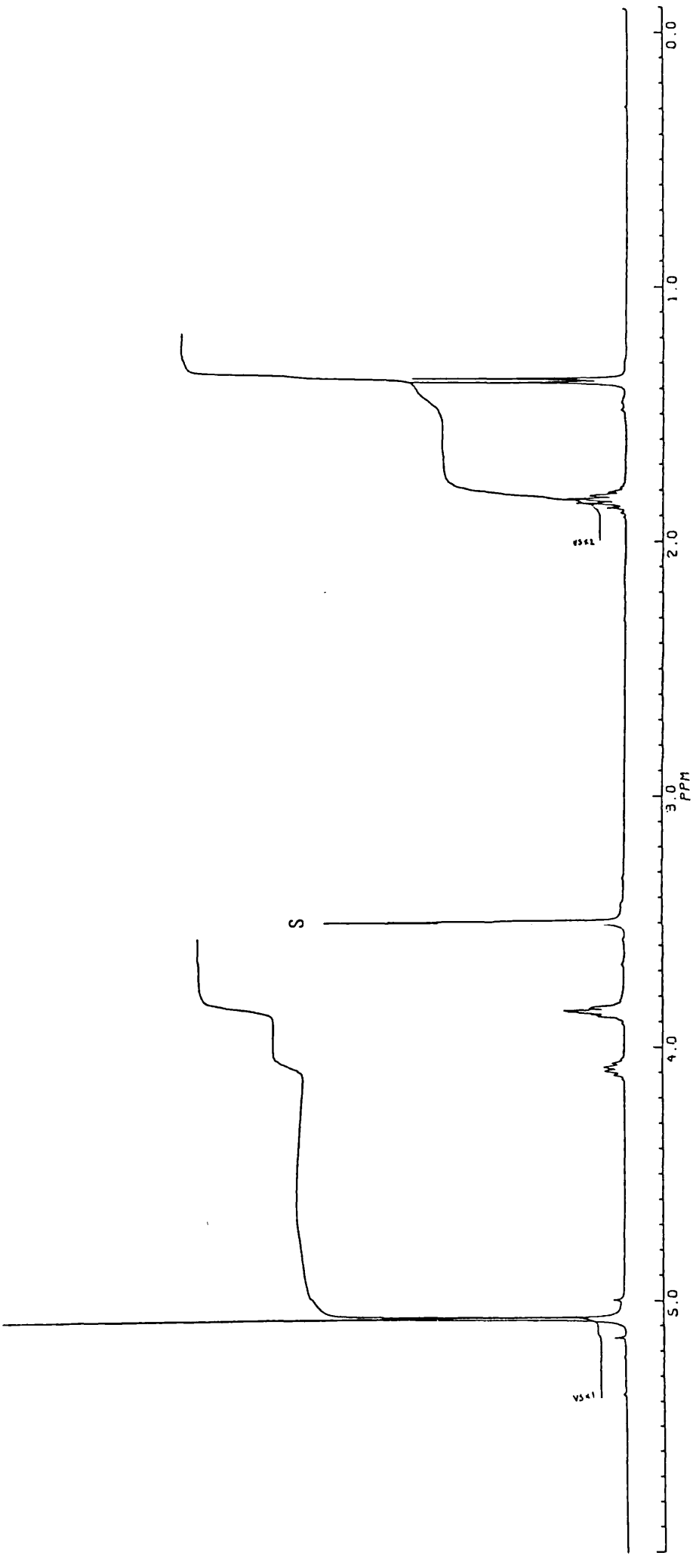

Fig. I.2.6(5) 400.13 MHz ^1H nmr spectrum of cis-Bis(butane-1,3-diolato)dioxomolybdenum (VI) in CD_3OD.

I.2.6b 100.62 MHz ^{13}C nmr of cis-Bis(butane-1,3-diolato) dioxomolybdenum (VI).

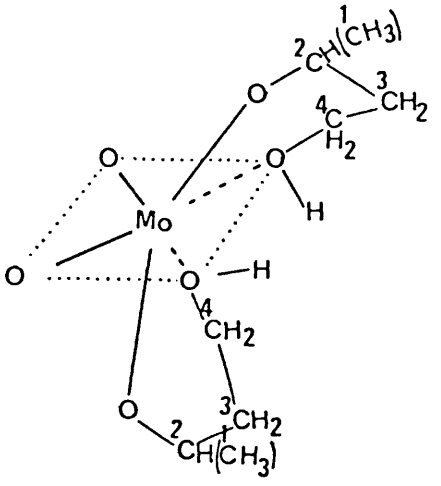

Fig. I.2.6(6)

	C-1	C-2	C-3	C-4
Chemical shift/ppm	24.06	66.56	42.76	60.67

Amongst our earlier findings in the case of ^{13}C spectrum of cis-Bis(S(+)propane-1,2-diolato)dioxomolybdenum (VI), with the aid of DEPT, Fig. I.2.5(9), we concluded that the $-CH_2O$ group was more shielded than the -CHO group. Therefore, the C-2 carbon in Fig. I.2.6(6) is at 66.56 ppm and the C-4 at 60.67 ppm. C-1 is in the expected region; hence it is assigned at 24.06 ppm.

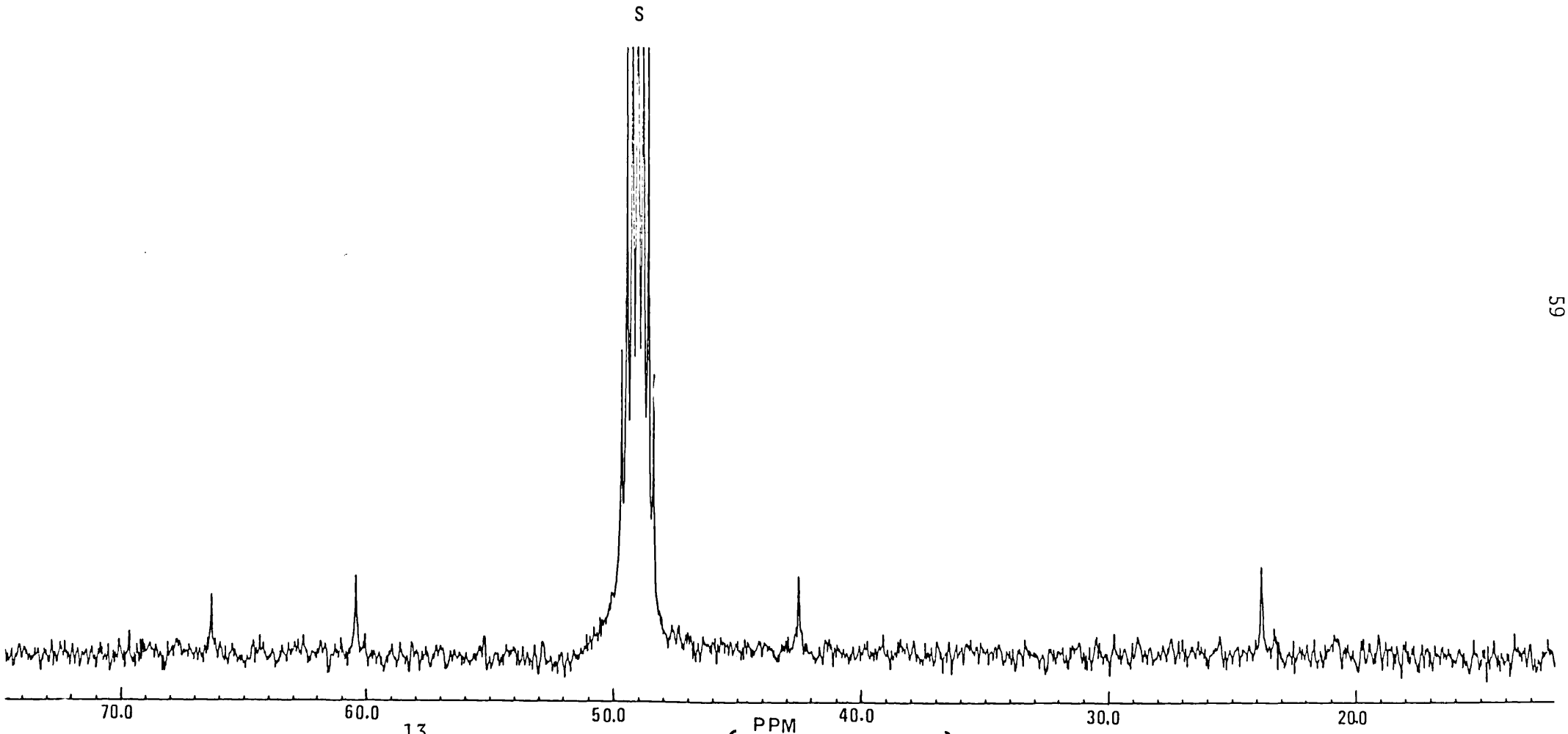

Fig. I.2.6(7) 100.61 MHz ^{13}C nmr spectrum of cis-Bis(butane-1,3-diolato)dioxomolybdenum (VI) in CD_3OD.

I.2.7 50.1 MHz ^{13}C CP/MAS NMR spectrum of cis-Bis(S(+)2(-)amino-1-phenyl propane-1,3-diolato)dioxomolybdenum (VI).

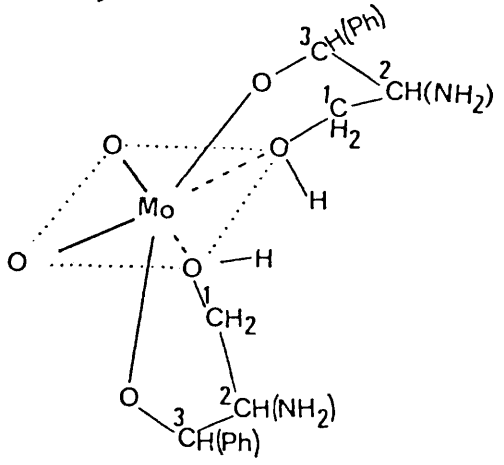

Fig. I.2.7(1)

The ^{13}C CP/MAS nmr spectrum revealed several spinning sidebands marked SSB. The chemical shifts, assignments, and percentage integrated intensities are as follows:-

Chemical shift/ppm	Assignment	% Integrated intensity
20.5	aliphatic carbon	5 ± 2
30.7	impurity	
60.5	methylene carbon, C-1	30 ± 5
62.9	amino-carbon, C-2	
90.4	methine carbon, C-3	14 ± 3
129.2	Aromatic C-H	35 ± 5
140.8	Aromatic C carbon	16 ± 3

SSB from Aromatic C-H

$\sim$ 178 ppm, $\sim$ 80 ppm, $\sim$ 32 ppm

SSB from Aromatic C

$\sim$ 189 ppm, $\sim$ 92 ppm, $\sim$ 44 ppm.

The broad line at 62.9 ppm is assigned to the amino-carbon as it is broadened by ^{14}N-^{13}C dipolar interaction. The ratio of Aromatic C-H to Aromatic C, in relation to the molecular formula ought to be 5:1; what we have is a ratio of 2.2:1. This could be explained by loss of intensity in the SSB. The true intensity of the peak consists of the summation of all the individual SSB and their addition to the central peak. The values quoted, do not included the intensities lost in SSB.

The empirical parameters quoted by Wehrli et al[25] for Benzyl alcohol, Fig. I.2.7(2), were as follows:-

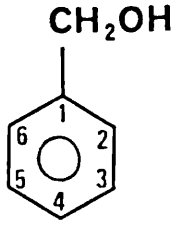

C-1	140.5 ppm
C-2, C-6	127.5 ppm
C-3, C-5	128.5 ppm
C-4	127.5 ppm

Fig. I.2.7(2)

The differences in chemical shift between the ortho, meta and para Aromatic C-H are only 1 ppm. The shift values obtained for the Phenyl group are in general agreement with these data. From this, one can infer that the five Aromatic C-H atoms fall under the broad peak at 129.2 ppm and the Aromatic C atom gives the peak at 140.8 ppm.

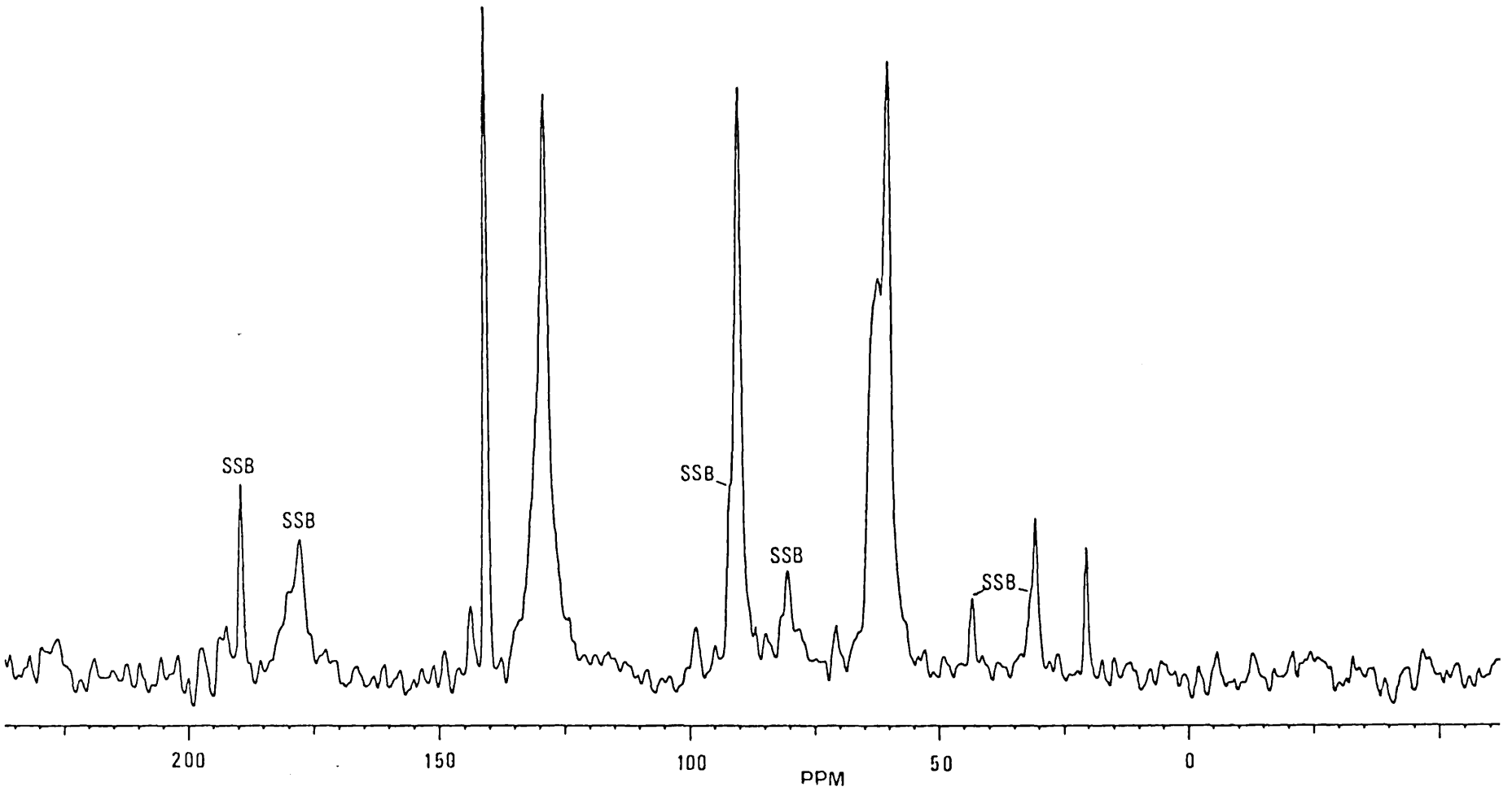

Fig. I.2.7(3) 50.1 MHz ^{13}C CP/MAS nmr spectrum of cis-Bis(S(+)2(-)amino-1-phenyl propane-1,3-diolato)dioxomolybdenum VI.

I.2.8a 100.62 Mlz ^{13}C nmr of Potassium tricarbonyl-L-Histidinato Molybdenum (VI).

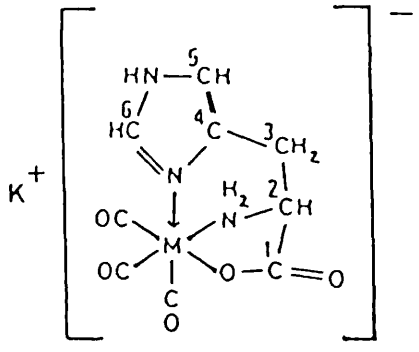

Fig. I.2.8(1).

The potassium salt of tricarbonyl-L-histidinato complex of molybdenum was first isolated by Beck et al [26] who quoted no NMR data. The 100.61 Mlz ^{13}C spectrum shown in Fig. I.2.8(2) was assigned as follows:-

	chemical shift/ppm
C-1	186.62
C-2	55.48
C-3	31.71
C-4	117.71
C-5	137.43
C-6	141.10
-CO	231.49

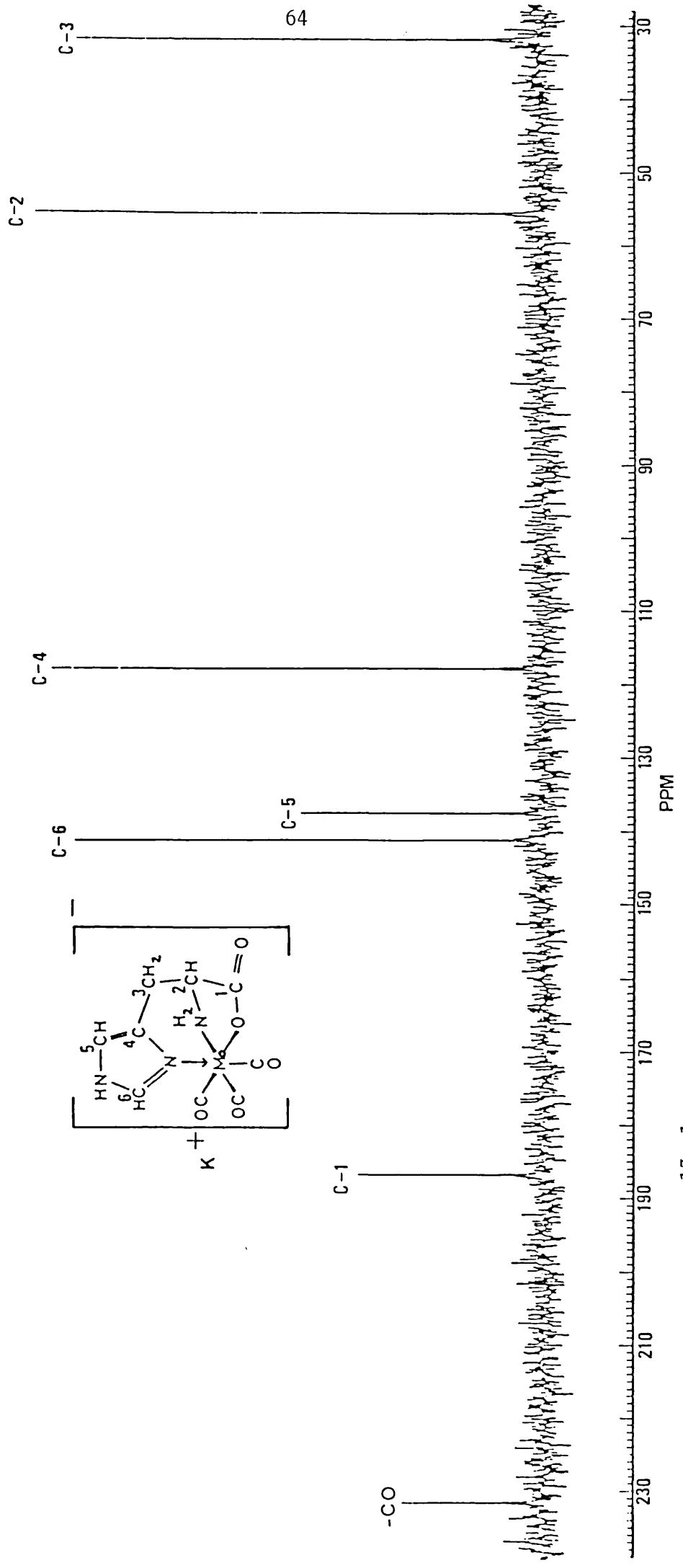

Fig. I.2.8(2) 100.62 MHz $^{13}C\{^{1}H\}$nmr spectrum of Potassium tricarbonyl-L-Histidinato Molybdenum (VI).

I.2.8b 90 MHz ^{1}H nmr of Potassium tricarbonyl-L-Histidinato Molybdenum (VI).

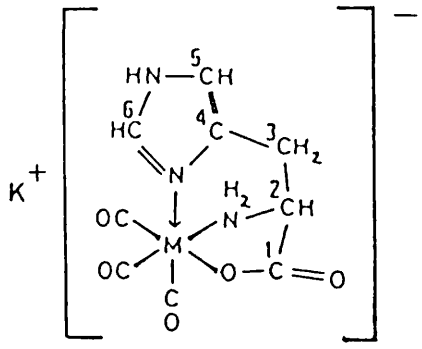

Fig. I.2.8(3)

The 90 MHz ^{1}H nmr spectrum gave the following shift values:-

^{2}CH	3.00ppm,m
$^{3}CH_2$	3.86ppm,t (3.9Hz)
^{5}CH	6.92ppm,s
^{6}CH	7.90ppm,s

I.2.8c 26.08 MHz ^{95}Mo nmr of Potassium tricarbonyl-L-Histidinato Molybdenum (VI).

The ^{95}Mo spectrum Fig. I.2.8(4) gave a singlet at 782ppm (referenced to external Molybdenum hexacarbonyl).

Fig. I.2.8(4) 26.08 MHz ^{95}Mo mnr spectrum of Potassium tricarbonyl-L-Histidinato Molybdenum (VI) (ref. to external $Mo(Co)_6$).

I.2.9 400.13MHz ^{1}H nmr of Potassium histidinatotrioxomolybdate VI - Water (1:1).

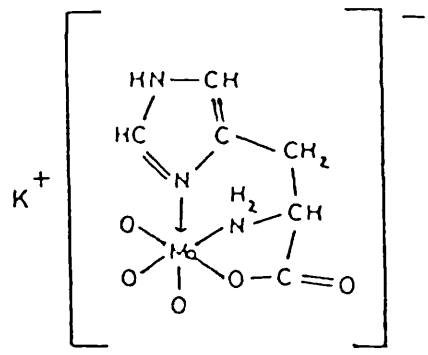

Fig. I.2.9(1)

From the spectra Fig. I.2.9(2) of the complex in D_2O, there is an equilibrium that exists between the complex and the free ligand which is summarised in Eqn. I.2.9(1).

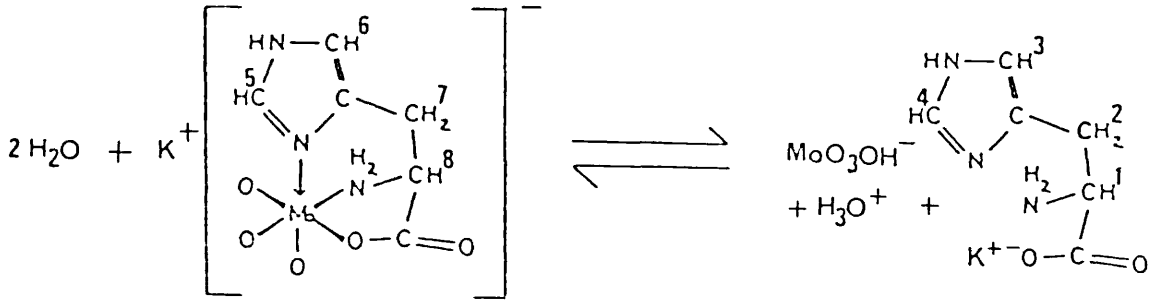

Eqn. I.2.9(1)

pD	Complex Hist / Free Hist	H^1	H^2	H_2^3	H^4	H^5	H^6	H_2^7	H^8
5.65	24:76	8.61,s	7.38,s	ν_A=3.40;ν_B=3.36;o J=12.7Hz	4.07,t J=6Hz	8.23,s	7.03,s	ν_A=3.24;ν_B=3.17;o J=12.8Hz	4.19,b
6.05	41:59	8.54,s	7.36,s	ν_A=3.38;ν_B=3.34;o J=12.8Hz	4.06,t J=6.4Hz	8.23,s	7.03,s	ν_A=3.25;ν_B3.17;o J=12.8Hz	4.20,t J=3.8Hz
6.50	61:39	8.35,s	7.27,s	ν_A=3.33;ν_B=3.29;o J=11.7Hz	4.03,b	8.20,s	7.00,s	ν_A=3.23;ν_B=3.15;o J=12.8Hz	4.18,b
6.75	62:38	8.35,s	7.27,s	ν_A=3.33;ν_B=3.29;o J=11.9Hz	4.04,b	8.20,s	7.00,s	ν_A=3.23;ν_B=3.15;o J=12.8Hz	4.19,b
6.95	68:32	8.25,s	7.24,s	ν_A=3.31;ν_B=?	4.03,b	8.21,s	7.01,s	ν_A=3.23;ν_B=3.15;o J=12.9Hz	4.19,b
8.35	5:95	7.74,s	7.04,s	ν_A=3.20;ν_B=3.11;o J=11.8Hz	4.07,t J=6.4Hz	8.20,s	7.00,s	3.15,b	4.18,b

Table I.2.9(1)

The complex, as expected, but unlike the free ligand does not show any variation in chemical shift with pD Table I.2.9.(1) .

Protonation of the complex leads to its dissociation. In free histidine, at low pH (acidic solution), both basic sites are protonated, however, at high pH (alkaline solution), both are free - this is represented by Eqn.I.2.9(2) below:-

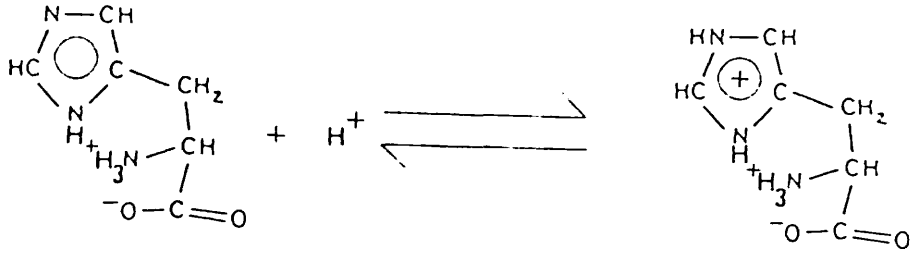

Histidine (Base)

Eqn. I.2.9(2)

Protonated Histidine (Acid)

This is clearly seen by nmr, and is recorded in the chemical shifts for H^1 and H^2 Table I.2.9(1) which move upfield in more basic solutions. The variation in chemical shift value is due to the charge deficiency in the imidazole ring that accounts for less shielding in acidic solutions.

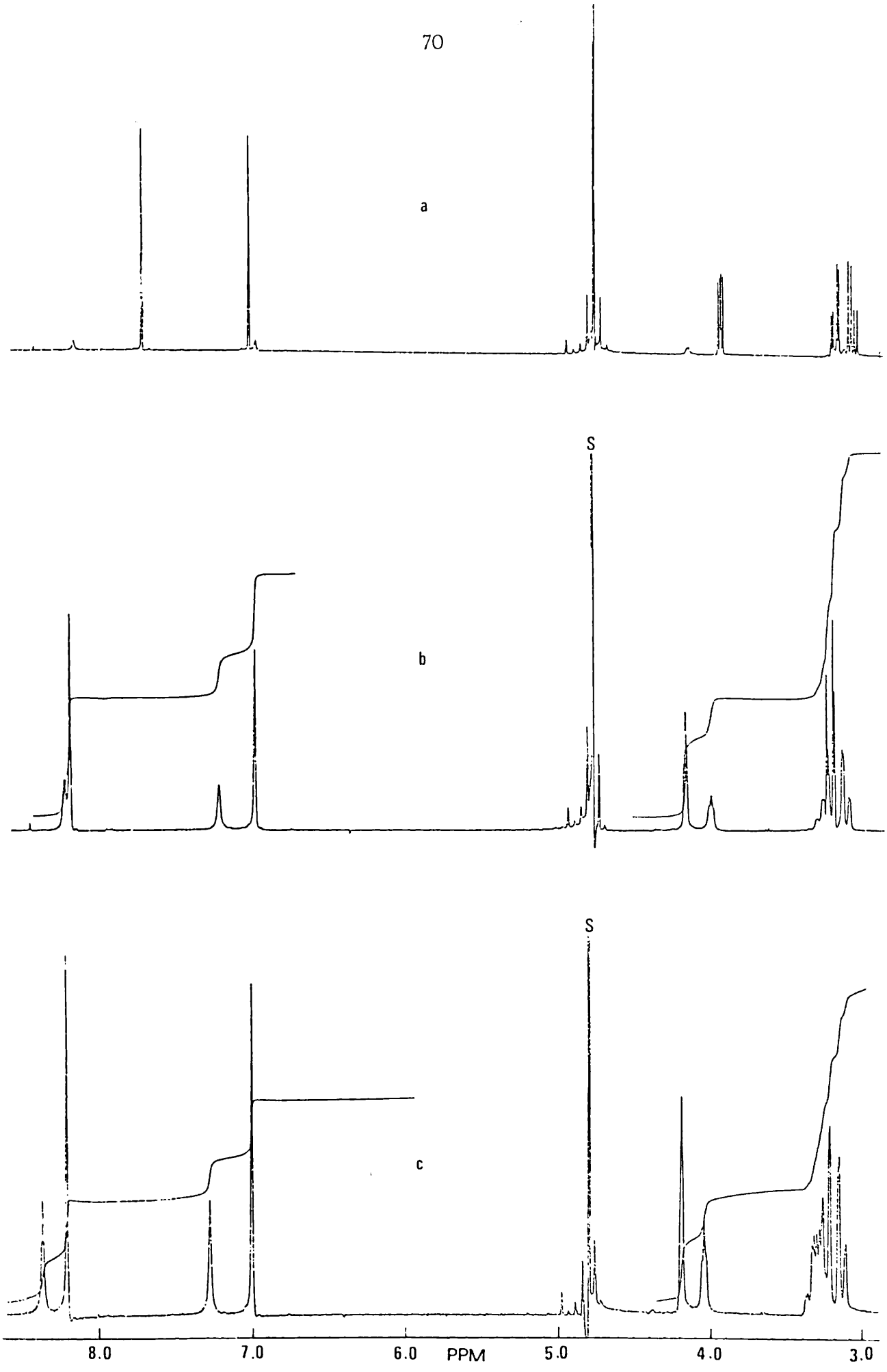

Fig. I.2.9.2 400.13 MHz ^{1}H nmr spectrum of Potassium Histidinatotrioxo-molybdate (VI) - Water in D_2O at a) pD = 8.35 b) pD = 6.95 c) pD = 6.35

CHAPTER I SECTION 3

I.3.1. Purification of Reagents

Acetonitrile was dried by shaking with molecular sieves (type 4A), filtered, and then refluxed with calcium hydride until no further hydrogen was evolved. The acetonitrile was then distilled and stored under nitrogen.

Benzene was dried with sodium wire, distilled under nitrogen and stored over molecular sieves (type 4A).

Chloroform was dried over molecular sieves (type 4A).

Diethyl ether was dried with sodium wire.

Diols used as ligands. All the diols were dried by refluxing with calcium hydride, until no further hydrogen was evolved, then vacuum distilled. The product was then dried using the 'magnesium-iodine' method, vacuum distilled and stored under molecular sieves (type 3A) in a vacuum desiccator over phosphorus pentoxide.

Propan-1-ol was dried by the 'magnesium-iodine' method, then distilled under nitrogen and stored under molecular sieves (type 3A).

THF was refluxed with sodium metal and benzophenone for 2 hrs., then distilled and stored under nitrogen.

L-2-amino-1-butanol was dried by refluxing with calcium hydride, until no further hydrogen evolved, then vacuum distilled and stored under molecular sieves (type 3A).

I.3.2 General Experimental Methods

All glassware was thoroughly cleaned and dried overnight in an oven. In all cases, ball and socket joints were used.

I.3.2a Procedure for making diol catalysts

The catalysts were made in a 250 ml round bottomed 'Schlenk flask' complete with a magnetic follower. To it was fitted a condenser with a nitrogen bubble tube (Fig. I.3.2(1)). General precautions were taken to ensure that all solvents were degassed and the system was kept under nitrogen. After completion of the reaction, a cold trap (Fig. I.3.2(2)) was fitted to the 'Schlenk flask' and the excess solvent removed under vacuum.

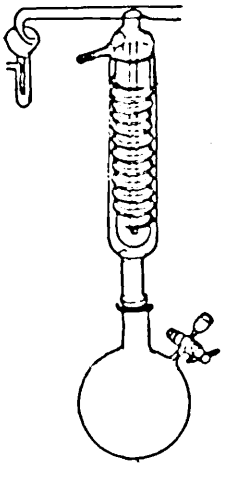

Fig. I.3.2.(1)

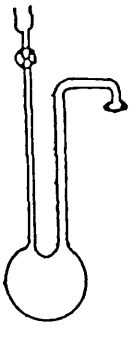

Fig. I.3.2.(2)

Fig. I.3.2.(3)

The cold trap was then removed from the 'Schlenk flask' and replaced by a tap (Fig. I.3.2.(3)). The system was then evacuated. Diethyl ether was condensed into the 'Schlenk flask' under vacuum. When this was completed, the tap was closed and the product stirred in an ice bath (this ensured that trituration was carried out in the absence of air).

The product was then filtered under nitrogen, dried, transferred to a Schlenk tube and stored under nitrogen.

I.3.2b Nuclear Magnetic Resonance

All samples were measured on a Bruker 400 MHz spectrometer. For ^{1}H spectra, samples were sealed in a 5 mm high precision NMR tube (10 mm tubes used for ^{13}C and ^{95}Mo). Unless stated, the spectrum were run at 297K. Several pulse methods were used to simplify the assignment of the spectrum. For a review of these methods, refer to Benn et al[27]. All chemical shifts are measured in ppm downfield from TMS.

I.3.2c Cross Polarisation Magic Angle Spin (CP/MAS) in Solid State NMR

In liquid nmr, due to the rapid molecular motion, ^{13}C - ^{1}H dipolar interactions and ^{13}C chemical shift anisotropies are averaged to zero. However, in solids, they have to be artifically removed; failure to do so, leads to extremely broad linewidth.

Linewidth due to chemical shift anisotropy can be removed by rotating a sample around the axis, making a 'magic angle' of 54.7^{o} with the static field. This process, known as magic angle spinning (MSA), makes the time-averaged shift tensor equivalent in x, y and z plane, resulting in the removal of the anisotropy.

High-resolution isotropic spectra in solids (comparable to liquids)

is obtainable by using heteronuclear dipolar decoupling and MAS. The relatively small magnetic moment and low natural abundance (1.1%) of ^{13}C along with the long ^{13}C spin-lattice relaxation in many solids makes the normal Fourier Transform (FT) NMR not practical. However, this problem is overcome by using a method called Cross Polarisation (CP)[28-30].

Finally, isotropic chemical shift spectra of dilute spins in solids can be obtained by the combined techniques[29,31] of high powered decoupling to remove the heteronuclear dipolar interaction, MAS to eliminate chemical shift anisotropy, and CP method to enhance the sensitivity. The combination of these three techniques is often called CP/MAS NMR.

I.3.2d Infra-red

Infra-red spectra were recorded for potassium chloride discs and nujol mull using a Perkin Elmer PE 983 Infra-red spectrometer. Knobler et al[22] and Butcher et al[12] have assigned $\nu(Mo\text{-}O_t)$, $\nu(Mo\text{-}O_b\text{-}Mo)$ and $\nu(M_o\text{-}O_\ell)$ stretching frequencies. O_t = terminal oxygen; O_b = core-bridging oxygen; O_ℓ = ligand oxygen.

I.3.2e Elemental Analysis

C, H, N elemental analysis were carried out on a Perkin Elmer PE240 Elemental Analyser by Mrs. E. Whitaker of this Department.

I.3.2f Melting Point

Melting points were measured using a Gallenkamp melting point apparatus.

I.3.3 Experimental Details for Chapter I.

I.3.3a Preparation of cis-Bis(D(-)butane-2,3-diolato)dioxomolybdenum (VI)-D(-)Butane2,3diol (1:1)

To finely ground $MoO_2(acac)_2$ (3g, 9.19 mmole), was added D(-)butane 2,3-diol(12ml, 131.4 mmole). After stirring under nitrogen for 1 hr at 75°, the excess glycol was removed in vacuo and the residue triturated with ether, giving a white powder; yield 3.30g, (91%). Recrystallisation from dry acetonitrile gave a white powder, m.p. 102-5° goes yellow (i.e. dimer forms).

Analysis:-

	C	H
CALCULATED	36.36	7.07
FOUND	35.92	6.97

Infra-red

2600-3400 cm^{-1} (broad, strong) Coordinated hydroxyl

935 cm^{-1} (strong); 928 cm^{-1} (strong) $\nu(Mo\text{-}O_t)$

620 cm^{-1} (strong); 532 cm^{-1} (medium) $\nu(Mo\text{-}O_\ell)$

I.3.3b Preparation of cis-Bis(butane-2,3-diolato)dioxomolybdenum (VI)-Butane2,3-diol (1:2)

To finely ground $MoO_2(acac)_2$ (5g, 15.3 mmole), was added butane 2,3-diol(20ml, 220.8 mmole). After stirring under nitrogen for 1 hr at 75°, the excess glycol was removed in vacuo and the residue, triturated with ether, giving a white powder; yield was 4.9g (66%). Recrystalisation from dry acetonitrile gave a white powder, m.p. 89° (lit 89°)[12].

Analysis:-

	C	H
CALCULATED	39.50	7.82
FOUND	39.40	7.93

Infra-red

2600-2400 cm^{-1} (broad, strong) Coordinated hydroxyl

932 cm^{-1} (strong); 918 cm^{-1} (strong) $\nu(Mo-O_t)$

608 cm^{-1} (medium); 538 cm^{-1} (medium $\nu(Mo-O_\ell)$

I.3.3c Preparation of μ-Oxo-Bis ([D(-)-dimethyl-2,3-butanediolato(1-)] [D(-)2,3-dimethyl-2,3-butanediolato (2-)]) oxomolybdenum (VI)

0.5g (1.53 mmole) of cis-Bis D(-)butane2,3-diolato dioxomolybdenum (VI)-D(-)Butane 2,3-diol (1:1), prepared by the method described in I.3.3.a, was heated under vacuum at 70°. The product formed, gave a yellow powder; yield was 0.4g (53%); m.p. 135-137° dec.

On cooling, the product reverted to its starting material hence, this catalyst was always made in situ. The starting material was insoluble in chloroform however, the product was extremely soluble. As the compound was stable in solution, it was confirmed by NMR.

I.3.3d Preparation of μ-Oxo-Bis ([2,3-dimethyl-2,3-butane diolato (1-)] [2,3-dimethyl-2,3-butanediolato(2-)]) oxomolybdenum (VI)

To finely ground $MoO_2(acac)_2$ (5g, 15.3 mmole), was added butane 2,3-diol (20ml, 220.8 mmole). After stirring under nitrogen for 1 hr at 75°, the excess glycol was removed in vacuo while the product vessel was heated to 100°. Trituration with ether gave a yellow powder; yield was 4.9g (54%). Recrystallisation from dry chloroform gave a yellow powder.

Analysis:-

	C	H
CALCULATED	32.32	5.72
FOUND	32.12	5.69

Infra-red

2600-3400 cm^{-1} (broad, strong)	Coordinated hydroxyl
953 cm^{-1} (strong); 929 cm^{-1} (strong)	$\nu(MoO_t)$
741 cm^{-1} (strong)	$\nu(MoO_bM_o)$
618 cm^{-1} (strong); 550 cm^{-1} (medium)	$\nu(Mo\text{-}O_\ell)$

I.3.3e Preparation of S(+) Propane 1,2-diol[32]

To a suspension of lithium aluminum hydride (26.45g, 0.7 mole) in 1ℓ dry ether was added dropwise, L(+) ethyl lactate (100g, 0.85 mole) in 200cm^3 dry THF with ice cooling. After the addition was complete, the mixture was stirred at room temperature overnight and hydrolysed under ice cooling by dropwise addition of 30cm^3 of water, 30cm^3 of 15% sodium hydroxide and 100cm^3 water. The reaction mixture was briefly refluxed and the precipitate filtered. The solvent was removed in vacuo and the residue distilled, b.p. 70-2°/10mm; yield 52.8g (82%).

I.3.3f Preparation of cis-Bis(S(+)propane-1,2-diolato) dioxomolybdenum (VI)

To finely ground $MoO_2(acac)_2$ (5g, 15.3 mmole) was added S(+) propane-1,2-diol(20 cm^3 272.2 mmole). After stirring under nitrogen for

1 hr at 75°, the excess glycol was removed in vacuo and the residue, triturated with ether, giving a white powder; yield was 3.85g (90%). Recrystallation from dry acetonitrile gave a white powder, m.p. 128° dec.

Analysis:-

	C	H
CALCULATED	25.89	5.03
FOUND	25.78	5.01

Infra-red

2600-3400 cm^{-1} (broad, strong)	Coordinated hydroxyl
950 cm^{-1} (strong)- 918 cm^{-1} (strong)	$\nu(Mo\text{-}O_t)$
620 cm^{-1} (strong); 550 cm^{-1} (strong)	$\nu(Mo\text{-}O_\ell)$

I.3.3g Preparation of cis-Bis(propane-1,2-diolato)dioxomolybdenum (VI)

The same method was employed as that used in Section I.3.3.f. Yield was 3.9g (91%), m.p. 132-133° (lit. 132-4°)[33].

Analysis:-

	C	H
CALCULATED	26.89	5.03
FOUND	25.46	5.01

Infra-red

2600-3400 cm^{-1} (broad, strong)	Coordinated hydroxyl
950 cm^{-1} (strong); 918 cm^{-1} (strong)	$\nu(Mo\text{-}O_t)$
620 cm^{-1} (strong); 547 cm^{-1} (medium)	$\nu(Mo\text{-}O_\ell)$

I.3.3h Preparation of cis-Bis(butane-1,3-diolato)dioxomolybdenum (VI)

To finely ground $MoO_2(acac)_2$ (5g, 15.3 mmol) was added butane 1,3-diol (20ml, 220.8 mmole). After stirring under nitrogen for 1 hr at 75°, the excess glycol was removed in vacuo and the residue triturated with ether giving a white powder; yield was 4.2g (90%), m.p. 155-9°dec.

Analysis:-

	C	H
CALCULATED	31.37	5.88
FOUND	31.20	5.79

Infra-red

2600-3400 cm^{-1} (broad, strong)	Coordinated hydroxyl
945 cm^{-1} (strong)- 918 cm^{-1} (strong)	$\nu(Mo-O_t)$
610 cm^{-1} (strong)	$\nu(Mo-O_\ell)$

I.3.3i Preparation of R(-)phenyl ethane 1,2-diol

To a suspension of lithium aluminium hydride (25g, 0.66 mole) in 1ℓ of dry ether was added dropwise R(-)mandelic acid (18g, 12 mmole) in 400ml dry ether with ice cooling. After the addition was completed, the mixture was refluxed for 1 hr and then hydrolysed with dilute hydrochloric acid and water. The aqueous and organic layers were separated; the organic layer, being washed successively with water, sodium carbonate, water and dried (magnesium sulphate). The excess solvent was removed in vacuo. R(-) phenyl ethane-1,2-diol crystallised out from ether; yield was 14.1g (86%), m.p. 63-4°.

Analysis:-

	C	H
CALCULATED	69.56	6.25
FOUND	69.54	6.24

NMR

^{1}H nmr: Phenyl group 7.24 ppm, m, 5 protons; -OH attached to methine 4.45 ppm, b, 1 proton; -OH attached to methylene 4.25 ppm, b, 1 proton; methine 4.68 ppm, d.d. J8.3 Hz, 1 proton; methylene ν_A = 3.53 ppm ν_B = 3.60 ppm, o, J = 10.7 Hz, 1 proton.

^{13}C nmr: methylene C, 68.09 ppm; methine C, 74.75 ppm; C-1 140.57 ppm; ortho 128.56 ppm; meta 128.01 ppm; para 126.10 ppm.

I.3.3 j Preparation of cis-Bis (S(+)phenyl ethane-1,2-diolato) dioxomolybdenum (VI)

To finely ground MoO_2 (acac)$_2$ (5g, 15.3 mmole), was added a solution of R(-)phenyl ethane-1,2-diol (8.28g, 6o mmole) dissolved in 40cm^3 of dry propanol. After stirring under nitrogen for 1 hr at 80^o, the white powder formed was filtered. Yield was 4.9g (80%), m.p. 116-118^{o}dec.

Analysis:-

	C	H
CALCULATED	47.76	4.47
FOUND	47.51	4.40

Infra-red

2600-3400 cm^{-1} (broad, strong)	Coordinated hydroxyl
950 cm^{-1} (strong); 918 cm^{-1} (strong)	$\nu(Mo-O_t)$
598 cm^{-1} (strong)	$\nu(Mo-O_\ell)$

I.3.3k Preparation of cis-Bis(S(+) 2(-)amino-1-phenyl Propane-1,3-diolato)dioxomolybdenum (VI).

To finely ground $MoO_2(acac)_2$ (5g, 15.3 mmole) was added a solution of S(+)2-amino-1-phenyl-1,3-propane diol dissolved in 40ml of dry propanol. After stirring under nitrogen for 1 hr at 80°, the white powder formed was filtered. Yield was 4.9g (69%), m.p. 156-8 dec.

Analysis:-

	C	H	N
CALCULATED	46.95	5.22	6.09
FOUND	46.52	5.29	6.09

Infra-red

2600-3400 cm^{-1} (broad, strong)	Coordinated hydroxyl
930 cm^{-1} (strong); 905 cm^{-1} (strong)	$\nu(Mo-O_t)$
570 cm^{-1} (medium)	$\nu(Mo-O_\ell)$

I.3.3l Preparation of cis-Bis(R(-)2(-)amino-1-butanato)dioxomolybdenum (VI)

To finely ground $MoO_2(acac)_2$ (5g, 15.3 mmole) was added R-(-)-2-amino-1-butanol (20mol, 211.6 mmole). After stirring under nitrogen for 1 hr at 100°, the excess amino alcohol was removed in vacuo and the residue, triturated with ether, giving a white powder; yield was 4.1g (88%), m.p. 209-14°dec.

Analysis:-

	C	H	N
CALCULATED	31.58	6.58	9.21
FOUND	30.21	6.41	9.02

Infra-red

2600-3400 cm^{-1} (broad, strong)	Coordinated hydroxyl
902 cm^{-1} (strong); 863 cm^{-1} (medium)	$\nu(Mo-O_t)$

I.3.3m Preparation of μ-Oxo-Bis(oxo[butane-1,2-diolato(1-)][butane-1,2-diolato(2-)])molybdenum (VI).

To finely ground $MoO_2(acac)_2$ (5g, 15.3 mmole) was added butane 1,2-diol (20ml, 220.8 mmole). After stirring under nitrogen for 1 hr at 75°, the excess glycol was removed in vacuo while the product vessel was heated to 100°. Trituration with ether gave a yellow powder; yield was 4.2g (46%). Recrystallisation from dry chloroform gave a yellow powder, m.p. 85-87°dec.

Analysis:-

	C	H
CALCULATED	32.32	5.72
FOUND	31.72	5.49

Infra-red

2600-3400 cm^{-1} (broad, strong)	Coordinated hydroxyl
950 cm^{-1} (strong)- 929 cm^{-1} (strong)	$\nu(Mo-O_t)$
940 cm^{-1} (strong)	$\nu(MoO_bMo)$
618 cm^{-1} (strong); 550 cm^{-1} (medium)	$\nu(Mo-O)$

I.3.3n Preparation of Potassium tricarbonyl-L-histidinato molybdenum (VI).

The salt was prepared by the same method used by Beck et al[26]. Yield was 80%, m.p. 216-220°dec.

Analysis:-

	C	H	N
CALCULATED	27.62	2.56	10.74
FOUND	27.22	2.09	11.26

I.3.3o Preparation of Potassium histidinatotrioxomolybdate (VI)-Water (1:1).

MoO_3 (2.16g, 15 mmole), L(-) Histidine (2.325g, 15 mmole) and potassium hydroxide (0.84g, 15 mmole) were refluxed in 150ml of water for 3 hr. The hot solution was filtered and allowed to evaporate. The clear tabular crystals were washed with a small quantity of ethanol/diethyl ether (50:50). Yield was 2.1g (40%), m.p. 187-190°dec.

Analysis:-

	C	H	N
CALCULATED	20.28	2.81	11.83
FOUND	20.17	2.69	11.80

Infra-red

895 cm^{-1} (strong); 840 cm^{-1} (strong) $\nu(Mo\text{-}O_t)$

NMR studies of potassium histidinatotrioxomolybdate (VI) with pD.

A saturated solution of potassium histidinatorioxomolybdenum (VI)

was made in D_2O. The nmr of the complex was carried out at different pH. pD was varied accordingly with KOD and a solution of perchloric acid in D_2O.

Chapter II

EPOXIDATION OF OLEFINS

CHAPTER II SECTION 1

II.1 INTRODUCTION

II.1.1 The Prilezhaev Reaction[34]

The most well established method for epoxidation of olefin hydrocarbons is the Prilezhaev reaction described by Eqn. II.1.1(1)

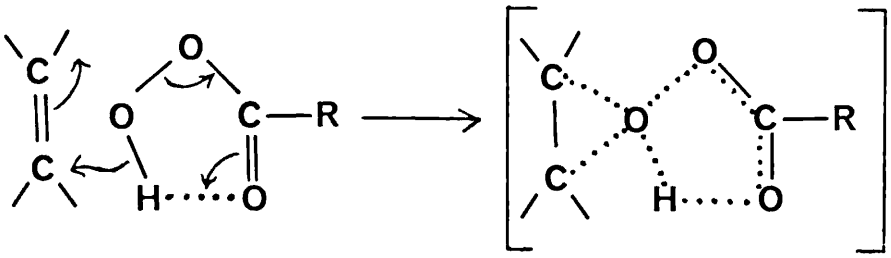

(I) (II) (III)

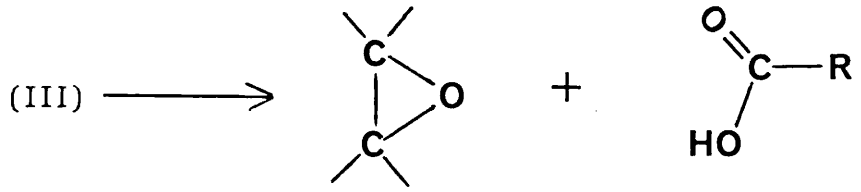

(IV) (V)

Eqn. II.1.1(1)

This method uses organic peroxyacids as oxidising agents. The reactions of many unsaturated compounds have been examined in detail.[35-37] Amongst the organic peroxyacids used are m-chloroperoxybenzoic acid, monoperoxyphthalic acid, performic acid and peroxybenzoic acid.

Kinetic studies have indicated that the reaction is first order with respect to both olefin and peroxyacid. In the case of the olefin, electron releasing substituents increase and electron attracting substituents decrease the reaction rate. The rate of reaction varies

according to the nature of the peroxyacid and the substituents on the olefin[38].

The epoxidation reaction, described in Eqn. II.1.1(1) proceeds via a heterolytic mechanism to give stereoselective addition of oxygen across the double bond. Variations and modifications on this general outline remain a subject of discussion[35-37,39].

Inspite of its wide applications, the Prilezhaev reaction has some disadvantages. On a large scale, the process is extremely dangerous and many epoxides undergo cleavage by secondary reactions.

II.1.2 Liquid phase oxidation of olefins using organic hydroperoxides in the presence of catalytic amounts of metal complexes.

The problems posed by the Prilezhaev reaction mentioned in Section II.1.1 has paved the way for modern methods of epoxidation. The most notable method now used for epoxidation involves the expoxidation of olefins using organic hydroperoxides, the reaction being catalysed by transition metals[40-42]. (Eqn. II.1.2(1)).

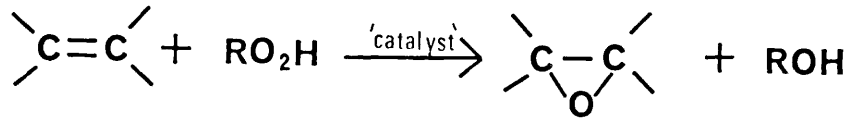

Eqn. II.1.2(1)

This reaction bears some resemblance to the epoxidation of olefins by peroxyacids in that the organic hydroperoxides possess the capability of heterolytic cleavage of the O-O bond, although to a lesser extent than organic peroxyacids. However, in the case of the organic hydroperoxides, cleavage is facilitated with the aid of metal catalysts.

The transition metal complexes of iron, manganese, cobalt and copper readily catalyse the homolytic decomposition of organic hydroperoxides, generating radicals [43,44] and hence give poor epoxide yields. However, soluble complexes of molybdenum, tungsten, vanadium and titanium which can effect heterolysis of the peroxy linkage in organic hydroperoxides, are generally used for epoxidation.

II.1.2.1 Kinetics and Mechanism

In the epoxidation of olefins using organic hydroperoxides, metal complexes in high oxidation states e.g. Mo(VI), W(VI), V(V) and Ti(IV), facilitate the heterolysis of alkyl hydroperoxides [8,45-54].

Metal catalysed epoxidations exhibit the following characteristics:- [33,48,49,55-57].

a) Metal complexes which are good Lewis acids and have low oxidation potentials are superior catalysts. For soluble transition metal catalysts, the following order of activity is observed: Mo>W>V,Ti.

b) The active catalyst contains the metal in its highest oxidation state.

c) Polar solvents, particularly alcohols and water, retard the reaction by competing with the hydroperoxide for coordination sites on the metal.

d) The high yield of epoxides and the stereospecificity of the reaction arises due to the heterolytic mechanism.

e) Reaction by-products arise from the competing metal-catalysed homolytic decomposition of the hydroperoxide.

f) Substituent effects indicate that the active epoxidising agent is an electrophilic species.

Scheme I, outlines the reaction scheme for molybdenum catalysis.[57-59]

Scheme I

$$Mo^{VI} + RO_2H \rightleftharpoons [Mo^{VI}RO_2H] \quad \text{Eqn. II.1.2(2)}$$
'active'

$$Mo^{VI} + ROH \rightleftharpoons [Mo^{VI}ROH] \quad \text{Eqn. II.1.2(3)}$$
'inactive'

$$[Mo^{VI}RO_2H] + C=C \longrightarrow \underset{O}{C-C} + Mo^{VI} + ROH \quad \text{Eqn. II.1.2(4)}$$

$$Mo^{VI} + RO_2H \longrightarrow Mo^{V} + RO_2\cdot + H^+ \quad \text{Eqn. II.1.2(5)}$$

$$Mo^{V} + RO_2H \longrightarrow Mo^{VI}OH + RO\cdot \quad \text{Eqn. II.1.2(6)}$$

Spectroscopic investigations carried out by Trifiro et al[60] indicated the presence of Catalyst/hydroperoxide complex as an 'active' species. It has been suggested by several workers[8,46,48,49,51,52,54,61] that a fast equilibrium is set up between the active catalyst and the hydroperoxide and the rate-determining step in the epoxidation reaction is the electrophilic attack on the olefin by the Catalyst/hydroperoxide complex. The final step is the heterolytic cleavage of the O-O bond in the hydroperoxide.

Kinetic studies[8,52,60] have shown that metal catalysed hydroperoxide epoxidation of olefins using molybdenum and tungsten is first order in olefin, catalyst and hydroperoxide (Eqn. II.1.2(7)) and the reaction is inhibited by alcohols, including the alcohol generated as as result of epoxidation (Eqn. II.1.2(4)).

$$\text{Rate} = k[\text{Olefin}][\text{Catalyst}][\text{Hydroperoxide}]$$

Eqn. II.1.2(7)

Sheng and Zajacek suggested Fig. II.1.2(1) or Fig. II.1.2(2) as possible transition states in the molybdenum catalysed epoxidation of olefins.

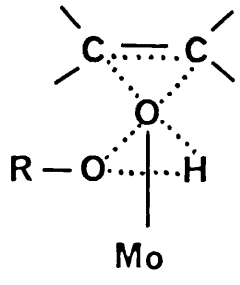

Fig. II.1.2(1)

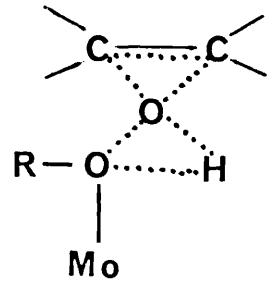

Fig. II.1.2(2)

Gould et al[51] proposed Scheme II for the epoxidation of cyclohexene by the tert-butyl hydroperoxide in the presence of vanadyl acetylacetonate. The co-product alcohol strongly retarded the reaction and the rate dependence on the hydroperoxide was found to be analogous to the Michaelis-Menten equation for enzyme catalysis in the presence of a competitive inhibitor[62]. This observation has been confirmed by a number of workers[52-54].

Scheme II

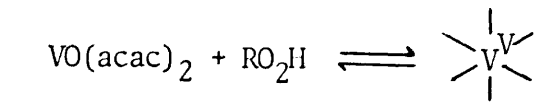

Eqn. II.1.2(8)

Catalyst activation (rapid, reversible)

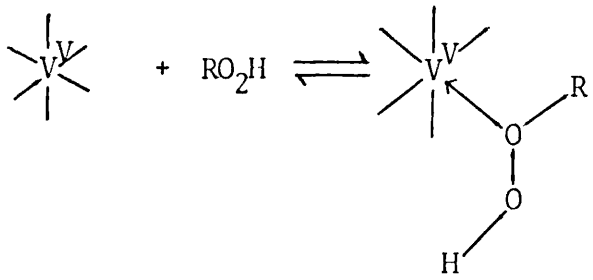

Eqn. II.1.2(9)

Complex formation (rapid, reversible)

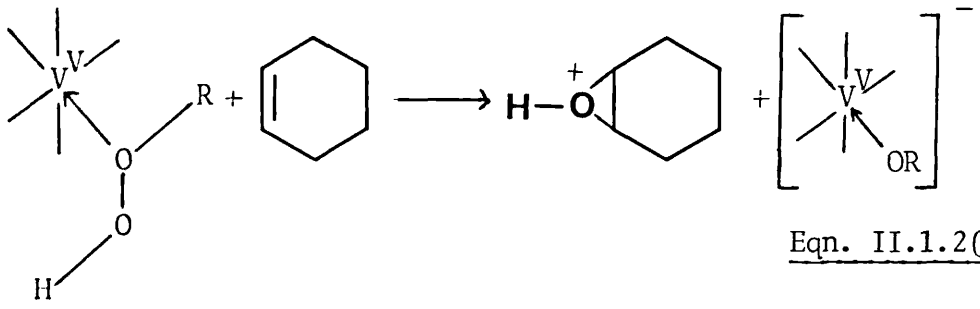

Eqn. II.1.2(10)

heterolysis (rate-determining)

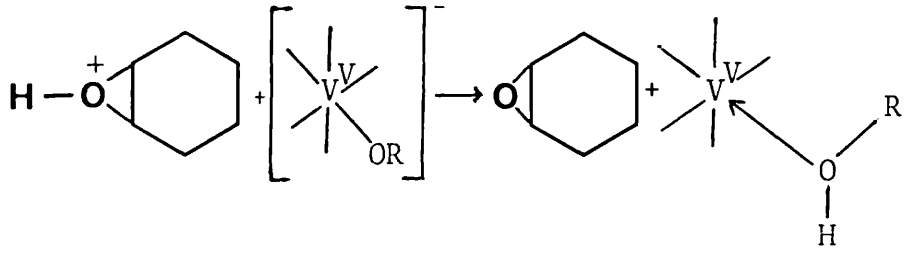

Eqn. II.1.2(11)

proton transfer (rapid)

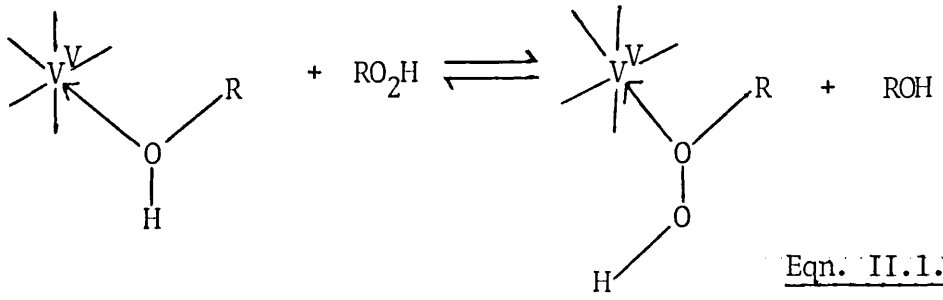

Eqn. II.1.2(12)

Ligand exchange (rapid, reversible)

Sheng and Zajacek[63] found that yields obtained in the reaction of allyl alcohol and 1,5-hexadiene-3-ol, catalysed by vanadium complexes, were higher than those obtained when molybdenum complexes were used as catalysts. However, contrary observations were made in the case of simple olefins. This arises, because of the ability of vanadium chelates to form inactive complexes with the coproduct alcohol more readily than their molybdenum counterparts.

Due to the capability of alcohols to complex with the catalysts, one would expect allylic alcohols to be less reactive than simple olefins. However, in the case of vanadium compounds, this in not the case[63]. Sheng and Zajacek[61,63] proposed the modified mechanism in Scheme III.

Scheme III

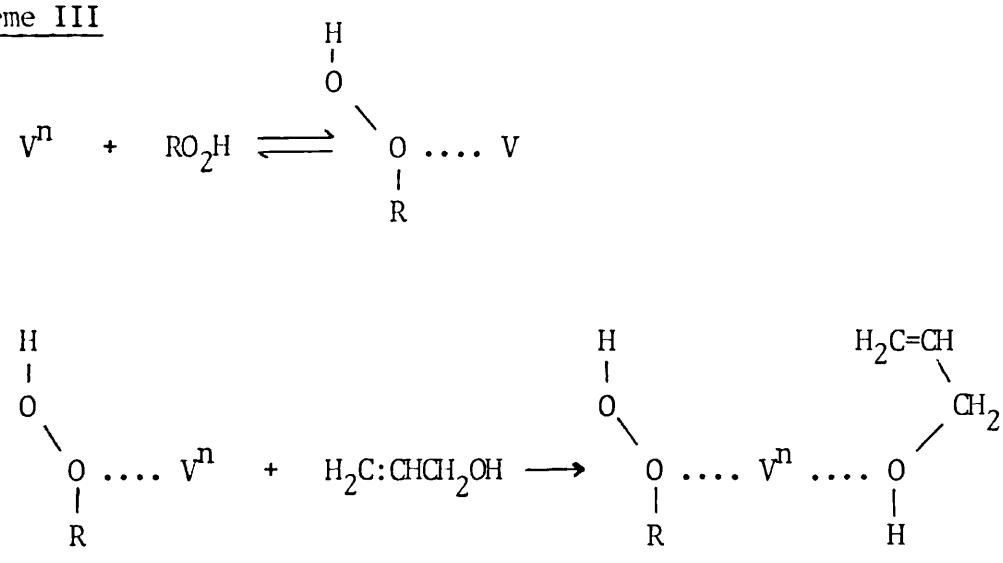

Scheme III, shows the active catalyst complexed with both the allylic alcohol and the hydroperoxide before the double bond is epoxidised. The geometry of the intermediate places the electron-deficient oxygen of the hydroperoxide in the vicinity of the double bond.

Chong and Sharpless[64] suggested that in the hydroperoxide/metal

complex intermediate, the metal is coordinated to the hydroperoxide through the oxygen farthest to the alkyl group. Hence, coordination takes place at a site which is less sterically hindered. In addition, such intermediates proposed also account for the reactivity of allylic alcohols in these systems. The geometry of the intermediates is favourable for simultaneous coordination at the metal centre of the hydroxyl group of an allylic alcohol and for the oxygen of the hydroperoxide farthest to the alkyl group.

Mimoun et al[65] discovered that molybdenum(VI)peroxo compounds (Fig. II.1.2(3)) stoichiometrically epoxidise olefins under anhydrous

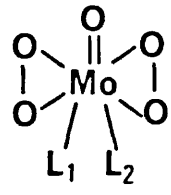

Fig. II.1.2(3)

$L_1;L_2$ = H.M.P.T., D.M.F.,D.M.A.C.

H.M.P.T. = hexamethyl phosphotriamide

D.M.F. = dimethyl formamide

D.M.A.C. = dimethyl acetamide

conditions in organic solvents. They speculated that the active oxidants in the catalytic systems might also be peroxo species generated in situ by reaction of the alkyl hydroperoxide with a metal oxo compound.

Sheldon[33], in his studies of molybdenum catalysed epoxidation using tert-butyl hydroperoxide, isolated intermediates which were considered to be Mo(VI)-1,2diol complexes. The structure of the diol is related to the structure of the substrate olefin being epoxidised and independent of the molybdenum compound.

Skibida and Kok[66], using catalysts of the general formula

MoO_2L_2 investigated complex formation in the catalytic epoxidation of cyclohexene and 2-methyl-2-pentene by tert-butyl hydroperoxide. NMR was used to identify intermediates in the reaction mixture and they concluded that diol complexes of Mo(VI) were involved in epoxidation.

In view of the diol interemediates in the epoxidation reaction, the question arises whether the organic hydroperoxide is truly coordinated to the metal complex during epoxidation. It is possible that there is an initial reaction of the hydroperoxide with the metal complex producing a metal diol species which epoxidises the olefin in the subsequent step.

However, ^{18}O labelled studies[64] of epoxidations with alkyl hydroperoxides have substantiated evidence that the intact hydroperoxide is present in the activated complex responsible for oxygen transfer to the olefin.

Mimoun[67] proposed a rather different mechanism for the metal catalysed hydroperoxide epoxidation of olefins. This mechanism, shown in Scheme IV involves the olefin initially attacking the metal, upon coordination to the metal, the olefin loses its nucleophilic character and the peroxy oxygen acting as a nucleophile attacks the coordinated olefin resulting in a five-membered peroxymetallocycle. This intermediate then decomposes to produce the epoxide and metal alkoxide.

Scheme IV

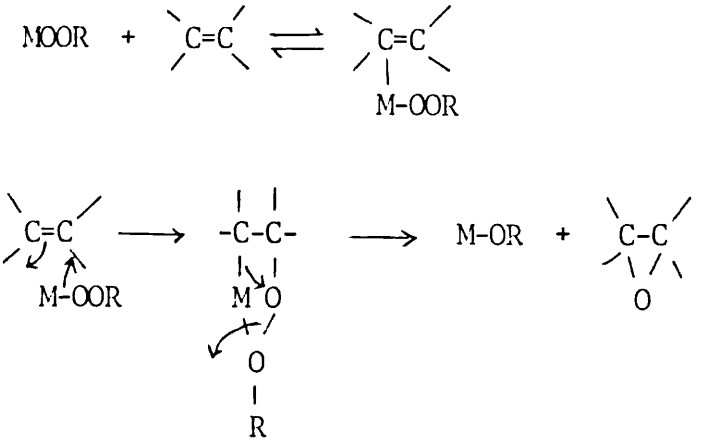

II 1.2.2 Competing reactions

The autoretardation of epoxidation that arises from complexing between the catalyst and the alcohol has been observed by many workers,[8,46,49-51,53,53,61] particularly for vanadium catalysed reactions. The catalyst/alcohol complex hinders both the formation of a catalyst/hydroperoxide complex and its subsequent reaction with the olefin.

The extent of autoretardation can be related to the equilibrium constants for the formation of catalyst/hydroperoxide and catalyst/alcohol complexes. Sheldon and Van Doorn[49] found that the autoretardation by tert-butanol increases in the order W<Mo<Ti<V for a series of complexes.

Sheng and Zajacek[8] found that the addition of large amounts of tert-butanol to molybdenum complex catalysed epoxidations has also resulted in a decrease of reaction. The effects of deliberate addition of tert-butanol on the rates of complexes of Mo, Ti and W catalysed reaction were compared, so as to determine the extent of

retardation in these reactions. The addition of alcohol had only slight but significant effect upon molybdenum and tungsten compounds whereas with both homogeneous and heterogeneous titanium compounds, reactions showed a marked decrease in reaction rate.

These results explain why kinetic investigations using molybdenum and tungsten complexes were first thought to be governed by simple first order kinetics (where alcohol interference is minimal), whereas for vanadium complexes, the rate of reaction was found to decrease throughout the epoxidation.

In cases where an alcohol has been used as a solvent for epoxidation reactions, severe retardation has been observed[8,68].

For oxidation of propene with a number of molybdenum complexes, alcohols have been placed in the following order according to their inhibitory power[69]:-

MeOH>EtOH>Pr^nOH>n-octanol>phenylethanol.

Another factor which can affect epoxide yields is the competing metal catalysed homolytic decomposition of organic hydroperoxides[48,49]. Many transition metal complexes such as those of iron, managanese, cobalt and copper, are known to initiate the decomposition of hydroperoxides via one-electron redox reactions Eqn. II 1.2.2(1) and Eqn II 1.2.2(2).

Reduction:

$$RO_2H + M^{(n-1)+} \longrightarrow RO\cdot + M^{n+} + HO^- \quad \text{Eqn. II 1.2.2(1)}$$

Oxidation:

$$RO_2H + M^{n+} \longrightarrow RO_2\cdot + M^{(n-1)} + H^+ \quad \text{Eqn. II 1.2.2(2)}$$

Metal complexes of molybdenum, tungsten, vanadium, chromium and titanium have been shown to initiate homolytic decomposition of organic hydroperoxides to a certain extent, in the absence of olefins or other suitable nucleophilic sites.[48,49]

Sheldon and Van Doorn,[49] in order to accentuate the differences in epoxide selectivity between various metal catalysts, purposely chose conditions which were not conducive to good epoxide yields and selectivity. The epoxidation of cyclohexene with a number of different catalysts yielded two major products, epoxycyclohexene and 3-tert-butylperoxy-1-cyclohexene together with trace amounts of 2-cyclohexene-1-ol and 2-cyclohexene-1-one.

The alkoxy and alkylperoxy radicals formed in Eqn. I.1.2.2(1) and Eqn. II.1.2.2(2) may abstract hydrogen from the olefin and subsequent reactions of radicals formed from the olefins can result in oxidation products such as alcohols and ketones.

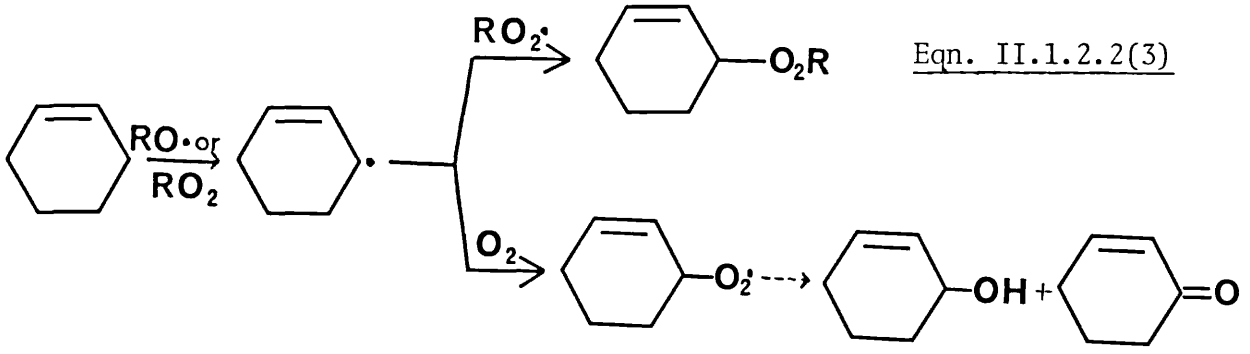

Eqn. II.1.2.2(3)

Eqn. II.1.2.2(4)

The addition of alkoxy and alkylperoxy radicals to the double bond may be at least partly responsible for the formation of epoxides, particularly in reactions using less reactive catalysts for the heterolytic reaction.

e.g.

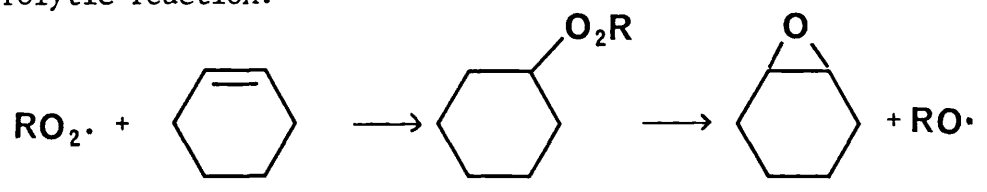

Eqn. II.1.2.2(5)

Brill and Indictor[42] obtained epoxide yields of 5 - 30% for reactions of 1-octene and cyclohexene with tert-butyl hydroperoxide in the absence of a catalyst at 100°C - a thermal homolytic decomposition of the hydroperoxide most probably occurred. Koelewyn prepared 1-phenyl-1,2-epoxyethane and 3,4-epoxy-1-butene using di-tert-butyl peroxide as a radical initiator.[70]

In solvents which possess reactive C-H bonds, the alkoxy and alkylperoxy radicals will abstract hydrogens from the solvent. The resulting solvent radicals (S·) may form oxidation products.

e.g.

$RO\cdot + SH \longrightarrow ROH + S\cdot$ Eqn. II.1.2.2.(6)

$RO_2\cdot + SH \longrightarrow RO_2H + S\cdot$ Eqn. II.1.2.2.(7)

$S\cdot + RO_2\cdot \longrightarrow SO_2R$ Eqn. II.1.2.2.(8)

$S\cdot + O_2 \longrightarrow SO_2\cdot \dashrightarrow$ ketones, alcohols etc. Eqn. II.1.2.2.(9)

In the absence of any abstractable hydrogens, normal radical induced chain decomposition of the organic hydroperoxide will take place.

i.e.

$RO\cdot + RO_2H \longrightarrow ROH + RO_2\cdot$ Eqn. II.1.2.2(10)

$RO_2\cdot \longrightarrow RO\cdot + \frac{1}{2}O_2$ Eqn. II.1.2.2(11)

The performance of transition metal catalysts and organic hydroperoxides in epoxidation is therefore dependent upon the relative rates of heterolytic and homolytic decomposition of the hydroperoxide and the susceptibility of the catalyst to complex with the co-product alcohol.

II.1.2.3 Comparison of Catalytic activity

Olefinic epoxidation by organic hydroperoxide has been claimed to have been carried out by several metals - some of which include chromium, molybdenum, nickel, niobium, rhenium, selenium, tantalium, titanium, tungsten, vanadium and zirconium.

With the exception of complexes of cobalt, manganese, copper and iron, comparative studies[8,47,49,71-75] have shown that most of these metals give a higher yield of epoxide than equivalent uncatalysed reactions, with molybdenum, vanadium and tungsten giving consistently high yields of epoxides. Molybdenum compounds seem to be catalysts with the best yield, selectivity and speed of reaction. The most common molybdenum compounds used include molybdenum hexacarbonyl and molybdenyl acetylacetonate. Tungsten compounds when used with organic hydroperoxides do not compare favourably with molybdenum, but in combination with hydrogen peroxide,[76,77] give the best yields.

Hiatt[78] reviewed an extensive list of catalysts without giving too much indication as to the reasons for the varying success of different metal compounds. Since then, several workers have investigated the activities of a number of catalysts and have drawn the following conclusions:-[46,49,52]

(a) The metals (e.g. Mo(VI), W(VI), V(V)) are small size, highly charged and have low-lying, although unoccupied, d-orbitals.

(b) The metal does not participate significantly in any one-electron redox reaction under strongly oxidising conditions.

(c) The metal forms complexes which are substitution labile.

Sheldon and Van Doorn[49] in their study of metal complexes have related their catalytic behaviour to the Lewis acidity and the redox potential of the central metal atom. The Lewis acidity of transition metal oxides decreases in the order, $CrO_3 > MoO_3 > WO_3 > V_2O_5 > TiO_2$[79]. Hence it becomes apparent why Mo(VI) compounds are such effective epoxidation catalysts. By the same argument, Cr(VI) compounds would be expected to be good epoxidation catalysts. This is not to be the case presumably because Cr(VI) compounds are strong oxidants and can cause ready decomposition of the hydroperoxide via radical pathways. The general ease with which transition metal ions or complexes catalyse the homolytic decomposition of organic hydroperoxides can be related to their redox potentials. Hydroperoxides are strong oxidants but weak reducing agents and hence redox reactions, indicated in Eqn. II.1.2.2(1) and Eqn. II.1.2.2(2) are easily accomplished with strong oxidants such as Co(III), Ce(IV) and Pb(IV)[80].

With the exception of vanadium, all successful epoxidation catalysts are weak oxidants in their highest oxidation states. This explains why vanadium catalysts tend to be less effective in olefin epoxidation reactions than molybdenum and tungsten. The low catalytic activity of other transition metal catalysts such as Th(IV) and Zr(IV) which are weak oxidants, is due to the fact that they are weak Lewis acids.

Sheldon and Van Doorn[49] also pointed out that the activity of the catalyst may be affected by the size of the metal ion which may be important in determining whether or not the geometry of the transition state for oxygen transfer is favourable. They also suggested that some, if not all, of the original ligands are removed in the early stages of

reaction to give effectively the same active catalyst for any particular metal[33,48,49].

Since the epoxidation step involves no change in the oxidation state of the metal, there is no reason why catalytic activity should be restricted to transition metal compounds. Non-transition metal compounds which are Lewis acids should also be capable of catalysing epoxidations. The Lewis acidity of a series of non-metallic oxides decreases in the order, $SeO_2 > B_2O_3 > SnO_2$[79]. SeO_2 is as acidic as MoO_3. Sheldon and Van Doorn[49] have found that SeO_2 catalyses the epoxidation of cyclohexene and 1-octene, but is much less effective than molybdenum, tungsten and vanadium compounds. This might be the case because SeO_2 is a relatively strong oxidant and will cause decomposition of the hydroperoxide via radical pathways.

Boron compounds have been used to catalyse epoxidations[56,81] but are less effective than transition metal complexes. Sheldon and Van Doorn[56] studied the catalytic effect of a number of boron compounds on epoxidation and concluded that the epoxidation is dramatically influenced by their structure. Electron-attracting substituents, by increasing the electrophilicity of the boron atom, enhance the catalytic activity. Even so, the most effective boron compound was approximately a thousand times less active than conventional molybdenum compounds. The boron catalyst has only a limited lifetime due to the deactivation via alcoholysis[82].

II.1.2.4 Reactivities of different olefins

Hiatt[78] reported a list of olefins that have been epoxidised. Since then many more have been reported including olefinic compounds with functional groups. Patent claims are extensive and generally cover all olefinic substances including high molecular weight polymers.

The effect of structure[48] on olefin activity parallels that for epoxidation by organic peroxyacids[37,83]. Increasing the number of alkyl substituents bonded to the carbon atom of the double bond results in enhanced rates of reaction due to increased olefin nucleophilicity.

Howe and Hiatt[50] studied the effect of some heteroatom substituents on the epoxidation of a series of ring substituted styrenes. A meta-nitro group decreased reaction rate and a para-methyl group increased it. The effect of halogen substituents was minimal.

Sheng et al[61,63] studied the epoxidation of a series of olefins, conjugated and non-conjugated dienes and allylic compounds. The reactivities of the dienes were found to be similar to mono-olefins although the reactivity of conjugated double bonds appears to be less than compounds with isolated double bonds. In the epoxidation of allylic compounds, groups capable of withdrawing electrons from the double bond tended to reduce reactivity towards epoxidation.

II.1.2.5 Influence of the structure of organic hydroperoxide

Several organic hydroperoxides have been claimed to be suitable for epoxidation[84,85]. Tert-Butyl hydroperoxide has been extensively used in mechanistic studies. Several comparative studies with various organic hydroperoxides have been carried out[8,55,78,86]. In a number of cases, these studies have used relatively reactive olefins e.g. cyclohexene and 1-octene.

Sheldon et al[55] have carried out a comparative study of a number of organic hydroperoxides using the relatively unreactive olefin, allyl chloride. Low selectivities were observed with alkyl-aromatic hydroperoxides due to their facile heterolytic decomposition, under reaction conditions, e.g.

$$PhC(CH_3)_2OOH \longrightarrow PhOH + (CH_3)_2C{=}O \qquad \text{Eqn. II.1.2.5(1)}$$

Competition from this reaction is diminished when such hydroperoxides possess electron-attracting substituents. A further complication in epoxidations using alkyl-aromatic hydroperoxides is the metal-catalysed dehydration of the co-product alcohol.

The purity of organic hydroperoxides does not appear to be critical in epoxidation reactions. In many cases, commercial grade tert-butyl hydroperoxide (70%) has been used which contains both di-tert-butyl peroxide and water. As di-tert-butyl hydroperoxide has been used as a radical initiator[70] in non-catalysed epoxidation reactions, it seems that the presence of this dialkyl peroxide could initiate radical formation leading to mixed products. In addition, the presence of water suggests that more diol than epoxide would be produced in these reactions.

Khcheyan et al[87] studied the effect of moisture content on the yield of propylene epoxide during the epoxidation of propylene using tert-butyl hydroperoxide. They concluded that at hydroperoxide concentrations of 30-60%, a moisture content of 2-3% was allowable.

As organic hydroperoxides may be prepared by the autoxidation of suitable hydrocarbons[88], a number of workers have used the raw reaction product from this oxidation directly in olefin epoxidation[89]. Seree de Roch et al[90] suggested that the use of raw oxidation products containing the organic hydroperoxide has a beneficial effect upon epoxidation.

Steric effects may play a role in the effectiveness of organic hydroperoxides. Allison et al[73] have reported that 4-methyl-2-butene-4-yl and 4-methyl-3-butene-2-yl hydroperoxides react at considerably different rates.

II.1.2.6 Stereospecificity and Stereoselectivity

The reactions of organic peroxyacids with olefins are stereospecifically cis. The same effects are observed in metal catalysed epoxidation using organic hydroperoxides.

As discussed in Section II.1.2.4, the rate of epoxidation is enhanced by increasing the number of alkyl substituents bonded to the carbon atom of the double bond. Where there is more than one double bond in the molecule, epoxidation takes place selectively at the double bond to which the greater number of alkyl groups is attached. Sheng and Zajacek[63] observed this substituent effect with 4-vinyl cyclohexene where only the ring olefin is epoxidised, and with 1,4-hexadiene the internal epoxide is the dominant product.

Steric hindrance may affect the ease with which different olefins are able to undergo epoxidation. Obekhov et al[91] studied the epoxidation of a number of butenes and have arranged them in the following series according to their reactivities:-

cis-but-2-ene	trans-but-2-ene	but-1-ene
36.6	14.2	1.0

Yur'ev et al[92] have reported that p-menth-1-ene (I) leads to the stereoselective epoxidation of the double bond to produce the diastereoisomer (II) where the epoxide ring is in the trans-position with respect to the isopropyl group. Epoxidation of (I) with organic peroxyacids, produce a mixture of the cis- and trans-diastereoisomers (II) and (III) (Fig. II.1.2.6(1)).

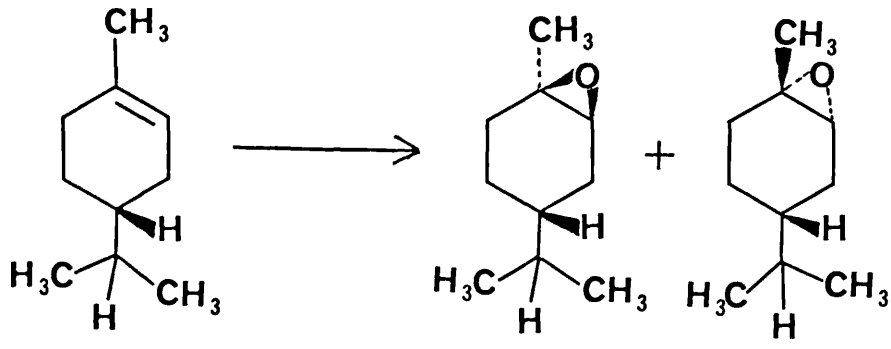

(I) (II) (III)

Fig. II.1.2.6(1)

In recent years, the epoxidation of allylic alcohols with organic hydroperoxides has attracted considerable interest.

Itoh et al[93] studied the epoxidation of a series of 'small to medium' ring cyclic allylic alcohols by both epoxidation methods. In contrast to the peroxyacid epoxidation, these workers found that the catalyst/hydroperoxide epoxidations selectively produced cis-epoxides with respect to the hydroxyl group.

Sharpless et al[94] studied the epoxidation of acyclic allylic alcohols. They observed that these reactions were highly stereospecific in comparison with isomeric mixtures obtained by peroxyacid epoxidations.

In the case where more than one double bond is present in an olefinic alcohol, epoxidation has been shown to take place exclusively at the allylic double bond.[94-96]

II.1.3 Liquid phase epoxidation of olefins using molecular oxygen

Many liquid phase oxidations, known as autoxidations proceed under relatively mild conditions of temperature and oxygen pressure.[97]

The oxidation of hydrocarbons, by molecular oxygen has been subject of many investigations.[98] The industrial processes for the production of oxygenated compounds include the preparation of ethylene and propylene epoxides.[99]

II.1.3.1 Homolytic Reactions

Autoxidations proceed via a free radical chain mechanism described by Scheme V.

Scheme V

Initiation

$$In_2 \longrightarrow 2In\cdot \qquad \text{Eqn. II.1.3.1(1)}$$

$$In\cdot + RH \longrightarrow InH + R\cdot \qquad \text{Eqn. II.1.3.1(2)}$$

Propagation

$$R\cdot + O_2 \longrightarrow RO_2\cdot \qquad \text{Eqn. II.1.3.1(3)}$$

$$RO_2\cdot + RH \longrightarrow RO_2H + R\cdot \qquad \text{Eqn. II.1.3.1(4)}$$

Termination

$$R\cdot + RO_2\cdot \longrightarrow RO_2R \qquad \text{Eqn. II.1.3.1(5)}$$

$$2RO_2\cdot \longrightarrow RO_4R \longrightarrow \text{non radical products} + O_2 \qquad \text{Eqn. II.1.3.1(6}$$

Initiation may be accomplished by the addition of initiators that yield free radicals on thermal decomposition. In the absence of added initiators, the hydrogen may be abstracted by radicals (In·) formed by the homolysis of organic hydroperoxides which are present in small quantities in most organic liquids.

The addition of the alkyl radical (R·) to oxygen indicated in Eqn. II.1.3.1(3) is extremely rapid and the rate of autoxidation is independent of oxygen even at low concentrations. The rate-determining step is the hydrogen transfer from substrate to the alkylperoxy radical described in Eqn. II.1.3.1(4).

Under most operating conditions, the termination step occurs almost exclusively by reaction of two alkyl peroxy radicals to form an unstable tetroxide Eqn. II.1.3.1(6).[100,101] The modes of decomposition of tetroxides are dependent on the structure of the alkyl group.[100-104]

Much of the present knowledge of autoxidation mechanisms has resulted from studies of the reactions of alkylperoxy radicals and the parent hydroperoxides, independent of autoxidation. The various modes of reaction or organic peroxides are now well characterised.[37,105]

II.1.3.1(1) Autoxidation of Olefins

In the autoxidation of olefins, chain propagation can occur via the usual abstraction mechanism to produce the allylic radical Eqn. II.1.3.1(7) or via the addition of the alkylperoxy radical to the double bond Eqn. II.1.3.1(8).

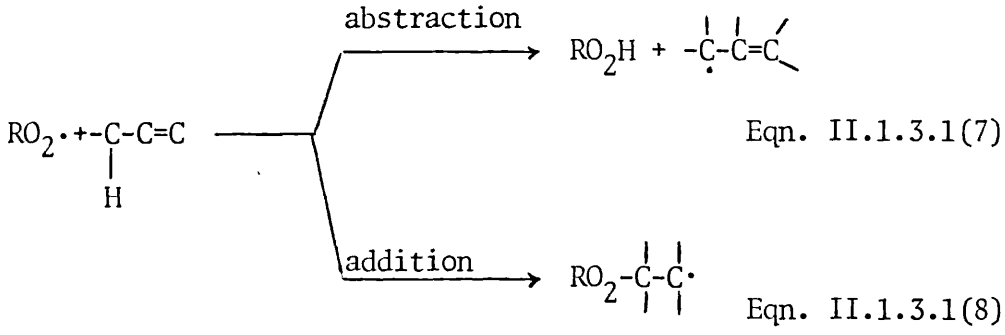

Eqn. II.1.3.1(7)

Eqn. II.1.3.1(8)

Addition can be followed by the unimolecular decomposition of the β-alkylperoxyalkyl radical giving an epoxide and an alkoxy radical, Eqn. II.1.3.1(9),

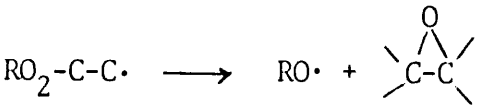

Eqn. II.1.3.1(9)

or by the reaction with oxygen, giving polyperoxides, Eqn. II.1.3.1(10)

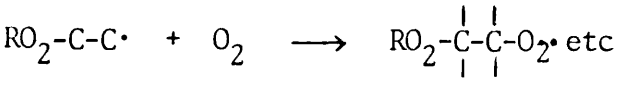

Eqn. II.1.3.1(10)

Much of the present knowledge of the addition mechanism for olefin autoxidation resulted from the studies of Mayo et al[106-109] and Brill et al.[41,110] The ratio of addition to abstraction is strongly dependent on the structure of the olefin.[106,111] Generally, epoxide selectivity is low in this type of reaction.

II.1.3.2 Heterolytic Reactions

The homolytic type of oxidation has been known and studied for sometime, however, the heterolytic oxidation of hydrocarbons is a more recent innovation. Such reactions involve the use of transition metal complexes, some of which are capable of catalysing homolytic reactions.

II.1.3.2(1) Epoxidation of Olefins

The direct reaction of olefins, particularly propylene, with molecular oxygen in the presence of catalysts such as molybdenum, tungsten and vanadium proceed via the initial formation of an allylic hydroperoxide followed by epoxidation of the olefin via the mechanism discussed in Section II.1.2.1.

Several studies have been reported in which the olefins cyclohexene,[71,73,99,112,113] 2- and 4-methyl pentenes[73] and propene[114-124] have been treated with oxygen in the presence of complexes of molybdenum, vanadium and tungsten. At low oxygen pressures, good epoxide selectivity with high yields are observed.

Gould and Rado[99] carried out the autoxidation of cyclohexene using oxides and soluble acetylacetonates of copper, chromium, manganese, iron, molybdenum and vanadium. With the exception of molybdenum and vanadium compounds, none of the catalysts gave more than 1-2% epoxide. Chromium and iron compounds produced high yields of cyclohexenone whilst the remainder tended to yield equal amounts of cyclohexenol and cyclohexenone.

Fusi et al[125] investigated the epoxidation of cyclohexene with oxygen using catalyst systems that comprise of two metal complexes. Complex (A) (generally a complex of iridium, rhodium, osmium or palladium) was capable of catalysing the radical autoxidation of cyclohexene to form its corresponding allylic hydroperoxide. Complex (B) (complex of molybdenum or vanadium) was capable of catalysing the selective heterolytic epoxidation of the olefin by the hydroperoxide formed in situ. It is believed that, in these catalytic systems, the two complexes act separately to give rise to a stepwise mechanism where there are two clearly defined processes, each corresponding to one well defined catalyst.

Stable metal-oxygen complexes of group (VIII) metals have been used and it has been suggested that these complexes may catalyse autoxidations via the direct transfer of oxygen from the metal-oxygen complex to the substrate. Such catalysts are generally phosphine containing complexes

of rhodium, iridium, osmium, platinum and palladium. These complexes first prepared by Vaska[126,127] are capable of adding oxygen reversible to the coordination sphere of the metal.

The role of these low valent phosphine transition metal complexes in olefin epoxidation has been interpreted in a number of ways. Several workers[128-131] favour a direct oxygen transfer mechanism, although this has been disputed. Van Gaal et al[132] reported that the iridium/ethylene complex IV indicated in Eqn. II.1.3.2(1) reacts with molecular oxygen to give a complex (V) which contains both coordinated oxygen and olefin and may be considered as a model complex for an intermediate in the oxidation of olefins.

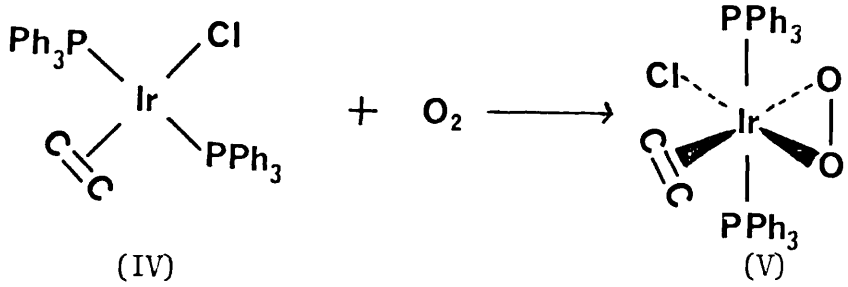

(IV) (V)

Eqn. II.1.3.2(1)

Takao et al[128,129] have investigated the oxidation of styrene in the presence of iridium (I) and rhodium (I) complexes and have suggested that the catalytic activity is due to coordination of oxygen at the metal centre which causes an increased oxygen-oxygen bond length and enhanced reactivity with the olefin.

Fusi et al[133] reported that the oxidation of cyclohexene, using phosphine-containing complexes of rhodium, iridium and platinum proceeds via a radical reaction involving the homolytic decomposition of the intermediate hydroperoxide.

Several reports have observed unusually high yields of epoxides which could not be accounted for by radical reactions. Lyons and Turner[134,135] suggested that the results obtained in such investigations are consistent with a mechanistic pathway in which the initial step is the autoxidation of the olefin to form an allylic hydroperoxide and a subsequent heterolytic epoxidation step catalysed by the metal complexes. This is comparable with the mechanism observed for complexes of molybdenum, vanadium and tungsten although it is not clear why certain low valent transition metal phosphine complexes behave under certain circumstances in this manner.

CHAPTER II SECTION 2

II.2. Results and Discussion

II.2.1 List of catalysts used for epoxidation.

For brevity, all catalysts used for epoxidation in this section will be referred to by the numerals listed below:

I. Molybdenum hexacarbonyl.

II. Molybdenyl acetylacetonate.

III. Sodium molybdate (VI).

IV. Sodium molybdate (VI) and 18-Crown-6.

V. Molybdenum (VI) oxide.

VI. cis-Bis(S(+)propane-1,2-diolato)dioxomolybdenum (VI).

VII. cis-Bis(propane-1,2-diolato)dioxomolybdenum (VI).

VIII. {cis-Bis(D(-)butane-2,3-diolato)dioxomolybdenum (VI)-D(-) Butane 2,3diol} (1:1).

IX. {cis-Bis(butane-2,3-diolato)dioxomolybdenum (VI)-Butane 2,3 diol} (1:2).

X. cis-Bis(butane-1,3-diolato)dioxomolybdenum (VI).

XI. cis-Bis(phenyl ethane-1,2-diolato)dioxomolybdenum (VI).

XII. cis-Bis(S(+)-2-amino-1-phenyl propane-1,3-diolato)dioxomolybdenum (VI).

XIII. cis-Bis(R(-)-2-amino-1-butanato)dioxomolybdenum (VI).

XIV. μ-Oxo-Bis(oxo[2,3-dimethyl-2,3-D(-)butane-2,3-diolato(1-)] [2,3-dimethyl-2,3-D(-)butane-2,3-diolato(2-)])molybdenum (VI) .

XV. μ-oxo-Bis(oxo[2,3-dimethyl-2,3-butane-2,3-diolato(1-)] [2,3-dimethyl-2,3-butane-2,3-diolato(2-)])molybdenum (VI) .

XVI. μ-Oxo-Bis(oxo[butane-1,2-diolato(1-)] [butane-1,2-diolato(2-)]) molybdenum (VI) .

XVII. Potassium tricarbonyl-L-histidinato molybdenum (VI).

XVIII. Potassium tricarbonyl-L-histidinato molybdenum I(VI) and 18-Crown-6.

XIX. Potassium histidinatotrioxomolybdate (VI)-Water (1:1).

XX. Potassium histidinatotrioxomolybdate (VI)-Water (1:1) and 18-Crown-6.

II.2.2 Catalytic Activity of Various Compounds on Formation of Decene Oxide[a].

CATALYST	AMOUNT OF CATALYST/g	CONVERSION OF EPOXIDE/%[b]	YIELD OF EPOXIDE[c]
I	0.0660	97	7.4g (95%)
II	0.0815	90	6.8g (87%)
III	0.0515	28	1.9g (24%)
IV	0.0515	39	3.0g (38%)
V	0.0360	65	5.1g (65%)
VI	0.0695	94	7.2g (93%)
VII	0.0695	93	6.8g (87%)
VIII	0.0991	89	6.8g (87%)
IX	0.1216	87	6.7g (86%)
X	0.0765	83	6.2g (80%)
XI	0.1006	96	7.2g (93%)
XII	0.1151	71	5.4g (69%)
XIII	0.0755	75	5.6g (72%)
XIV	0.1482	94	7.0g (90%)
XV	0.1482	94	7.0g (90%)
XVI	0.1482	92	6.9g (89%)
XVII	0.0933	9	0.6g (8%)
XVIII	0.0933	33	2.4g (31%)
XIX	0.0843	7	0.5g (6%)
XX	0.0843	33	2.3g (30%)

a See Section II.3.2f for experimental details.
b Conversion obtained by glc using tridecane as an internal standard.
c Isolated yields obtained by vacuum distillation.

Table II.2.2(1)

II.2.3 Catalytic Activity of Various Compounds on Formation of Dodecene Oxide[a].

CATALYST	AMOUNT OF CATALYST/g	CONVERSION OF EPOXIDE/%[b]	YIELD OF EPOXIDE[c]
I	0.0660	89	8.1g (88%)
II	0.0815	86	7.7g (84%)
III	0.0515	26	2.1g (23%)
IV	0.0515	35	3.1g (34%)
V	0.0360	64	5.8g (63%)
VI	0.0695	90	8.1g (88%)
VII	0.0695	89	8.0g (87%)
VIII	0.0991	83	7.4g (80%)
IX	0.1216	81	7.4g (80%)
X	0.0765	78	7.1g (77%)
XI	0.1006	89	7.9g (86%)
XII	0.1151	69	6.2g (67%)
XIII	0.0755	69	6.3g (68%)
XIV	0.1482	89	8.0g (87%)
XV	0.1482	88	8.0g (87%)
XVI	0.1482	85	7.7g (84%)
XVII	0.0933	8	0.6g (6%)
XVIII	0.0933	29	2.3g (25%)
XIX	0.0843	5	0.4g (4%)
XX	0.0843	29	2.6g (28%)

a See Section II.3.2f for experimental details.

b Conversion obtained by using tetradecane as an internal standard.

c Isolated yields obtained by vacuum distillation

Table II.2.3(1)

II.2.4(1) Molybdenum catalysed epoxidation of 1-Decene and 1-Dodecene.

The kinetics of the epoxidation of 1-decene and 1-dodecene with tert-butyl hydroperoxide at 70^{o} in the presence of various molybdenum catalysts were studied. All the reactions were followed by measuring the rate of disappearance of the hydroperoxide by iodometric titration. The reaction rate is first order in tert-butyl hydroperoxide, olefin and molybdenum catalyst Eqn. II.2.4(1).

$$\text{Rate} = \frac{[\text{d epoxide}]}{dt} = k_3[\text{TBHP}][\text{Olefin}][\text{Catalyst}] \qquad \text{Eqn. II.2.4(1)}$$

As long as the catalyst remains unchanged during the reaction, Eqn. II.2.4(1) reduces to:

$$\text{Rate} = k_2[\text{Olefin}][\text{TBHP}] \qquad \text{Eqn. II.2.4(2)}$$

which for a high olefin/hydroperoxide ratio, reduces further to the pseudo-first order rate equation.

$$\text{Rate} = k_1[\text{TBHP}] \qquad \text{Eqn. II.2.4(3)}$$

where $k_1 = k_2[\text{Olefin}] = k_3[\text{Catalyst}][\text{Olefin}]$

The rates of epoxidation for 1-decene and 1-dodecene using different molybdenum catalysts, summarised on Tables II.2.4(1) and II.2.4(2) were compatible for equimolar concentrations of the reactants (Fig. II.2.4(1)). When a ten-fold excess (see Fig. II.2.4(2)) of substrate over tert-butyl hydroperoxide was used, the epoxide

selectivity was high, demonstrating that hydroperoxide decomposition was insignificant (this also being verified by the concentration of tert-butanol being ∿ 100 times less than that of the epoxide on the glc trace). From Tables II.2.4(1) and II.2.4(2), the overall rate constants for similar types of catalysts give the same order of magnitude.

Other workers[8,45,46,52,63,84] concluded that the rates and selectivities of metal catalysed epoxidation with hydroperoxides increase as the olefin becomes more substituted with alkyl groups, demonstrating that the active epoxidising agent is an electrophilic species. The comparison of relative rates of epoxidation for 1-decene and 1-dodecene for comparative experiments using various molybdenum complexes show that the rate of epoxidation for 1-decene is faster - this probably being so due to steric factors.

Overall rate constant k_3 for the epoxidation of 1-decene and 1-dodecene using various molybdenum catalysts.

CATALYST	$k_3 \times 10^2 / s^{-1} mol^{-2} dm^6$ 1-DECENE	$k_3 \times 10^2 / s^{-1} mol^{-2} dm^6$ 1-DODECENE
I	0.78	0.73
II	0.75	0.73
III	0.48	0.39
IV	0.49	0.41
V	0.48	0.42
VI	0.82	0.75
VII	0.82	0.74
VIII	0.79	0.73
IX	0.78	0.73
X	0.80	0.76
XI	0.85	0.77
XII	0.73	0.71
XIII	0.73	0.71
XIV	0.77	0.75
XV	0.77	0.75
XVI	0.76	0.74
XVII	0.40	0.35
XVIII	0.43	0.37
XIX	0.40	0.37
XX	0.43	0.39

[OLEFIN] = 0.1 mol dm^{-3}
[TBHP] = 0.1 mol dm^{-3}
[CATALYST] = 10^{-4} mol dm^{-3}

Table II.2.4(1)

Observed rate constants $k_1 x 10^{-3}/s^{-1}$ for 1-decene and 1-dodecene using various Molybdenum catalysts[a].

CATALYST	$k_1 x 10^{-3}/s^{-1}$ for 1-decene	$k_1 x 10^{-3}/s^{-1}$ for 1-dodecene
I	1.58	1.57
II	1.52	1.45
III	0.96	0.73
IV	0.96	0.76
V	0.92	0.80
VI	1.70	1.58
VII	1.64	1.48
VIII	1.59	1.46
IX	1.63	1.47
X	1.62	1.50
XI	1.63	1.56
XII	1.49	1.41
XIII	1.51	1.44
XIV	1.56	1.50
XV	1.55	1.52
XVI	1.50	1.49
XVII	0.82	0.66
XVIII	0.86	0.70
XIX	0.81	0.69
XX	0.85	0.73

[a] Calculated first order rate constants for hydroperoxide disappearance. For overall rate constant k_3, divide by the product of the concentration of olefin times catalyst.

$[TBHP] = 0.01 \text{ mol dm}^{-3}$ $[OLEFIN] = 0.1 \text{ mol dm}^{-3}$

$[CATALYST] = 2x10^{-4} \text{ mol dm}^{-3}$

Table II.2.4(2)

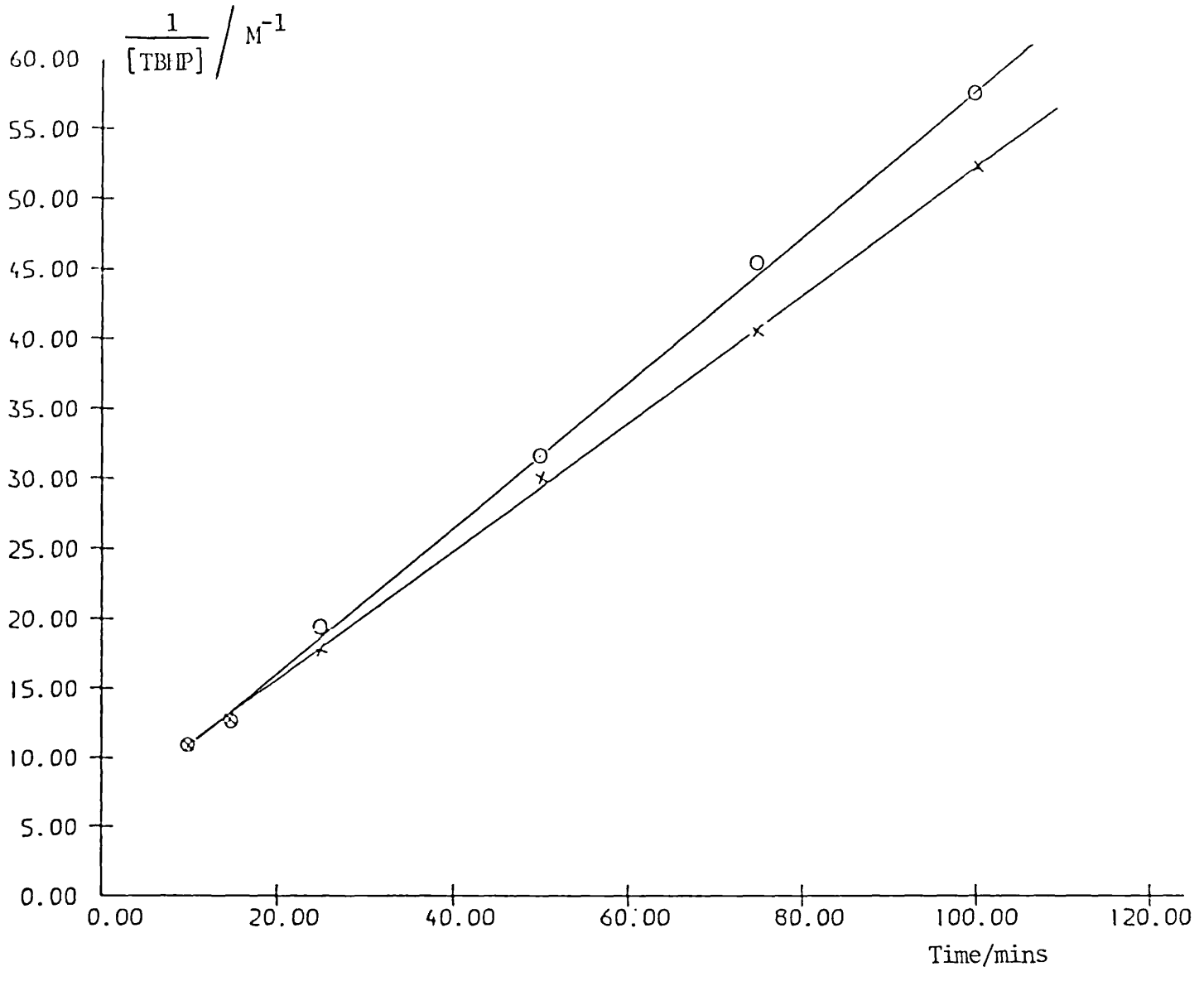

Fig. II.2.4(1) Reaction of tert-butyl hydroperoxide with 1-decene (O) and 1-dodecene (X) in 1,2 dichloroethane at 70° in the presence of Catalyst (XI) (TBHP 0.1M; olefin 0.1M; Catalyst 0.0001M).

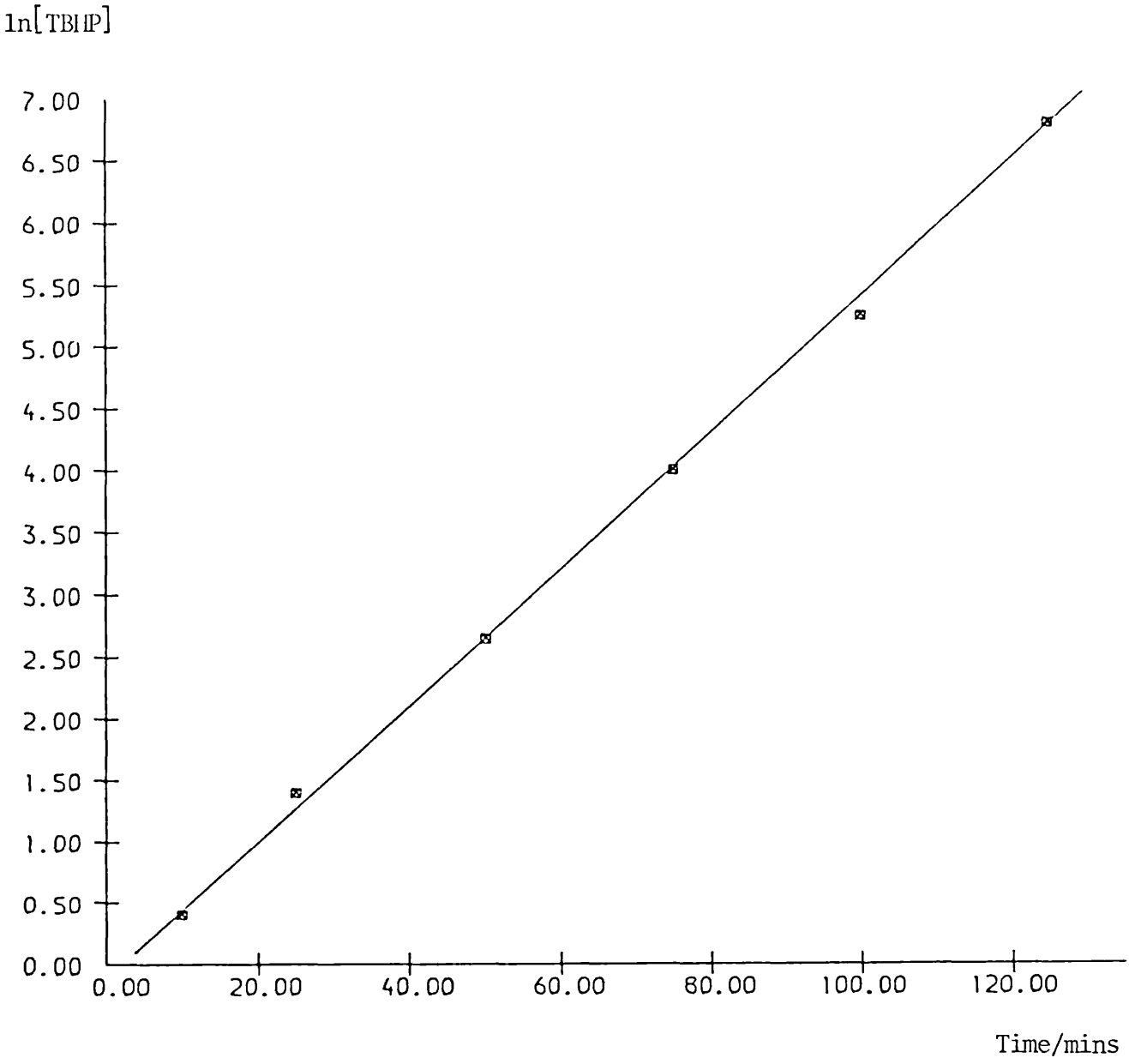

Fig. II.2.4(2) Reaction of tert-butyl hydroperoxide with 1-decene in 1,2 dichloroethane at 70^{o} in the presence of Catalyst XI (TBHP 0.01M; 1-decene 0.1M Catalyst 0.0001M).

II.2.4.2 Dependence on catalyst concentration.

Parallel experiments with the same initial concentrations of olefin and tert-butyl hydroperoxide, but differing concentrations of molybdenum catalyst indicate a first order dependence on molybdenum concentrations, see Tables II.2.4(4) and II.2.4(4).

For Catalyst XI, using 1-decene as substrate the values given in Table II.2.4(3) confirm this first order dependence approximately.

CATALYST	Observed Rate Const.$x10^{-2}/M^{-1}s^{-1}$
$4x10^{-4}$	3.34
$2x10^{-4}$	1.64
1.10^{-4}	0.89

$$\frac{4x10^{-4}}{2x10^{-4}} = \frac{3.34}{1.64} = 2.03$$

$$\frac{2x10^{-4}}{1x10^{-4}} = \frac{1.64}{0.89} = 1.84$$

$$\frac{4x10^{-4}}{1.10^{-4}} = \frac{3.34}{0.89} = 3.75$$

Table II.2.4(3)

For all the other catalysts, the rate constants are summarised in Tables II.2.4(4) and II.2.4(5).

Observed rate constants, $k_2 x 10^{-2}/M^{-1}s^{-1}$ obtained for 1-decene using different concentrations of Catalyst[a].

CATALYST	CONCENTRATION OF CATALYST/mol dm^{-3}		
	$1x10^{-4}$	$2x10^{-4}$	$4x10^{-4}$
I	0.78	1.54	3.16
II	0.72	1.50	3.12
III	0.52	0.95	1.79
IV	0.52	0.97	1.85
V	0.49	0.96	1.90
VI	0.81	1.66	3.27
VII	0.81	1.65	3.26
VIII	0.78	1.60	3.19
IX	0.77	1.56	3.16
X	0.79	1.61	3.24
XI	0.89	1.64	3.34
XII	0.70	1.50	2.97
XIII	0.71	1.48	2.99
XIV	0.73	1.56	3.15
XV	0.77	1.53	3.15
XVI	0.76	1.50	3.12
XVII	0.39	0.80	1.62
XVIII	0.43	0.85	1.68
XIX	0.40	0.79	1.64
XX	0.44	0.84	1.71

[a] Calculated second order rate constants for hydroperoxide disappearance. For overall rate constant k_3, divide k_2 by the concentration of catalyst.

[TBHP] = 0.1 mol dm^{-3} [DECENE] = 0.1 mol dm^{-3}

Table II.2.4(4)

Observed rate constants, $k_2 x10^{-2}/M^{-1}s^{-1}$ obtained for 1-dodecene using different concentrations of Catalyst[a].

CATALYST	CONCENTRATION OF CATALYST/mol dm^{-3}		
	$1x10^{-4}$	$2x10^{-4}$	$4x10^{-4}$
I	0.72	1.49	2.95
II	0.73	1.47	2.94
III	0.40	0.77	1.59
IV	0.41	0.79	1.64
V	0.43	0.83	1.69
VI	0.74	1.50	2.99
VII	0.73	1.47	2.98
VIII	0.72	1.45	2.92
IX	0.73	1.45	2.90
X	0.76	1.54	3.05
XI	0.77	1.57	3.07
XII	0.71	1.44	2.85
XIII	0.71	1.43	2.86
XIV	0.75	1.49	2.96
XV	0.76	1.50	2.95
XVI	0.73	1.51	2.95
XVII	0.36	0.69	1.40
XVIII	0.40	0.72	1.44
XIX	0.38	0.75	1.44
XX	0.42	0.77	1.46

[a] Calculated second order rate constants for hydroperoxide disappearance. For overall rate constant k_3, divide k_2 by the concentration of catalyst.

[TBHP] = 0.1 mol dm^{-3} [DECENE] = 0.1 mol dm^{-3}

Table II.2.4(5)

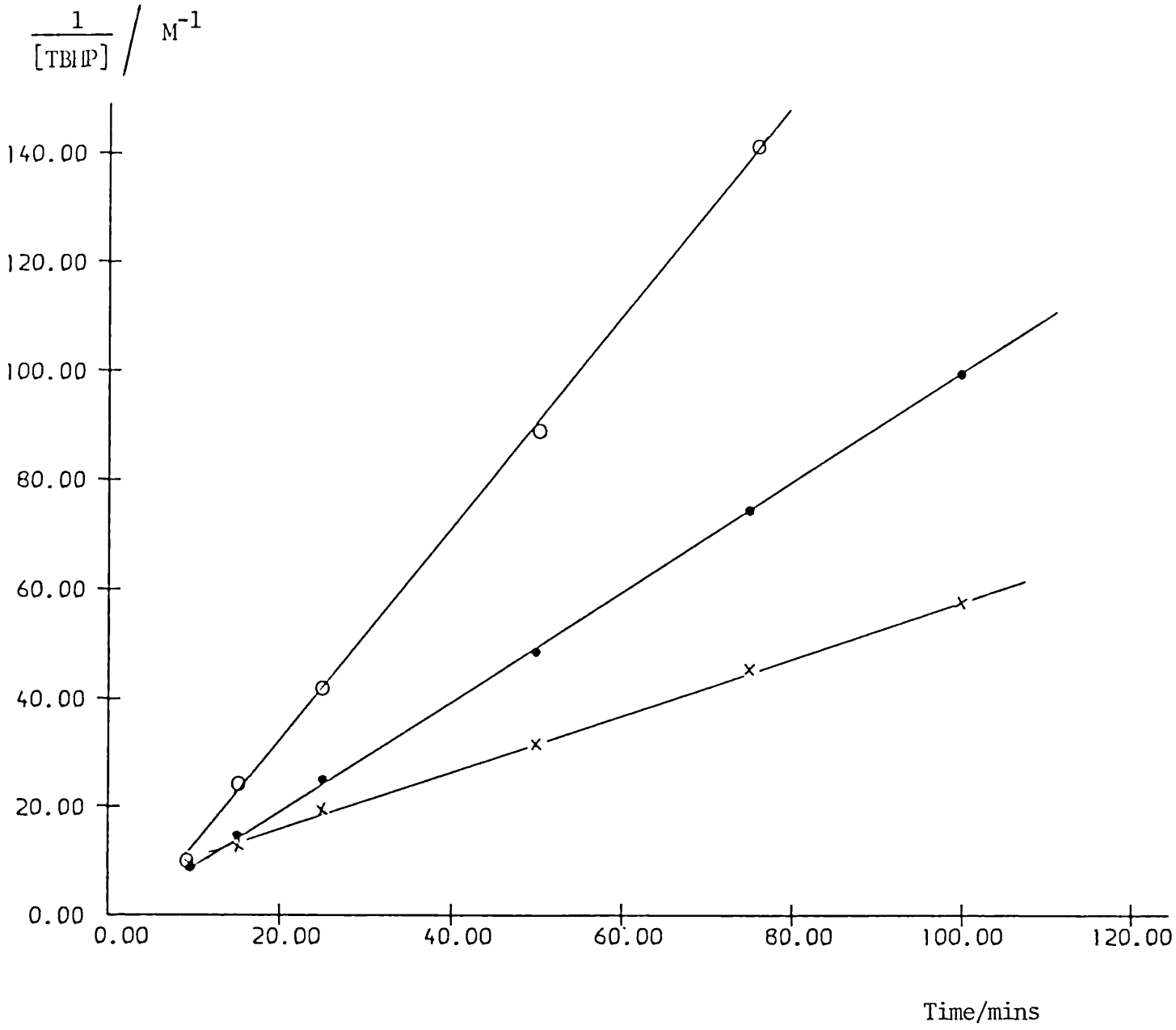

Fig. II.2.4(3) Reaction of tert-butyl hydroperoxide with 1-decene in 1,2 dichloroethane at 70° in the presence of Catalyst XI (O = 0.0004M; • = 0.0002M; X = 0.0001M); 1-decene 0.1M; TBHP 0.1M).

II.2.4.3 Reactions of molybdenum complexes with tert-butyl hydroperoxide in the absence of olefin.

A plot of ln[TBHP] against time for the decompositon of tert-butyl hydroperoxide by molybdenum complexes in the absence of olefin gave a straight line. The gradients of the plots are summarised as overall rate constants in Table II.2.4(6). What is apparent from Table II.2.4(6) is the rate of decomposition of tert-butyl hydroperoxide is about ten times slower than that of epoxidation (cf Table II.2.4(1)).

Overall rate constants for molybdenum catalysed decomposition of TBHP at 70°.

CATALYST	kx10/s^{-1} [a]
I	0.58
II	0.54
III	0.33
IV	0.38
V	0.36
VI	0.45
VII	0.46
VIII	0.45
IX	0.43
X	0.44
XI	0.43
XII	0.47
XIII	0.47
XIV	0.64
XV	0.62
XVI	0.65
XVII	0.28
XVIII	0.30
XIX	0.27
XX	0.28

[a] Calculated first order plots for hydroperoxide disappearance.

[TBHP] = 0.1 mol dm^{-3} [CATALYST] = 10^{-4} mol dm^{-3}

Table II.2.4(6)

II.2.4.4 Conclusions

The results are consistent with Scheme VI, involving two competing reactions - molybdenum catalysed homolytic decomposition of the hydroperoxide and molybdenum catalysed epoxidation.

Scheme VI

$$Mo^{V} + RO_2H \xrightarrow{fast} Mo^{VI} + RO^{\cdot} + HO^{-} \qquad \text{Eqn. II.2.4(4)}$$

$$Mo^{VI} + RO_2H \rightleftharpoons \left[Mo^{VI}.RO_2H \right] \rightarrow Mo^{V} + RO_2^{\cdot} + H \qquad \text{Eqn. II.2.4(5)}$$

$$\left[Mo^{VI}.RO_2H \right] \rightarrow \text{epoxide} + ROH + Mo^{VI} \qquad \text{Eqn. II.2.4(6)}$$

Molybdenum catalysed homolytic decomposition is initiated by electron transfer reactions of Mo (V) and Mo (VI) complexes of hydroperoxides. The hydroperoxide decomposition for Catalysts XIV-XVI (inclusive) is faster than that obtained for all the other catalysts. Previous work[48] concluded that the dimer complexes decomposed to give the alkoxy radicals, the reaction for Catalyst XIV being described by Eq. II.2.4(7).

$$\left(Mo_2O_3\left[OCH(CH_3)CH(CH_3)O\right]_2\left[OCH(CH_3)CH(CH_3)OH\right]_2\right) + 2RO_2H \longrightarrow$$

$$2\{MoO_2\left[OCH(CH_3)CH(CH_3)OH\right]_2\} + 2RO^{\cdot} + \tfrac{1}{2}O_2 \qquad \text{Eqn. II.2.4(7)}$$

Hence, the reaction described by Eqn. II.2.4(4) will be faster than that described by Eqn. II.2.4(5), the latter being the rate determining step. Homolytic decomposition is commonly found when

cobalt, iron and manganese are used as metal catalysts - this being due to the high oxidation potential between differing oxidation states which exist in these metals. The oxidation potential of the Mo (VI)/Mo (V) couple is low ($\sim$ 0.2V)[136].

The molybdenum catalysed epoxidations show a small induction period during which the rates are different but after this induction period is over, settle to similar values. This is in agreement with previous studies[35] where it was reported that the catalyst was modified to the same structure.

With the hydroperoxide being a strong oxidising agent, it is highly unlikely that Mo^{VI} complexes would be reduced in these experiments. Hence if the active catalyst is the same in all these reactions, it must be a Mo^{VI} species. Complex formation between the metal catalyst and the hydroperoxide renders the peroxidic oxygens more electrophilic and hence, more liable to attack by an olefinic double bond. In so doing, the catalyst acts as a Lewis acid.

A possible mechanism for the metal catalysed epoxidation is described in Scheme VII (overleaf).

SCHEME VII

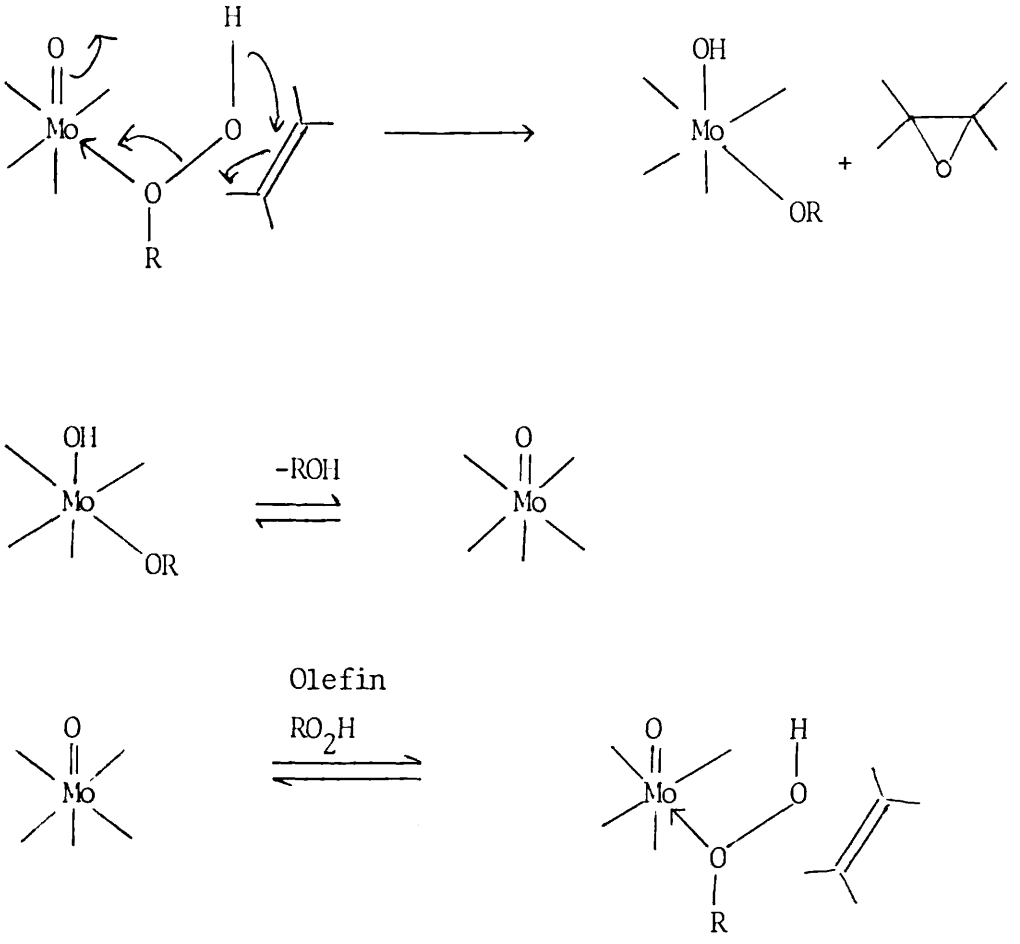

CHAPTER II SECTION 3

II.3.1 Purification of reagents

Diethyl ether was dried over sodium wire.

1,2-dichloroethane was dried over calcium hydride and distilled under nitrogen. It was then stored over molecular sieves (type 4A).

Tert-butyl hyproperoxide (TBHP) [137]

The TBHP used was TBHP-70 (30% W/W H_2O) (Aldrich). The water was removed by the following method:-

TBHP-70 (100 cm^3) and 170 cm^3 of reagent grade 1,2 dichloroethane were combined in a 1ℓ separation funnel and swirled (not vigourously) for 1 min. The organic phase is poured into a 500 cm^3 round bottomed flask. A few boiling stones were added and the solution distilled in a steam bath. The earlier fraction was cloudy and separated in the collection vessel into organic and aqueous layers. After ca. 70 cm^3 of solvent was removed, the distillate became clear and homogeneous. A total of ca. 98 cm^3 of distillate was collected, leaving ca. 159 cm^3 of an anhydrous solution of TBHP in dichloroethane. The anhydrous TBHP solution was allowed to cool before storing.

II.3.2 General Experimental Methods

II.3.2a Measurement of concentration of 'Anhydrous TBHP-70' using iodometric method.

To a mixture of glacial acetic acid (2 cm^3) and isopropanol (25 cm^3) in a 250 cm^3 volumetric flask was added 10 cm^3 of freshly prepared sodium iodide-isopropanol solution (22g sodium iodide in 100 cm^3 isopropanol, reflux for 5 mins, cool to room temperature and then filter). To this was added an accurately measured sample of TBHP

solution. The solution was refluxed for 30 sec., diluted with 100 cm^3 of distilled water, then immediately titrated with 0-1N sodium thiosulphate. Freshly prepared starch solution was used to enhance the end-point.

The concentration is calculated according to the equation:-

$$\text{Molarity of TBHP solution} = \frac{SXM}{2x(cm^3 \text{ of sample of TBHP})}$$

S = Volume of sodium thiosulphate used as titre.

M = Molarity of sodium thiosulphate.

II.3.2b Measurement of concentration of 'Anhydrous TBHP-70' using ^1H nmr.

The values obtained by ^1H nmr were within (±6%) agreement with those obtained by titration.

The tert-butyl resonance is at ∿ 1.25ppm, 1,2-dichloroethane resonance is at 3.70ppm.

$$\text{Molarity} \sim \frac{A}{(0.10A+0.18B)}$$

A = Integral height of tert-butyl resonance

B = Integral height of 1,2-dichloroethane resonance.

II.3.2c NMR

^1H and ^{13}C nmr samples were run of a Brüker spectrometer at 400.13MHz and 100.62 MHz respectively. In all cases, $CDCl_3$ was the solvent used.

II.3.2d GC/MS

A Pye Unicam 104, interfaced to a Kratos MS25 mass-spectrometer was used for analysis of all products. Electron-Impact (E.I.) mass-spectra were recorded.

glc conditions

Column : OV101

Column length : 2.8m

Column diameter : 0.5mm

Carrier gas : Helium

Column Temperature : Decene Oxide 120° (isothermal)

Dodcene Oxide 140° (isothermal)

II.3.2e GLC

A Varian AU3900 gas liquid chromatograph was used.

glc conditions

Column : SE30 Capillary Column

Column length : 25m

Column diameter : 0.25 mm I.D.

Carrier gas : Helium

Splitter ratio : 30:1

Column Conditions : a) Decene Oxide, b) Dodecene Oxide.

a)

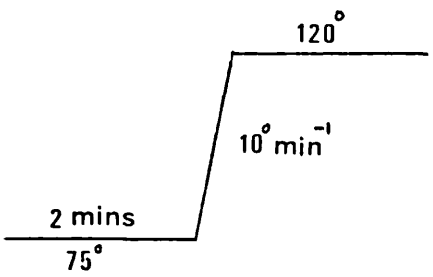

b)

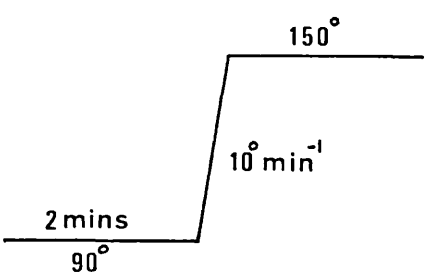

II.3.2f Experimental details for epoxidation reactions

All glassware was thoroughly dried overnight in an oven. In all cases, standard Quickfit glassware was used.

To a 250 cm^3 three neck round bottomed flask fitted with a teflon magnetic stirrer, reflux condenser, a 250 cm^3 dropping funnel and a nitrogen inlet was added olefin (0.05 mol.), catalyst (0.125 mmol.), freshly ground anhydrous disodium hydrogen phosphate (0.35 mmol.) and 100 cm^3 of 1,2 dichloroethane. The dropping funnel was charged with TBHP (24.5 cm^3, 0.05 mol.) previously prepared by the method described in Section II.3.1, the entire system being maintained under nitrogen. The reaction was brought to a gentle reflux upon which dropwise addition of the TBHP was commenced (during the addition of TBHP, the heat source was removed). When the TBHP addition was completed, the heat source was reapplied to the reaction vessel, the reflux being maintained for 10 hr.

The reaction vessel was then cooled in an ice bath and $\sim$ 150 cm^3 of a freshly prepared 10% solution of sodium sulphite was added dropwise with stirring. After the addition was completed, the ice bath was removed and the stirring continued for 3 hr. at autogenous temperature. At this point, the organic phase ought to give a negative peroxide test using acidified starch iodide test paper (TBHP reacts very slowly with startch-iodide test paper, therefore the commercially available starch iodide test paper is acidified with a few drops of 1-3M hydrochloric acid solution). If the test was positive, additional aqueous sulfite solution was added and stirring continued till the test proved negative.

The aqueous and organic layers were then separated and the milky white organic layer was extracted twice with 100 cm^3 water and once

with 100 cm^3 brine, dried (magnesium sulphate) and concentrated to give an oil. The oil was distilled under vacuum to give the pure epoxide.

II.3.3 Kinetic measurements

All glassware was thoroughly dried overnight in an oven. In all cases, standard Quickfit glassware was used. The reactionswere carried out under an atmosphere of nitrogen.

50 cm^3 of a solution of TBHP (10 mmol.) and olefin (100 mmol.) in 1,2-dichloroethane (100 cm^3) was warmed to 70°. The catalyst (1×10^{-4} mol., 2×10^{-4} mol., 4×10^{-4} mol) was added to the solution with stirring. Aliquots (10 cm^3) were removed at regular intervals and added to a mixture of acetic acid (10 cm^3) and a saturated aqueous solution of sodium iodide (2 cm^3). The mixture was allowed to stand for 15 min. and the liberated iodine titrated with 0.1N sodium thiosulphate solution. The rate of appearance of epoxide was followed by quenching the reaction aliquots with excess triphenylphosphine and analysing for epoxide by glc using chlorobenzene as an internal standard.

glc conditions for Kinetics

A Pye Unicam GCD105 gas chromatograph was used.

Column : 10% Carbowax 20M (Chromasorb W AW)

Detector Temp : 230°

Injector Temp : 240°

Length of Column : 2.8m

Column Diameter : 0.4mm

Column Temp : a) For Decene Oxide 120° (isothermal)

b) For Dodecene Oxide 140° (isothermal)

The rates of hydroperoxide disappearance in the absence of olefin were measured by the procedure described in Section II.3.2a.

Equimolar concentrations of TBHP (100mmol) and olefin (100mmol) in 1,2dichloroethane (150 cm^3) was warmed to 70^o. 10^{-4}mol of catalyst was added to the solution with stirring. Aliquots (10 cm^3) were removed at regular intervals and measured for the rate of disappearance of hydroperoxide by the procedure described in Section II.3.2a.

A plot of $^1/_{TBHP}$ vs time gave a straight line, in accord with a first-order dependence in both olefin and hydroperoxide.

II.3.4 Spectroscopic Data

II.3.4a 400.13 MHz ^{1}nmr spectrum of Decene Oxide

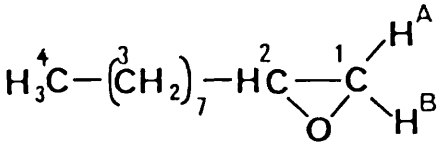

$^1CH^A$ 2.44ppm, d.d; $J_{HH}A$ = 3.0Hz, J_HA_HB = 5.0Hz

$^1CH^B$ 2.72ppm, d.d; $J_{HH}B$ = 4.5Hz, J_HA_HB = 5.0Hz

^2CH 2.88ppm, m.

$^3(CH_2)_7$ 1.26ppm, m.

$^4CH_3$ 0.86ppm, t; J = 6.5Hz.

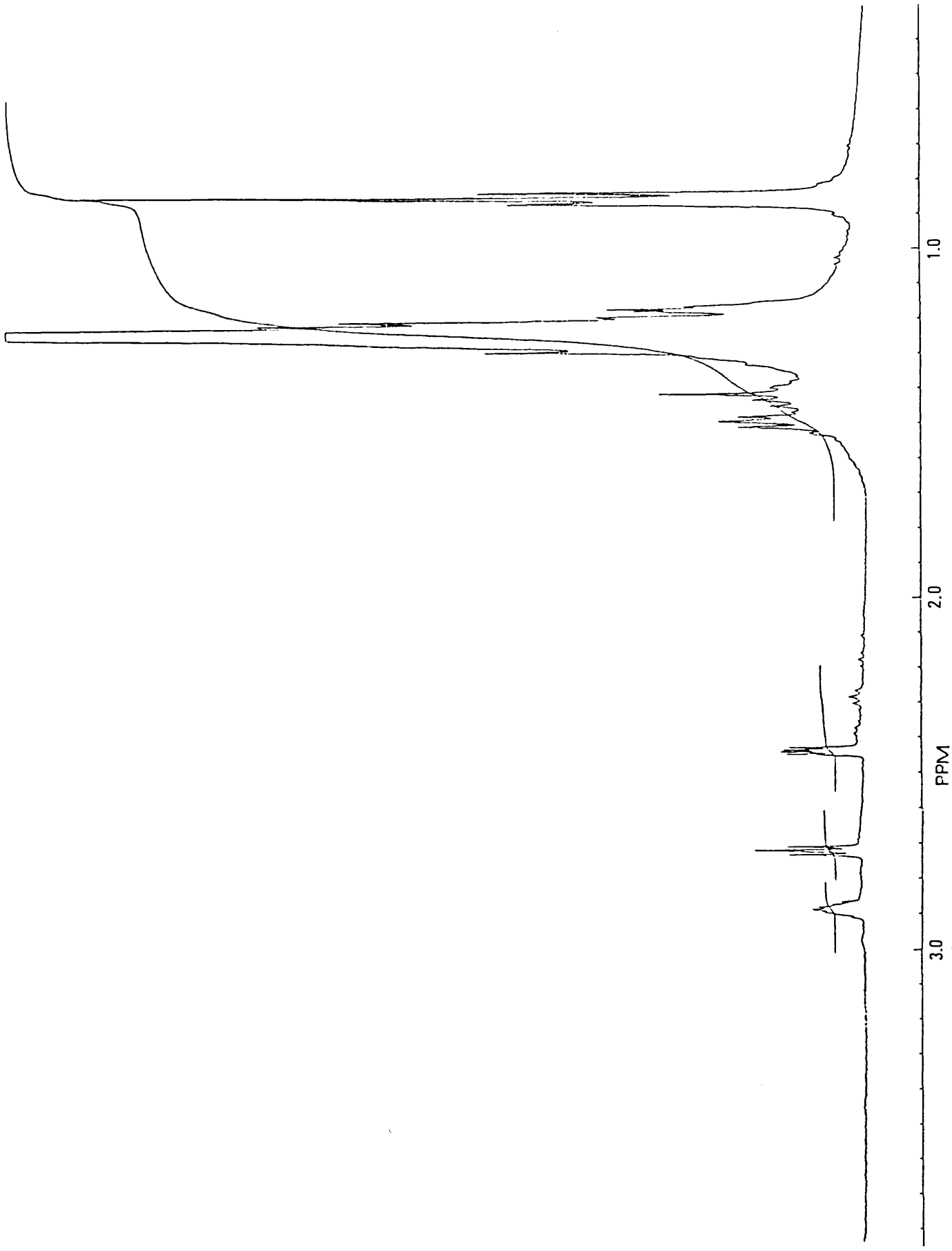

Fig. II.3.4(1) 400.13 Mhz ^{1}H nmr spectrum of Decene Oxide in $CDCl_3$.

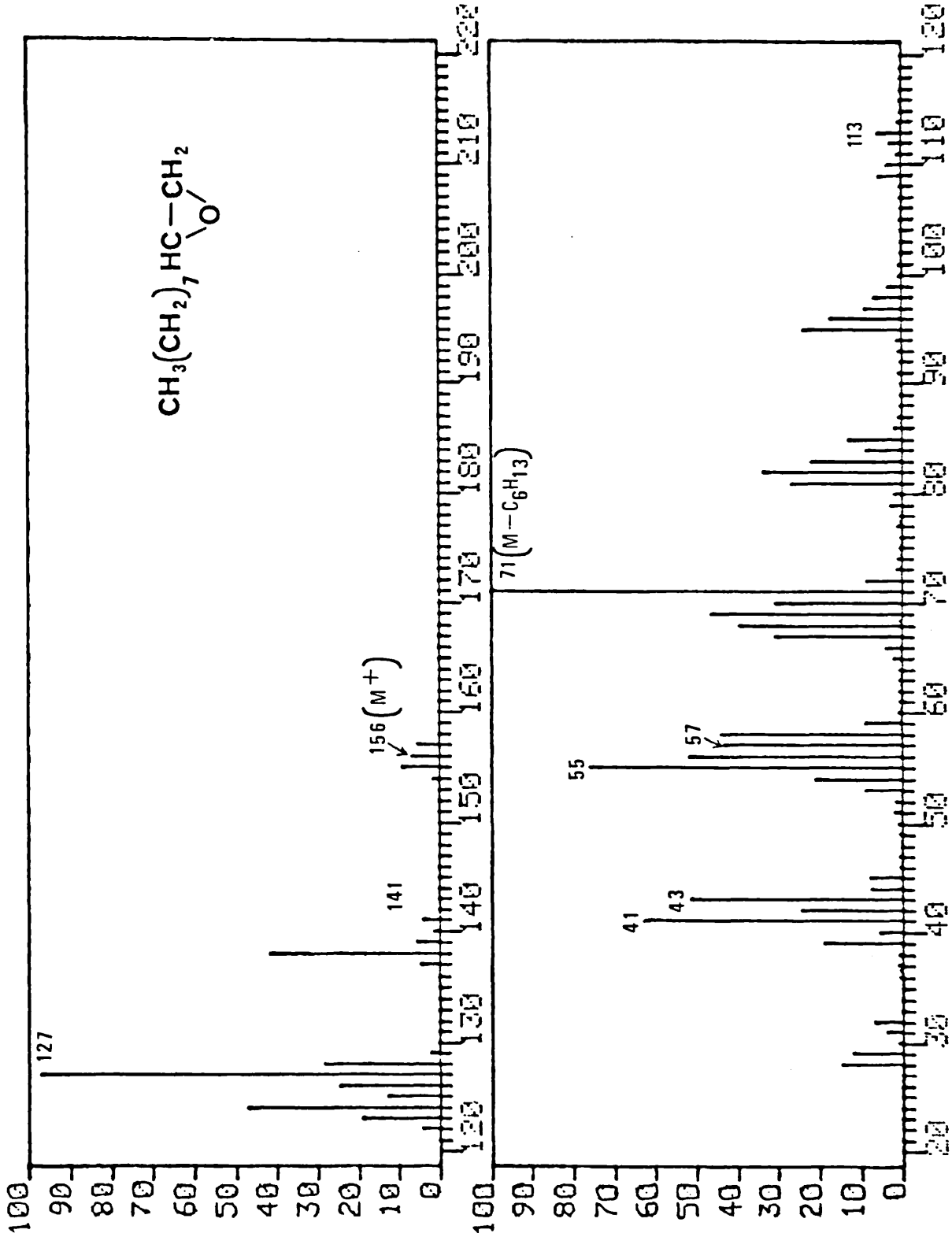

Fig. II.3.4(2) EI/MS of Decene Oxide

II.3.4b 400.13MHz ^{1}H nmr spectrum of Dodecene Oxide

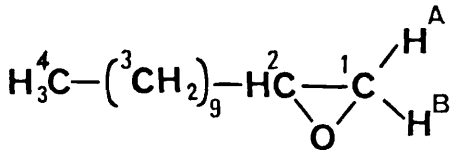

$^{1}CH^{A}$ 2.42ppm, d.d; $J_{HH}{}^{A}$ = 3.0Hz, $J_{H}{}^{A}{}_{H}{}^{B}$ = 5.0Hz

$^{1}CH^{B}$ 2.70ppm, d.d; $J_{HH}{}^{B}$=4.0Hz, $J_{H}{}^{A}{}_{H}{}^{B}$ = 5.0Hz

^{2}CH 2.86ppm, m.

$(^{3}CH_{2})_{9}$ 1.24ppm, m.

$^{4}CH_{3}$ 0.85ppm, t; J = 7.0Hz.

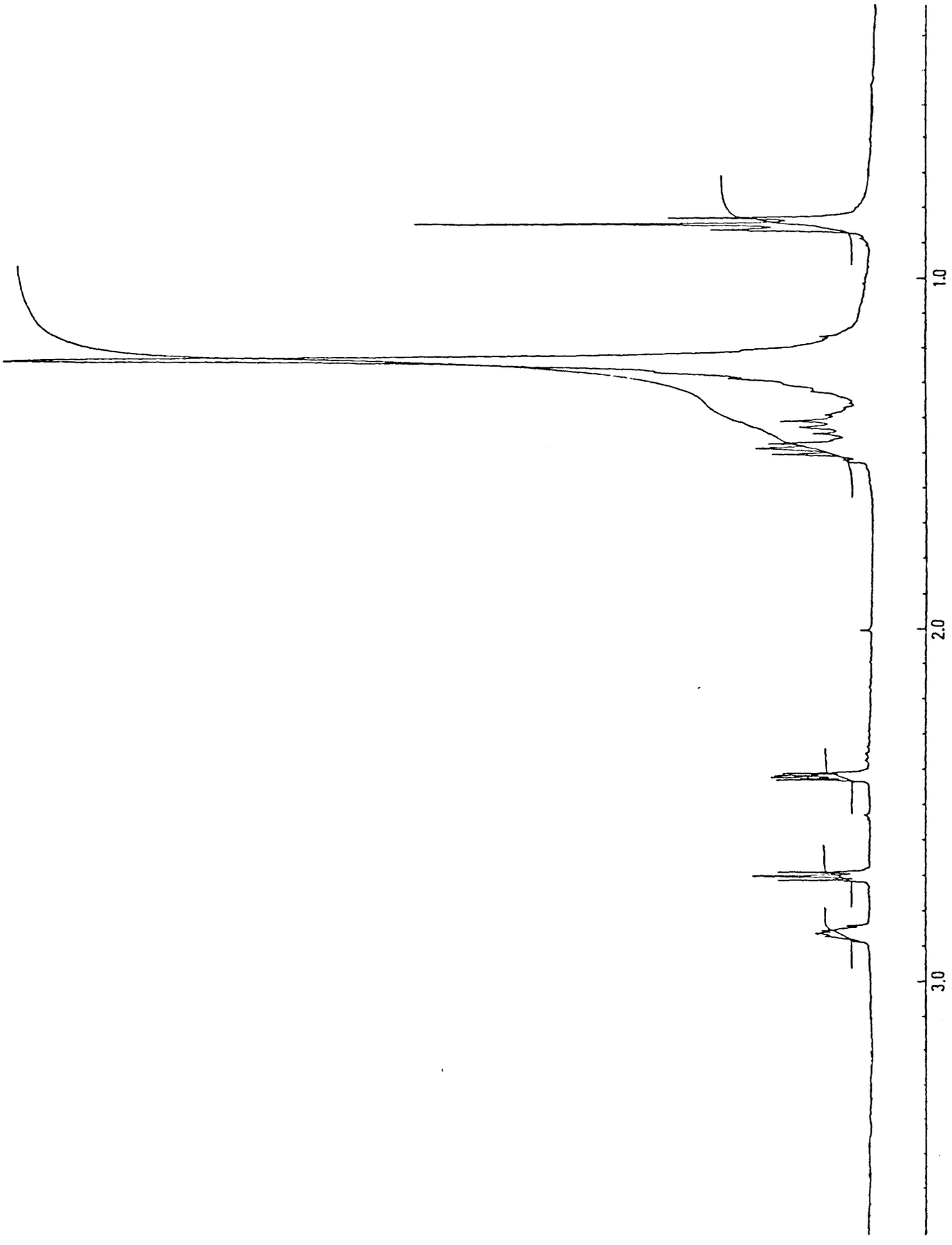

Fig. II.3.4(3) 400.13MHz ^{1}H nmr spectrum of Dodecene Oxide in $CDCl_3$

II.3.4c 100.62Mz ^{13}C nmr spectrum of Dodecene Oxide

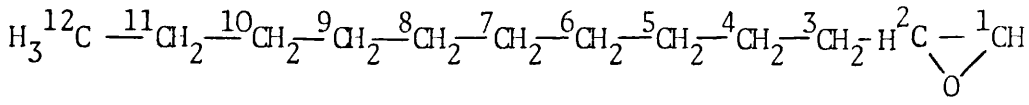

	ppm
C-1	46.82
C-2	52.14
C-3	32.38
C-4	31.79
C-5 - C-8 (inc.)	29.45
C-9	29.20
C-10	25.85
C-11	22.55
C-12	13.92

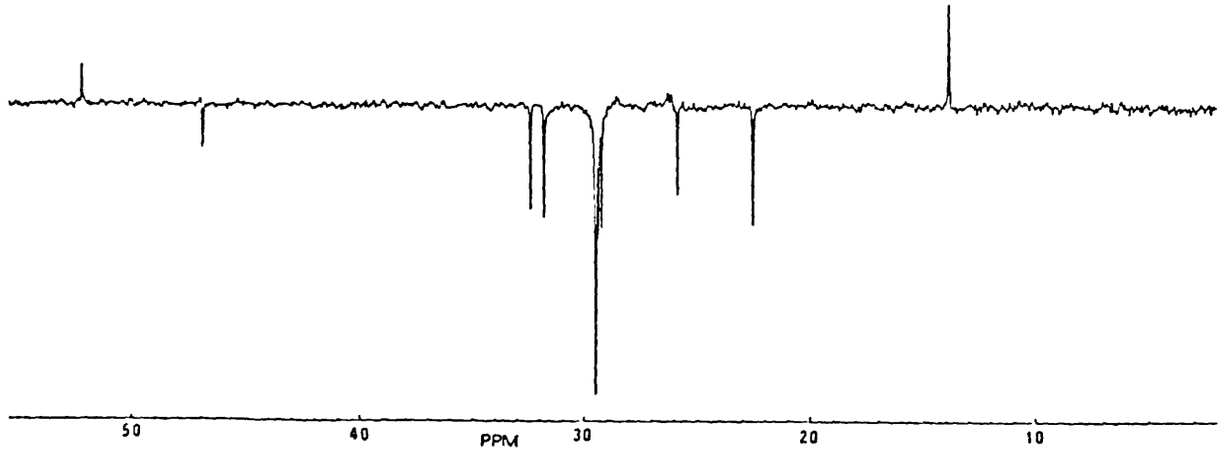

(i) 100.61MHz DEPT spectrum of Dodecene Oxide in $CDCl_3$.

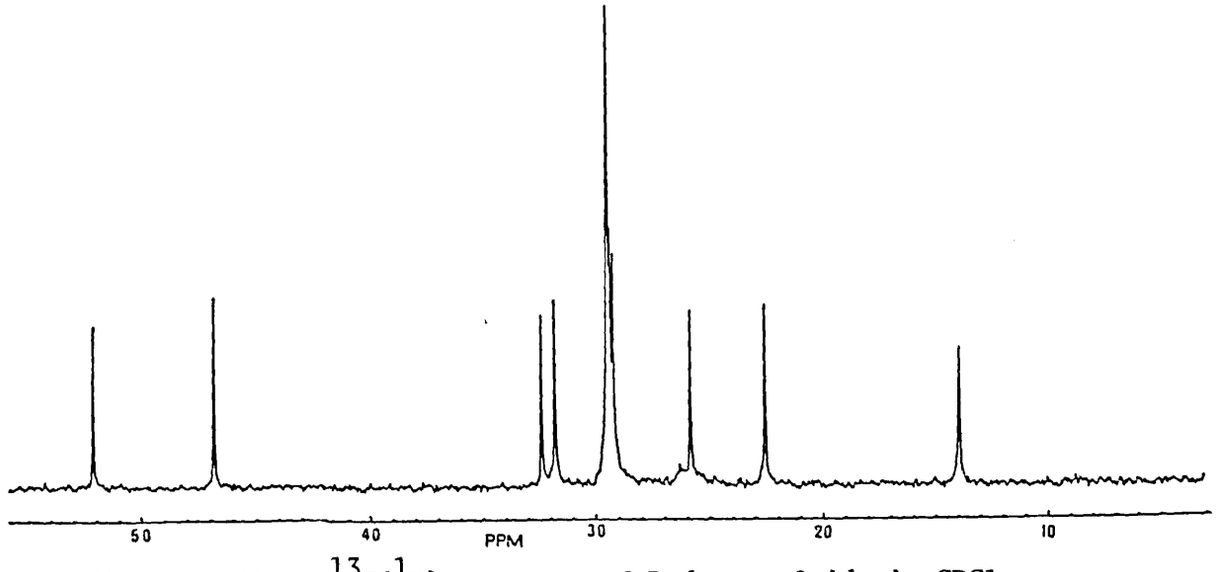

(ii) 100.61MHz $^{13}C\{^{1}H\}$ spectrum of Dodecene Oxide in $CDCl_3$

Fig. II.3.4(4).

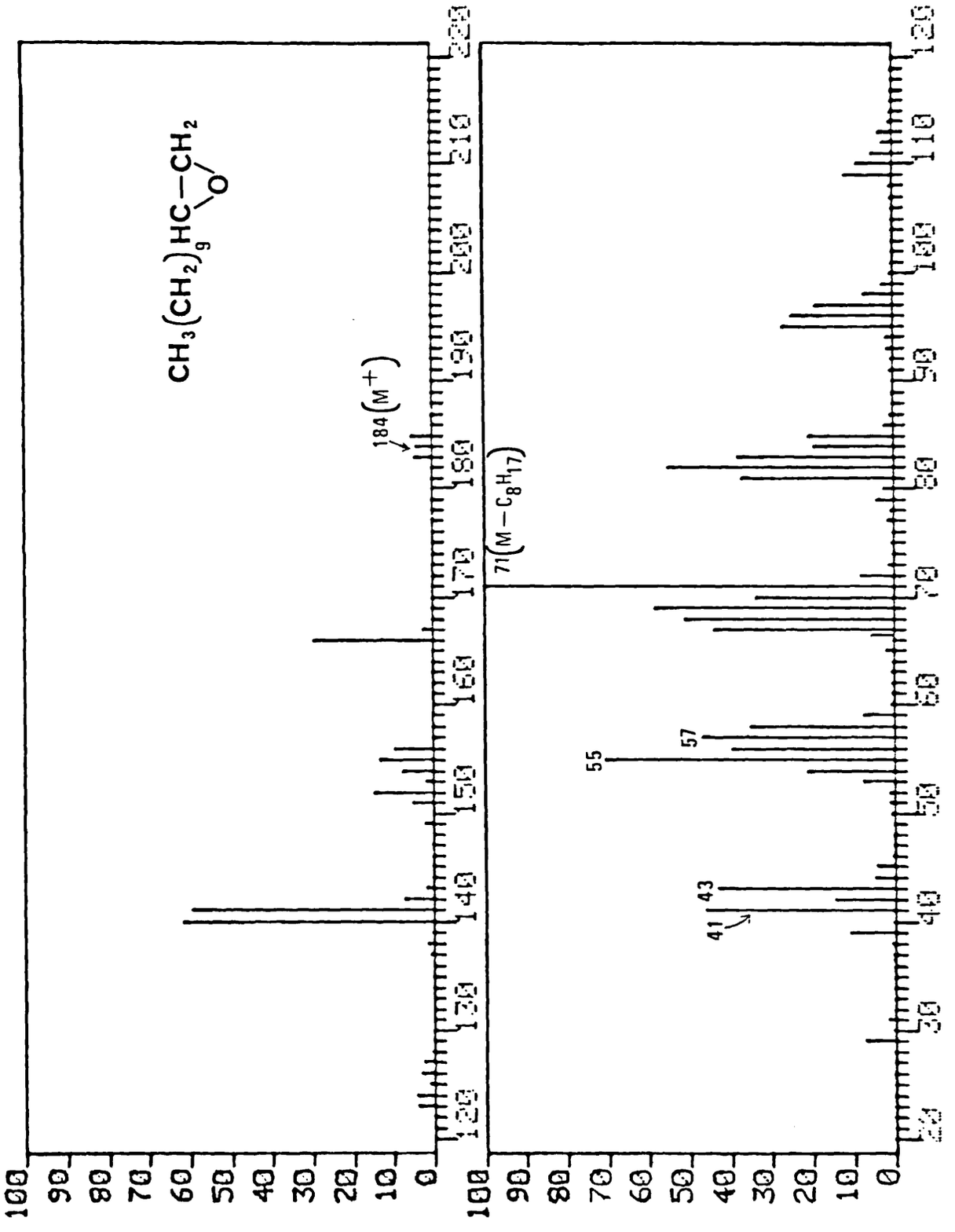

Fig. II.3.4(5) EI/MS of Dodecene Oxide.

Chapter III

ASYMMETRIC EPOXIDATION USING MOLYBDENUM CATALYSTS

CHAPTER III SECTION 1

III.1. INTRODUCTION

Emil Fischer was the first person to outline the concept of asymmetric synthesis which he based on his experiments in the conversion of one sugar to the next higher homolog via the cyanohydrin reaction[138]. Since then, chemists have sought to induce asymmetry into organic reactions. In the interim, our knowledge of chiral inducing reactions has greatly increased, though not as rapidly as our acquaintance of achiral reactions [139,140].

Resolutions and asymmetric inductions are the methods most frequently used for obtaining chiral compounds[140,141].

Resolutions involve the physical or chemical separation of enantiomeric pairs. However, resolutions suffer from the limitation that only fifty per-cent of the starting material is utilised.

Asymmetric inductions, are those reactions which produce an optically active centre from a symmetrical but prochiral centre or group. Potentially, all of the starting material can be converted into the desired product. However, asymmetric induction reactions also present difficult problems:-

i) Since the extent of optical induction is a function of energy difference in the competing diastereomeric transition states ($\Delta\Delta G^{+}$), the optical inductions cannot be increased without changing the nature of the reaction.

ii) There has to be a known chiral inducing reaction for the desired transformation.

However, for both resolutions and asymmetric inductions, an asymmetric reagent is necessary. The most economical use of this required 'species' is through catalysis. Bredig and Fiske[141] reported the first example of catalytic asymmetric induction by using optically active amines to catalyse the formation of chiral cyanohydrins. It was not till very recently that catalytic asymmetric expoxidation systems have been reported. Many oxidation reactions, tend to destroy chiral centres rather than generate them - epoxidation however, is an exception.

The epoxide is one of the most important and versatile functionalities in organic chemistry [142,143]. The synthetic importance of the epoxide group is due to the existence of regio and stereoselective methods both for construction and controlling its subsequent reactions. When the face of an olefin is oxygenated, Eqn. III.1(1), one (if $R_1 \neq R_2$, $R_3 = R_4$) or two (if $R_1 \neq R_2 \neq R_3 \neq R_4$) potentially chiral centres are generated. Hence, the simple transformation from a prochiral olefin into a chiral epoxide would have great potential in asymmetric synthesis.

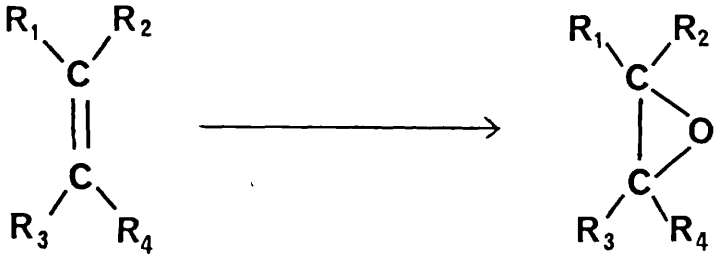

Eqn. III.1(1)

The first example of an asymmetric epoxidation was reported by Henbest et al [144,145] in 1965. This involved the reaction of (+)-mono-peroxycamphoric acid, Fig. III.1(1) with various mono-substituted ethylenes to yield optically active epoxides. However, the greatest

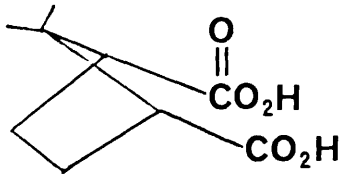

Fig. III.1(1)

amount of asymmetric induction achieved was 4%. Since the original reports of Henbest et al [144,145] the asymmetric epoxidation of olefins with chiral peroxyacids has been applied by several workers [146-153]. The best asymmetric induction observed was 10% [152], even though a wide variety of chiral peroxyacids has been tested. Pirkle and Rinaldi[154] found that the usual method of preparation of (+)-mono-peroxycamphoric acid yields a mixture of peroxyacids as well as a small amount of bis peroxy acid, Eqn. III.1(2). After separation, it was found that

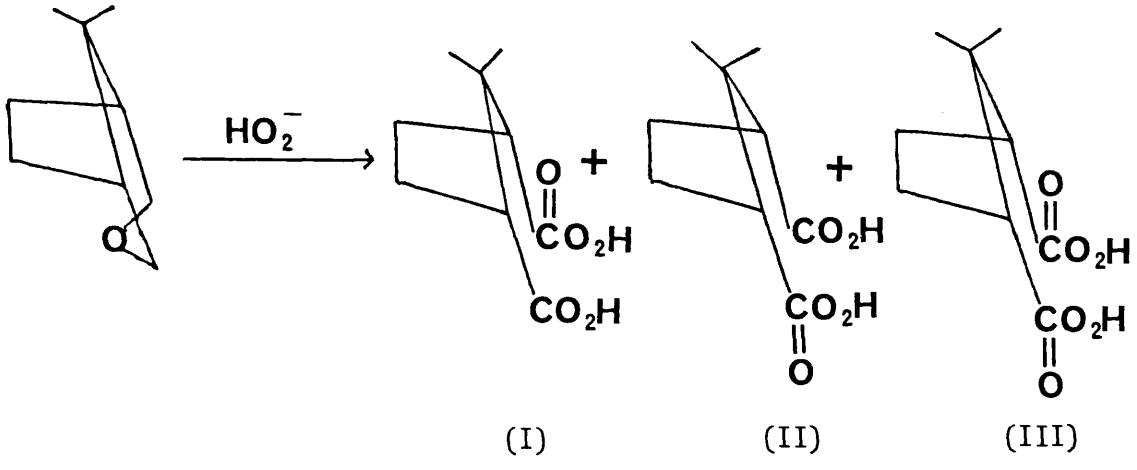

(I) (II) (III)

Eqn. III.1(2)

from Eq. III.1(2), (I) and (II) induce opposite stereochemistry in several cases, and that the use of purified (I) led to higher asymmetric induction. However, this method still gives chiral epoxides with optical purity less than 10%.

The base catalysed epoxidation of ℓ-menthyl alkylidene-cyanoacetates with H_2O_2/Na_2WO_4 yielded optically active epoxides Eqn. III.1(3), although the percentage of enantiomeric excess is unknown[155].

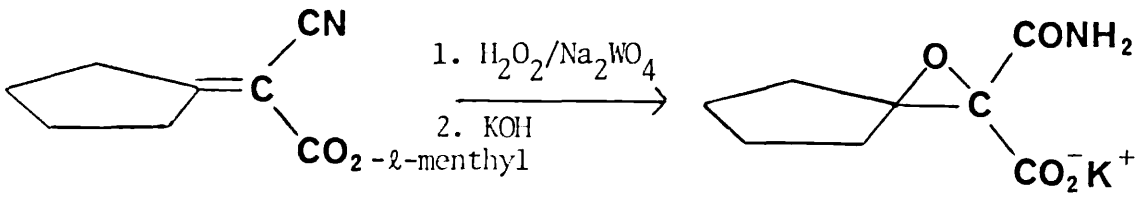

OPTICALLY ACTIVE

Eqn. III.1(3)

Chiral tertiary amines were used to catalyse the reaction between molecular oxygen and (1-phenyl-alkylidene)malo-nitriles to give low levels of enantiomeric excess (<10%)[156].

Another base catalysed epoxidation used hydrogen peroxide or tert-butyl hydroperoxide along with a quaternary ammonium salt of quinine acting as a phase-transfer reagent Eqn. III.1(4). The maximum enantiomeric excess determined was 25%[157].

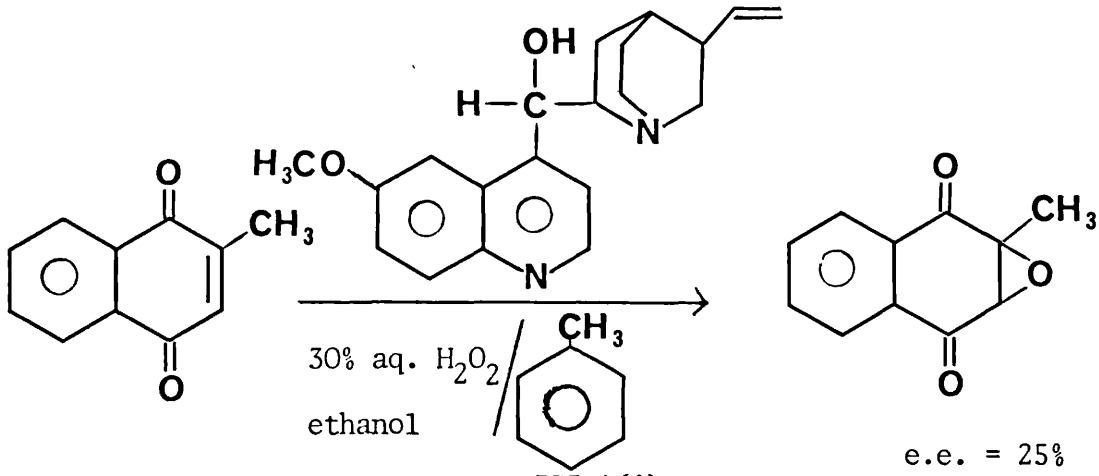

e.e. = 25%

Eqn. III.1(4)

The first examples of metal catalysed asymmetric hydroperoxide epoxidations were reported independantly by Yamada et al[18] and Sharpless et al[158].

Yamada and coworkers[18,19,159] exploited the use of an asymmetric catalyst to minimise the loss of precious chiral source. They asymmetrically epoxidised allylic alcohols with cumene hydroperoxide Eqn. III.1(5) in the presence of a chiral molybdenum catalyst, (acetylacetonato)-(-)-N-alkylephedrinato dioxomolybdenum, Fig. III.1(2).

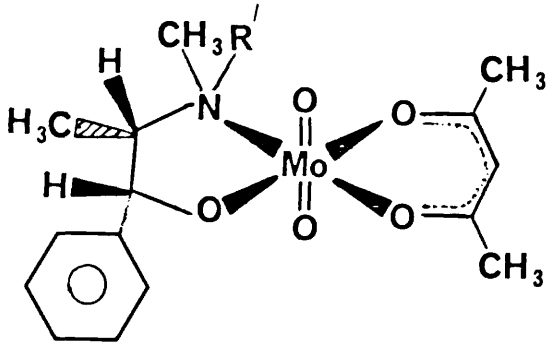

Fig. III.1(2)

Thus, epoxidation of 3-Methyl-2-butene-1-ol gave the epoxide with an enantiomeric excess of 33% Eqn. III.1(5)

Eqn. III.1(5) e.e. = 33%

Vanadium, in the presence of chiral hydroxamic acid, Fig. III.1(3), catalysed the asymmetric epoxidation of allylic alcohols [158]. Using

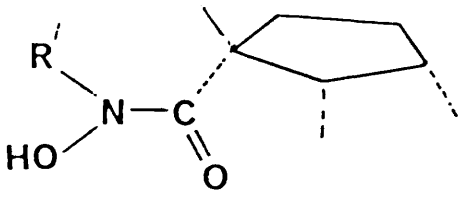

$R' = CH_3$; Ph; $2,6\text{-}Me_2Ph$

Fig. III.1(3)

this method, α-phenylcinnamyl alcohol was asymmetrically epoxidised to yield epoxy alcohols, with an enantiomeric excess of 50% (Eqn. III.1(6)).

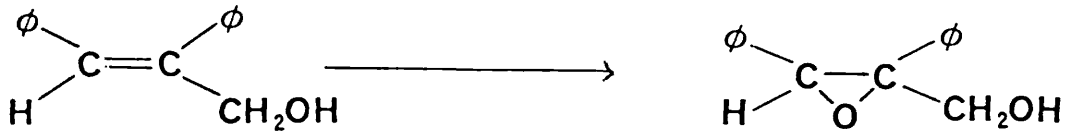

e.e. = 50%

Eqn. III.1(6)

Kagan et al[160] reported the asymmetric epoxidation of olefins using Molybdenum (VI) oxodiperoxo complexes, $MoO(O_2)_2L$ (L=pyridine, hexamethylphosphoric triamide, HMPA) Fig III.1(4).

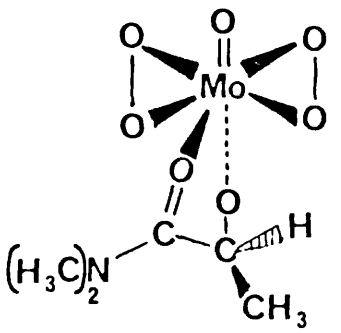

Fig. III.1(4)

The epoxidation of trans-2-butene afforded the chiral trans-dimethyl-oxirane with an enantiomeric excess of 35% (Eqn. III.1(7)).

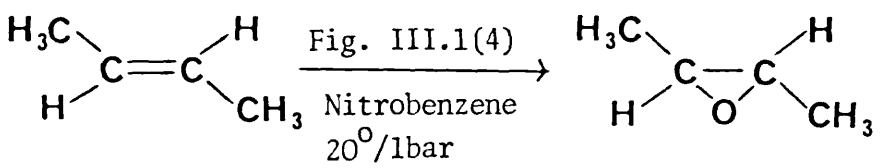

Eqn. III.1(7)

Hydrocarbon olefins were epoxidised by tert-butyl hydroperoxide with Mo (VI) catalysts in the presence of optically active diols[161]. The best induction was obtained in the presence of (+)-diisopropyl tartrate when squalene was epoxidised to afford (35)-2,3-oxidosqualene, Eqn. III.1(8).

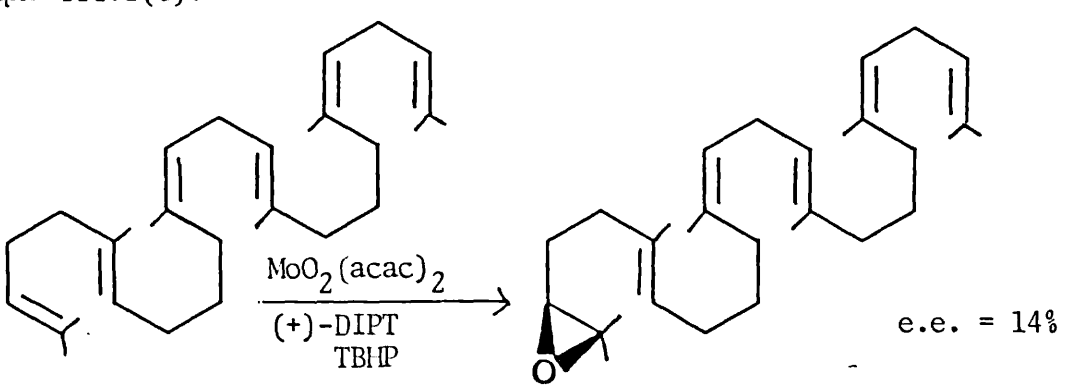

Eqn. III.1(8)

Oshima et al [162], successfully epoxidised and then acetylated geraniol and α-phenyl cinnamyl alcohol to their epoxy esters, Fig. III.1(5) and Fig. III.1(6) respectively. Asymmetric epoxidation was achieved by the use of aluminium alkoxides with tert-butyl

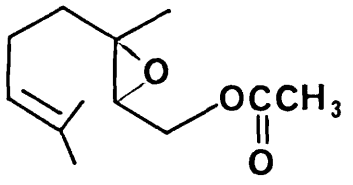

e.e. = 34%

Fig. III.1(5)

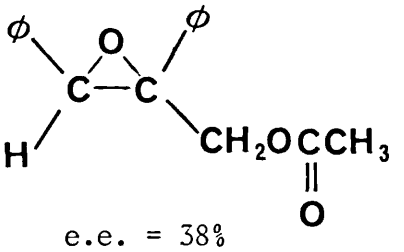

e.e. = 38%

Fig. III.1(6)

hydroperoxide in the presence of the chiral ligand Fig. III.1(7).

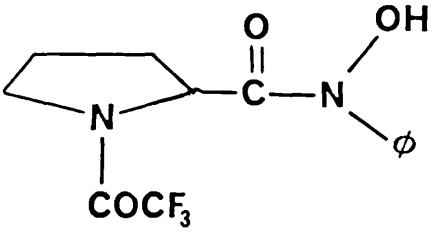

Fig. III.1(7)

The asymmetric epoxidation of olefins with chiral α-amino hydroperoxides and chiral hydroperoxy ketals and orthoformates gave at best an enantiomeric excess of 5% [163].

Sharpless and Katsuki [164] reported a major breakthrough in which geraniol was asymmetrically epoxidised to 2(S), 3(S)-epoxy geraniol, giving an enantiomeric excess of 87%. The system they used was titanium tetraisopropoxide in the presence of chiral tartaric acid

esters and tert-butyl hydroperoxide (Scheme I).

Scheme I

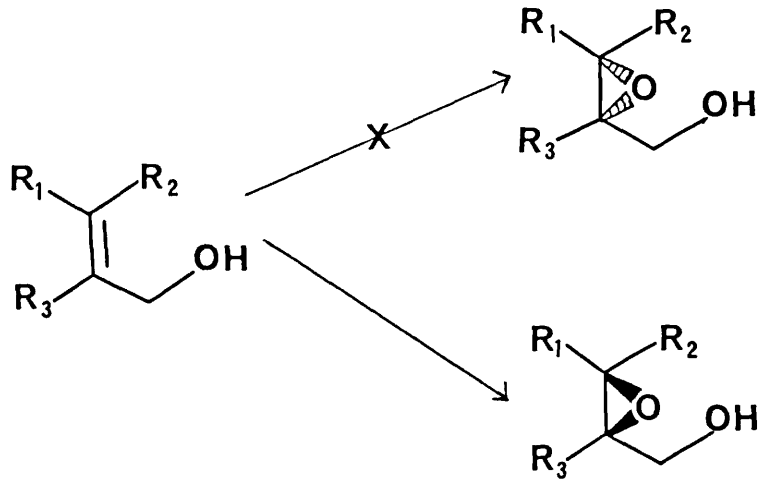

Without exception, all the variously substituted primary allylic alcohols studied were asymmetrically epoxidised yielding epoxy alcohols with high enantiomeric excess. They also found that the stereochemical outcome was completely predictable, utilising the simple model in Fig. III.1(8) (R^1,R^2=H). When tartrate esters derived from naturally occuring L-(+)-tartaric acid were used, epoxidation always occured on the bottom face of the olefin Fig. III.1(8), whereas esters derived from the unnatural D-(-)-tartaric acid, directed epoxidation on to the upper face.

Sharpless and coworker[165] found that secondary allylic alcohols were kinetically resolved under the same conditions. Hence when cyclohexylpropenyl-carbinol was reacted under the conditions described

D(-)-diethyl tartrate (unnatural)

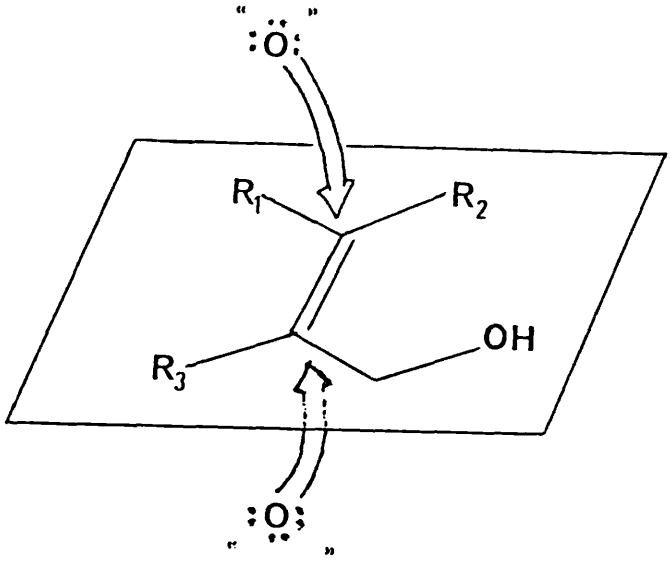

L-(+)-diethyl tartrate (natural)

Fig. III.1(8)

in Eqn. III.1(9), the recovered unreacted alcohol was found to be > 96% optically pure.

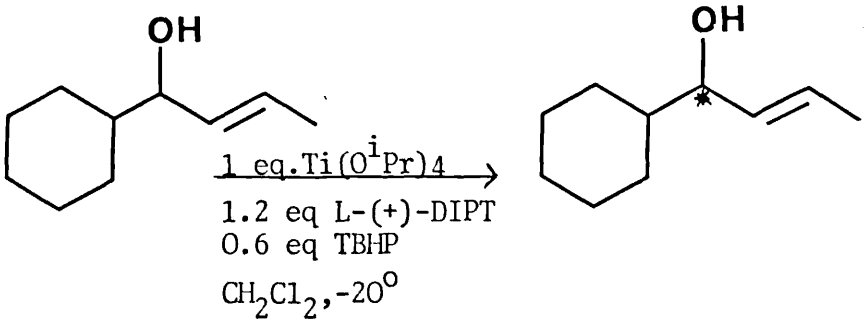

Eqn. III.1(9)

Stereoselectivity was also observed in the epoxyalcohol products as depicted in Scheme II.

Scheme II

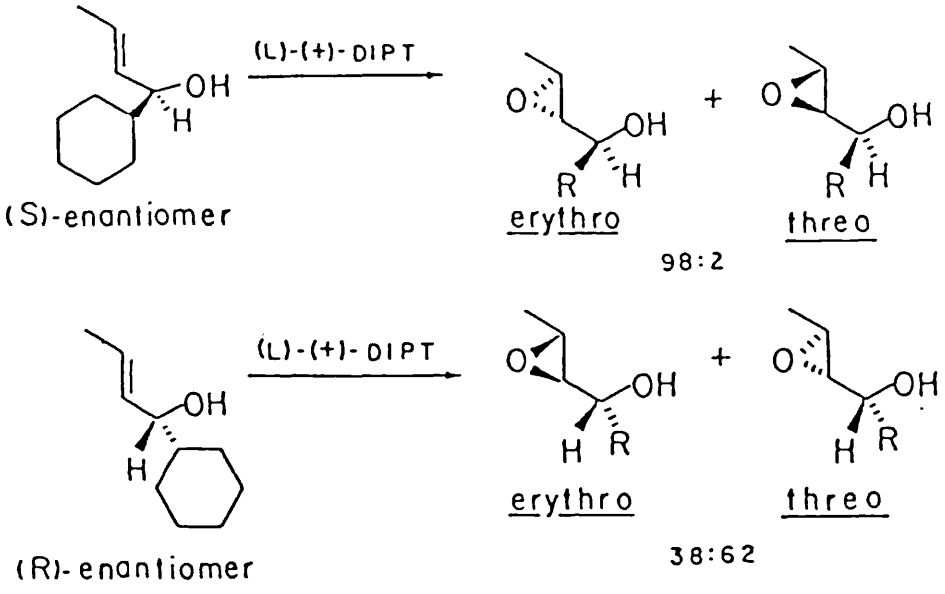

By stopping the reaction at various degrees of completion, the erytho and threo epoxy alcohols could be isolated with high enantiomeric excess. This new kinetic resolution process, provides an excellent route to optically pure allylic alcohols. In another paper by Sharpless and coworkers[166], it was shown that the kinetic resolution was not restricted to secondary allylic alochols in which the chirality resides at the carbinol carbon. Amongst the kinetic resolutions presented

include the resolutions of allenic alcohols, α-acetylenic carbinols, β-hydroxy sulfides and dienols.

The 2,3-epoxy alcohol moiety is a useful substrate for nucleophilic ring-opening reaction[166,167]. There are three reactive sties for nucleophilic substitution in a 2,3-epoxy alcohol, Fig. III.1(9)

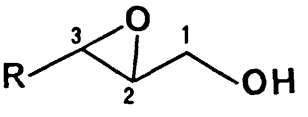

Fig. III.1(9)

Substitution at C-1 arises by virtue of the Payne rearrangement[152] in which an equilibrium is established between (I) and its 1,2-epoxy alcohol isomer (II) (Scheme III).

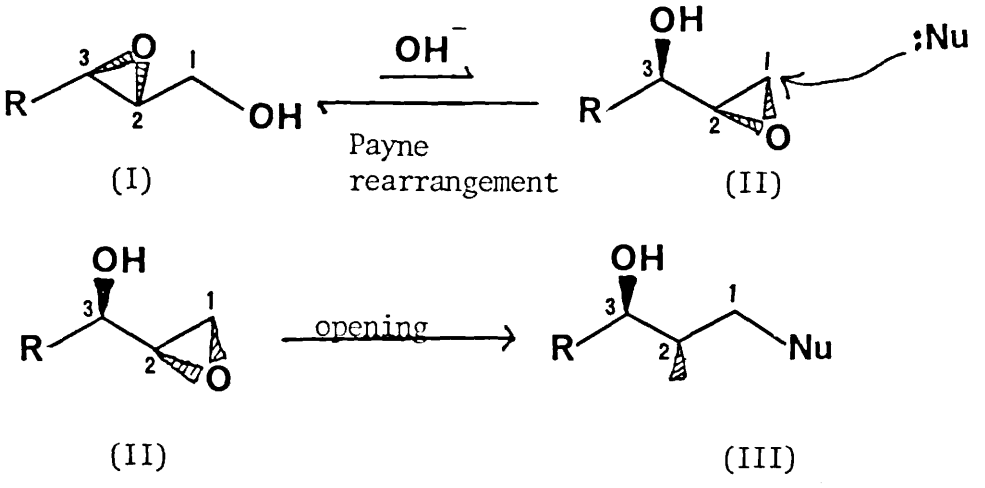

Scheme (III)

Typical nucleophiles include PhS^-, BH_4^-, CN^- and $TsNH^-$.

Suppressing the Payne rearrangement by use of buffered conditions, directs the nucleophilic attack to C-2 and C-3. However, certain reagents which are delivered intramolecularly by virtue of attachment

to the hydroxyl can exhibit high selectivity for C-2. Ring opening reactions of 2,3-epoxy alcohols with external nucleophiles may lead to selective attacks at either C-2 or C-3. When the substituent on C-3 is not sterically demanding and does not exert an electron-withdrawing inductive effect, there is a preference for ring opening at C-3. However, when R is sterically demanding and/or inductively electron withdrawing, the favoured approach is to C-2.

2,3-Epoxy acetals appear to be opened at C-3 by a variety of nucleophiles, 2,3-epoxy acids at C-2 while the 2,3-epoxy amides at C-3 [167](Scheme IV).

Scheme IV

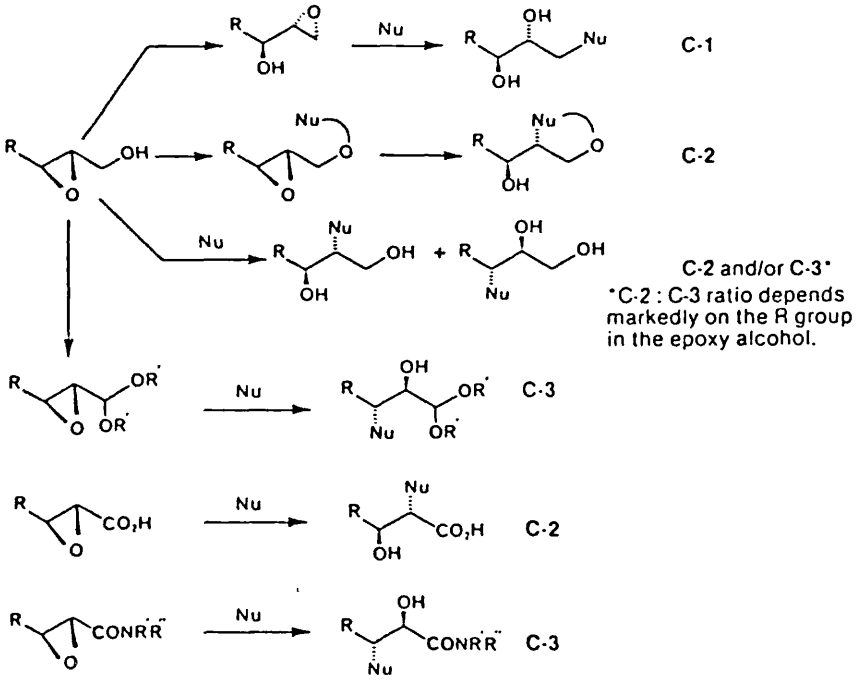

Also catalogued is an extensive list of compounds synthesised using asymmetric epoxidation as a step[166].

Coleman-Kammula and Duim-Koolstra[169] asymmetrically epoxidised 3-Methyl-2-butene-1-ol using cumene hydroperoxide and (acetylacetonato)-(L-N methylprolinol)dioxomolybdenum (VI), Fig. III.1(10), obtaining an enantiomeric excess of 50%.

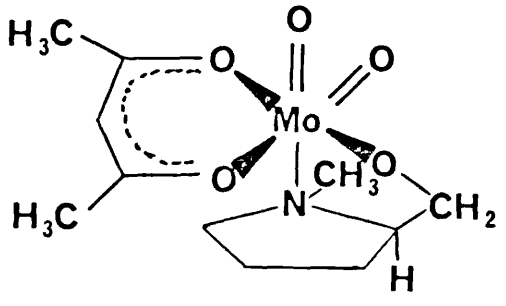

Fig. III.1(10)

Davis et al [170,171] described the synthesis of a new class of optically active oxidising reagents, chiral-2-(d-α-bromo-π-camphorsulphonyl-3-(2-chloro-5-nitrophenyl)oxaziridine (Fig. III.1(11) and Fig. III.1(12)). These reagents successfully epoxidised various olefins with differing success.

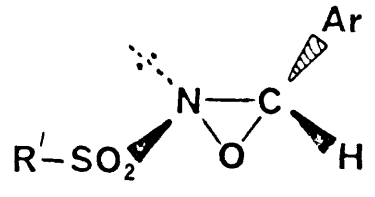

(-)(S,S)
Fig. III.1(11)

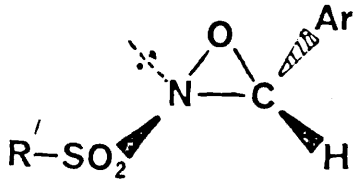

(+)(R,R)
Fig. III.1(12)

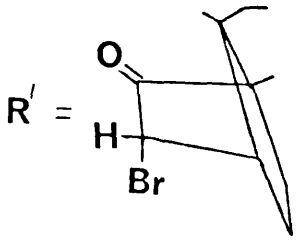

Ar = 2-chloro-5-nitrophenyl

The best enantiomeric excess value was obtained for 1,2-epoxy-1-phenyl-cyclohexane (40%) Eqn. III.1(10).

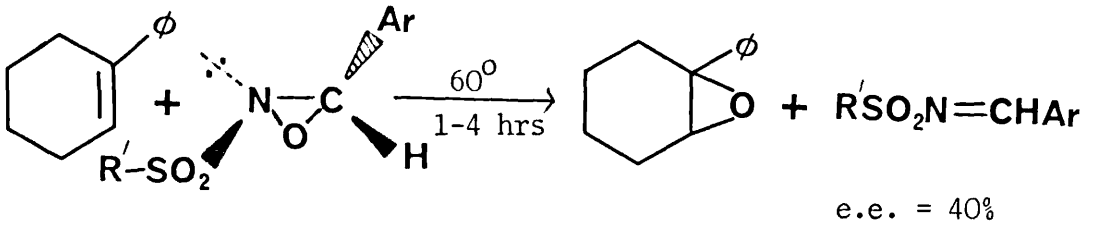

Eqn. III.1(10)

CHAPTER III SECTION 2

III.2 Results and Discussion

III.2.1 List of catalysts used for asymmetric epoxidation

For brevity, all catalysts used for asymmetric epoxidation in this section will be referred to by the alphabet.

A. cis-Bis(D(-)butane-2,3-diolato)dioxomolybdenum(VI)-D(-) Butane 2,3-diol(1:1).

B. μ-Oxo-Bis(oxo[2,3-dimethyl-2,3-D(-)butane-2,3-diolato(1-)] [2,3-dimethyl-2,3-D(-)butane-2,3-diolato(2-)])molybdenum(VI) .

C. {cis-Bis(S(+)phenyl ethane-1,2-diolato)dioxomolybdenum(VI)}.

D. {cis-Bis(S(+)2(-)amino-1-phenylpropane-1,3-diolato) dioxomolybdenum(VI)}.

E. {cis-Bis(S(+)propane-1,2-diolato)dioxomolybdenum(VI)}.

F. {cis-Bis(R(-)2(-)amino-1-butanato)dioxomolybdenum(VI)}.

III.2.2 Temperature Studies

The transition state discussed in Chapter II.1.2.1 showed the active catalyst complexed with both the olefin (or allylic alcohol) and the hydroperoxide before the double bond is oxidised. Hence, the diastereomeric transition states are controlling factors in the stereochemical course of the reaction. In these processes, the ground state free energies of the reactants for the competing pathways must be identical ($\Delta G^{\Theta}=0$). Only the free energies of

activation ($\Delta G^{\ddagger}$) of the two pathways differ, the extent of asymmetric transformation depends only upon the difference in the free energies ($\Delta\Delta G^{\ddagger}$) of the competing pathways.

Fig. III.2.2(1) shows the kinetically controlled asymmetric process in which the reactant, a_o, gives stereoisomeric products A_1 and A_2 in unequal quantities. The stereoisomer A_2 is formed predominantly because $\Delta G_2^{\ddagger} < \Delta G_1^{\ddagger}$; A_2 represents the less stable stereoisomer in case I and the more stable isomer in case II.

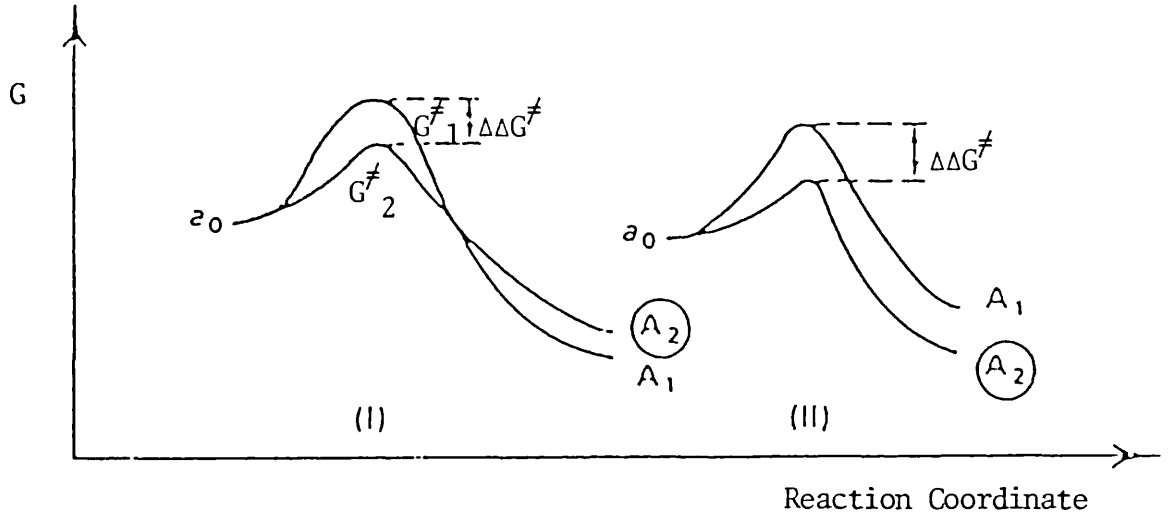

Fig. III.2.2(1)

Optimising reaction conditions often creates problems. Several independent studies[159,160,164,166] concluded that a marked increase in

enantiomeric excess is observed in reducing the reaction rate by lowering the temperature. However, this led to a drop in chemical conversion. This trend was observed in all the experiments carried out, an example of which at 60^{o} and $28\text{-}32^{o}$ is shown in Fig. III.2.2(2) and Fig. III.2.2.(3) using Catalyst C and geraniol. Another observation from Fig. III.2.2(2) is the drop in enantiomeric excess at 60^{o} after approximately 4 hrs., from e.e. 21% to $\sim$ 10%. This could be due to the dechiralisation of the catalyst that can occur either by the reversible replacement of the chiral ligand by product alcohol (Eqn. II.1.2(3))[57-59] or by reaction with the epoxide to form Mo(VI) diol complexes[33].

The pure epoxy alcohols isolated from the reaction at $28\text{-}32^{o}$ were converted into diastereomeric esters of Moshers acid[172]. The diastereomeric ratios determined by ^{19}F nmr, Fig. III.2.2(4), were in general agreement with those obtained in Fig. III.2.2(3).

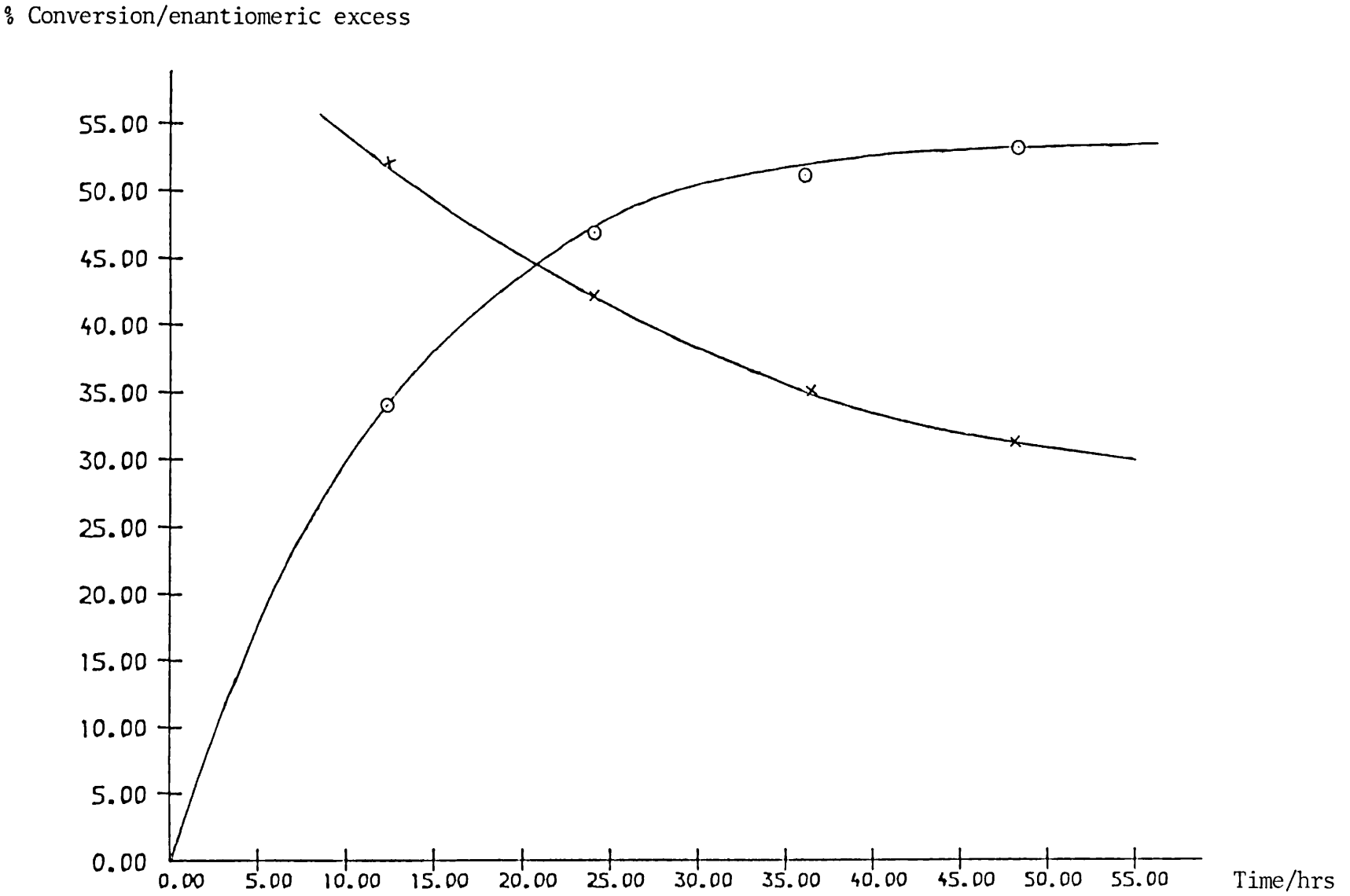

Fig. III.2.2(2) Conversion and optical purity vs. time in the enantioselective epoxidation of geraniol with TBHP catalysed by Catalyst C at 28°

$$o = \frac{\text{epoxy alcohol}}{\text{epoxy alcohol + allyl alcohol}} \times 100 \qquad x = \% \text{ optical purity}$$

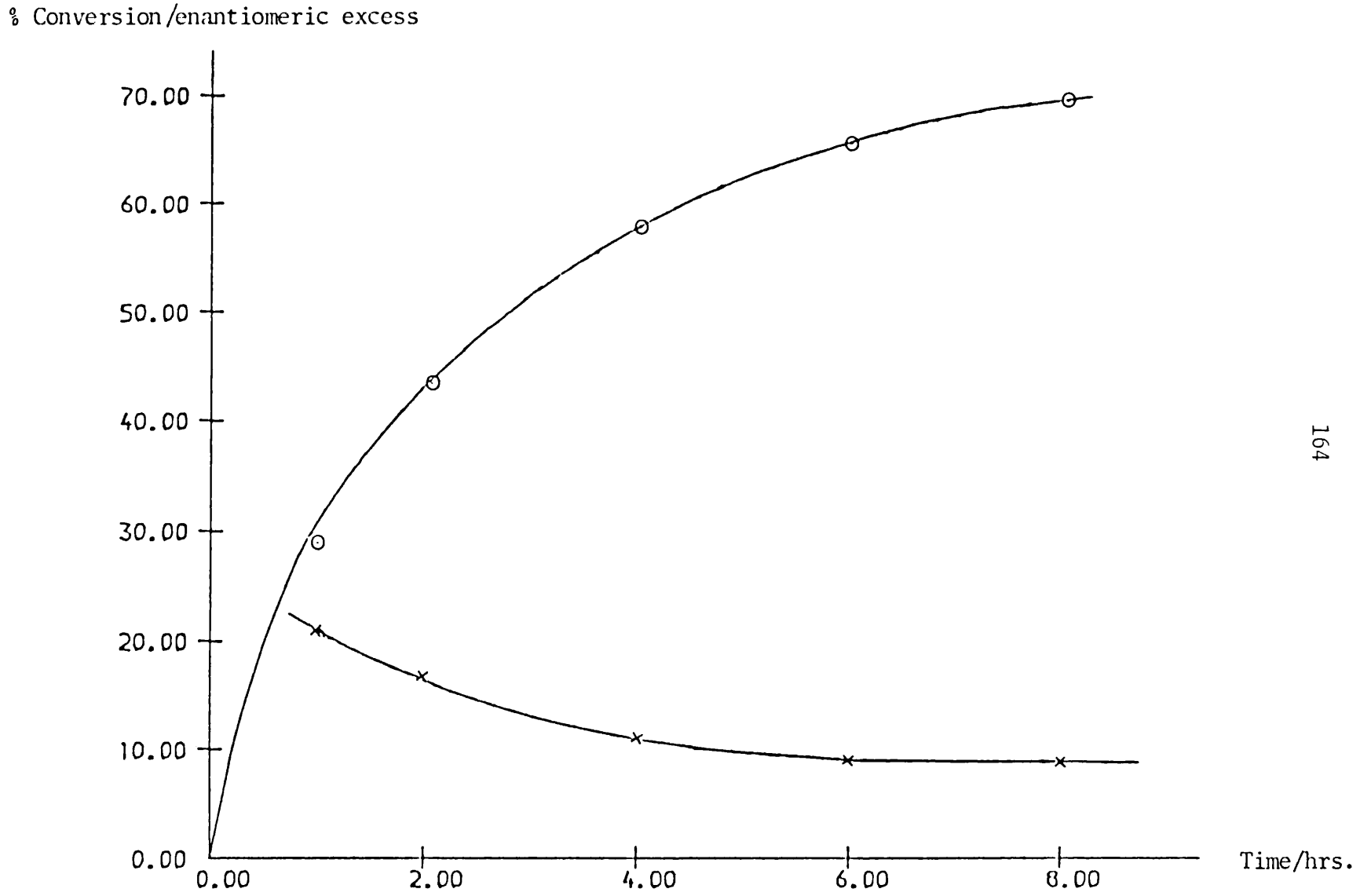

Fig. III.2.2(3) Conversion and optical purity vs. time in the enantioselective epoxidation of gernaiol with TBHP catalysed by Catalyst C at 60°.

$$O = \frac{\text{epoxy alcohol}}{\text{epoxy alcohol + allyl alcohol}} \times 100 \qquad x = \% \text{ optical purity.}$$

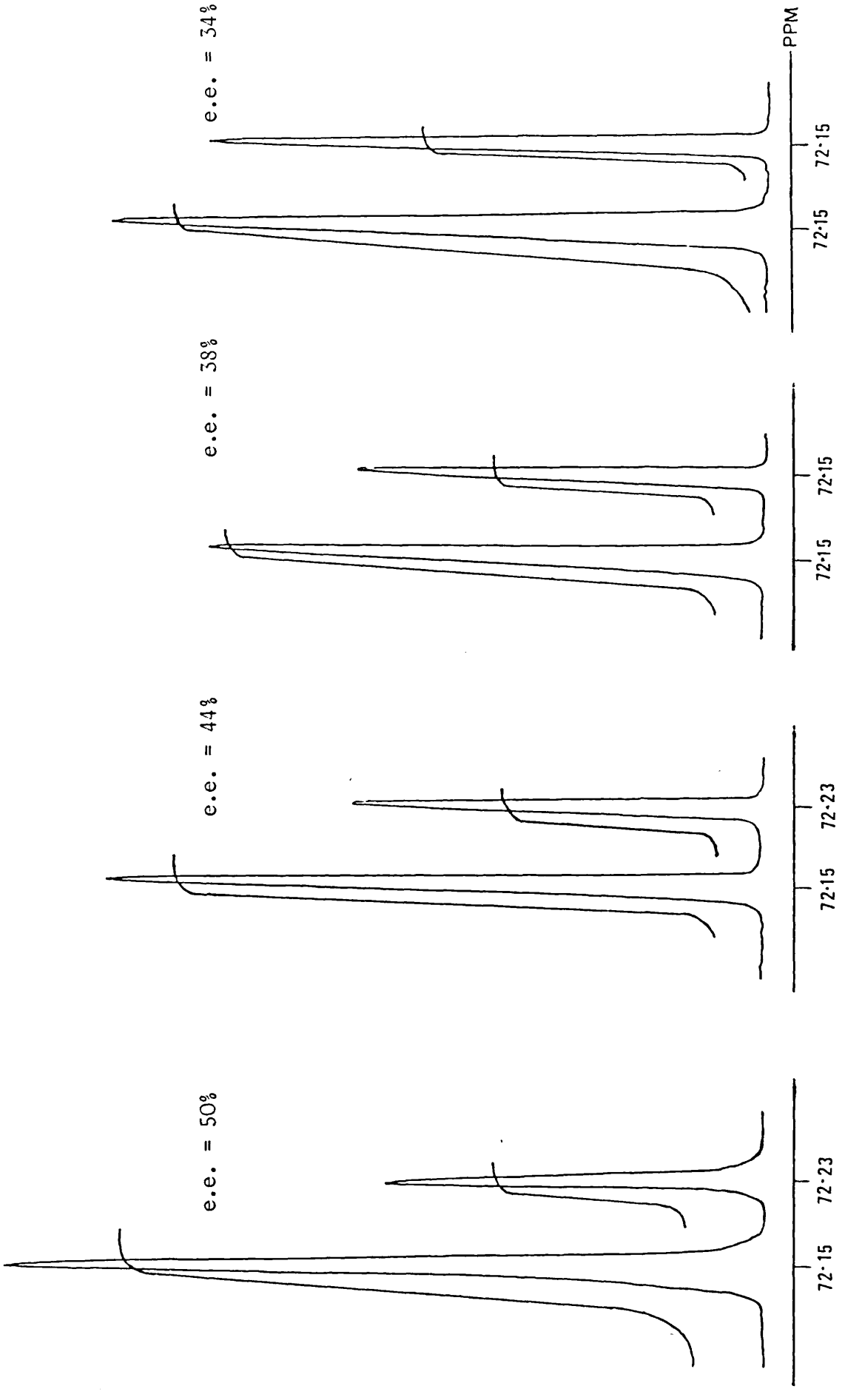

Fig. III.2.2(4) 235.36 Mlz ^{19}F nmr spectra of Diastereomeric esters of Moshers acid and geraniol oxide.

III.2.3a Asymmetric Epoxidation of Geraniol

Tables III.2.3(1) and III.2.3(2) show data obtained using similar reaction conditions, the only difference being choice of solvent. The performance of Catalysts D, E and F is not appreciably affected by a change of solvent. This is probably because these three catalysts are not very soluble in either of the solvents - a reflection of which is seen in low optical yields. However, this does not apply to Catalysts A, B and C. For Catalyst A, the asymmetric bias is higher in cyclohexane while for Catalysts B and C, the preference is for 1,2-dichloroethane These differencies in stereoselectivity with solvent change must be due to the preferential solvation of one of the competing transition states.

As discussed in the section on temperature studies (III.2.2), lowering the reaction rate leads to an increase in enantiomeric excess and a drop in chemical conversion. This is clearly observed when the data in Table III.2.3.(3) is compared with Tables III.2.3.(1) and III.2.3.(3). However this could become counterproductive as seen by Table III.2.3(4) where lowering the temperature to -20^{o} gave the best chemical conversion of only 6%.

The optical yields obtained by Catalysts B (e.e 69%) and C (e.e 60%) are higher than any of the data obtained by previous workers using molybdenum complexes - the previous best giving an optical yield of 50% [153].

III.2.3b Asymmetric Epoxidation of 3-Methyl-2-butene-1-ol

As discussed in Section III.2.3a (above), the same trends are followed when 3-methyl-2-butene-1-ol is epoxidised. However, from Tables III.2.3(5) and III.2.3(6), the striking feature is the higher chemical conversion and enantiomeric excess obtained by Catalysts A, B and C using 2-Methyl-2-butene-1-ol as substrate (cf geraniol). Using Catalysts D, E and F, similar enantiomeric excess is achieved with 3-Methyl-2-butene-1-ol and geraniol but higher chemical conversions are obtained with 3-Methyl-2-butene-1-ol. The higher chemical conversion could imply that there is a greater steric effect in geraniol.

In spite of the low concentrations of catalyst used in the asymmetric epoxidation summarised in Tables III.2.3(1) - III.2.3(8) inclusive, the enantiomeric excess values obtained tend to be favourable when compared with other groups[18,158,166] where considerably larger amounts of catalyst was employed.

Sharpless[173,174] found that (+)-2,3-butane diol as a ligand gave at best an enantiomeric excess of 10%. However, in this study, the best value obtained was 70% using Catalyst A. One of the problems posed in preparing the diol catalysts was getting rid of the excess diol - this being done as described earlier in Section I.3.2a. Failing to follow the process described in Section I.3.2a inevitably led to a large excess of diol in the reaction medium which presumably inhibited the formation of the epoxide (Section II.1.2.2).

III.2.3c Asymmetric Epoxidation of 1-Methylcyclohexene

See Tables III.2.3(7) and III.2.3(8).

Asymmetric Epoxidation of Geraniol (1g, 6.5mmole) at 28-32° using 1,2-dichloroethane as solvent .

Reaction Time 48 hr.

Catalyst	Mole equival. of Catalyst to substrate	Chemical[a] Yield/%	$[\alpha]_D^{25}$(C,$CHCl_3$)	Optical[b] Yield/%
A	0.02	50	-0.48°(19.5)	7
B	0.02	55	-1.50°(52.0)	21
C	0.02	53	+2.29°(42.2)	31
D	0.02	46	+0.29°(10.3)	4
E	0.02	48	+0.29°(82.1)	4
F	0.02	46	-0.05°(121.5)	1

a Calculated by glc, the percent of epoxy alcohol product plus the percent of unreacted allylic alcohol equals 100%.

b Expressed as percent enantiomeric excess. The optical rotation of optically pure 2,3-geraniol oxide was determined to be $[\alpha]_D^{20}$ = +7.33°($CHCl_3$) [18].

Table III.2.3(1)

Asymmetric Epoxidation of Geraniol (1g, 6.5mmole) at 28-32° using cyclohexane as solvent.

Reaction Time 48hr.

Catalyst	Mole equival. of Catalyst to substrate	Chemical[a] Yield/%	$[\alpha]_D^{25}(C,CHCl_3)$	Optical[b] Yield/%
A	0.02	51	-1.91°(48.1)	26
B	0.02	52	-0.46°(66.1)	6
C	0.02	52	+0.53°(49.2)	7
D	0.02	47	+0.15°(6.8)	2
E	0.02	48	+0.36°(66.1)	5
F	0.02	46	-0.16°(12.3)	2

a Calculated by glc, the percent of epoxy alcohol product plus the percent of unreacted allylic alcohol equals 100%.

b Expressed as percent enantiomeric excess. The optical rotation of optically pure 2,3-geraniol oxide was determined to be $[\alpha]_D^{20} = +7.33°(CHCl_3)$ [18].

Table III.2.3(2).

Asymmetric Epoxidation of Geraniol (1g, 6.5mmole) at 5°.

Reaction Time 14 days.

Catalyst	Mole equival. of Catalyst to substrate	Chemical[a] Yield/%	$[\alpha]_D^{25}(C,CHCl_3)$	Optical[b] Yield/%
A[c]	0.02	33	-2.79°(22.2)	38
B	0.02	36	-5.04°(27.8)	69
C	0.02	36	+4.39°(5.8)	60
D	0.02	29	+0.35°(18.6)	5
E	0.02	30	+0.42°(31.2)	6
F	0.02	28	-0.18° (14.8)	3

a Calculated by glc, the percent of epoxy alcohol product plus the percent of unreacted allylic alcohol equals 100%.

b Expressed as percent enantiomeric excess. The optical rotation of optically pure 2,3-geraniol oxide was determined to be $[\alpha]_D^{20} = +7.33°$ ($CHCl_3$).[18]

c With the exception of Catalyst A, the solvent used for the reactions was cyclohexane.

Table III.2.3(3)

Asymmetric Expoxidation of Geraniol (1g, 6.5mmole) at -20°.

Reaction Time 20 days.

These experiments were abandoned as the yields of the reaction were extremely low, making isolation of a sufficient quantity of pure geraniol oxide to measure enantiomeric excess difficult. However, epoxide yields were as follows:-

Catalyst	Mole equivalent of Catalyst to Substrate	Chemical[a] Yield/%
A	0.02	5
B	0.02	6
C	0.02	6
D	0.02	2
E	0.02	2
F	0.02	2

a Calculated by glc, the percent of epoxy alcohol product plus the percent of unreacted allylic alcohol equals 100%.

b With the exception of Catalyst A, the solvent used for the reactions was 1,2-dichloroethane. For A, the solvent used was cyclohexane.

Table III.2.3(4)

Asymmetric Epoxidation of 3-Methyl-2-butene-1-ol (1g, 11.61mmole) at 23-4°

Reaction Time 48 hr.

Catalyst	Mole equival. of Catalyst to substrate	Chemical[a] Yield/%	$[\alpha]_D^{25}$(c,$CHCl_3$)	Optical[b] Yield/%
A[c]	0.02	54	-8.50°(52.4)	46
A	0.02	53	-0.69°(49.1)	4
B	0.02	55	-2.22°(38.4)	12
C	0.02	58	+11.42°(18.9)	62
D	0.02	43	+0.46°(26.8)	3
E	0.02	46	+0.31°(44.9)	2
F	0.02	49	-0.75°(74.2)	4

a Calculated by glc, the percent of epoxy alcohol product plus the percent of unreacted allylic alcohol equals 100%.

b Expressed as a percent enantiomeric excess. The optical rotation of optically pure 3-methyl-2-butene-1-ol oxide was determined to be $[\alpha]_D^{20}$= +18.4° ($CHCl_3$) [18].

c Solvent used was cyclohexane. In all other examples, 1,2-dichloroethane was used as solvent.

Table III.2.3(5)

Asymmetric Epoxidation of 3-Methyl-2-butene-1-ol (1g, 11.61mmole) at 5°.

Reaction Time 14 days.

Catalyst	Mole equival. of Catalyst to substrate	Chemical[a] Yield/%	$[\alpha]_D^{25}$(c,$CHCl_3$)	Optical[b] Yield/%
A[c]	0.02	41	-12.95°(11.3)	70
B	0.02	42	-11.11°(15.9)	60
C	0.02	42	+15.67°(13.4)	85
D	0.02	37	+1.06°(38.3)	6
E	0.02	38	+0.55°(4.5)	3
F	0.02	36	-0.96°(16.0)	5

a Calculated by glc, the percent of epoxy alcohol product plus the percent of unreacted allylic alcohol equals 100%.

b Expressed as a percent enantiomeric excess. The optical rotation of optically pure 3-methyl-2-butene-1-ol oxide was determined to be $[\alpha]_D^{20}$= +18.4° ($CHCl_3$).[18]

c With the exception of Catalyst A, the solvent used for the reactions was 1,2-dichloroethane. For A, the solvent used was cyclohexane.

Table III.2.3(6)

Asymmetric Epoxidation of 1-Methylcyclohexene (1g, 10.39mmole) at 23.4°

Reaction Time 48 hr.

Catalyst	Mole equival. of Catalyst to substrate	Chemical[a] Yield/%	$[\alpha]_D^{25}$(c,$CHCl_3$)	Optical[b] Yield/%
A[c]	0.02	76	-1.67°(18.4)	9
B	0.02	81	-2.23°(42.6)	12
C	0.02	78	+7.17°(12.6)	38
D	0.02	65	+1.12°(18.3)	6
E	0.02	72	+0.75°(44.8)	4
F	0.02	69	-0.93°(8.4)	5

a Calculated by glc, the percent of epoxy alcohol product plus the percent of unreacted allylic alcohol equals 100%.

b Expressed as percent enantiomeric excess. The optical rotation of optically pure 1-methylcyclohexene oxide was determined to be $[\alpha]_D^{20}$ = -18.65°(neat)[161].

c With the exception of Catalyst A, the solvent used for the reactions was 1,2-dichloroethane. For A, the solvent used was cyclohexane.

Table III.2.3(7).

Asymmetric Epoxidation of 1-Methylcyclohexene (1g, 10.39mmole) at 5°

Reaction Time 14 days.

Catalyst	Mole equival. of Catalyst to substrate	Chemical[a] Yield/%	$[\alpha]_D^{25}$(c,$CHCl_3$)	Optical[b] Yield/%
A[c]	0.02	65	-2.98°(14.3)	16
B	0.02	68	-3.54°(10.1)	19
C	0.02	64	+10.15°(18.6)	54
D	0.02	58	+1.58°(11.3)	8
E	0.02	60	+1.72°(12.4)	9
F	0.02	55	-1.43°(10.3)	7

a Calculated by glc, the percent of expoxy alcohol product plus the percent of unreacted allylic alcohol equals 100%.

b Expressed as percent enantiomeric excess. The optical rotation of optically pure 1-Methylcyclohexene oxide was determined to be $[\alpha]_D^{25}$ = -18.65°(neat)[161].

c With the exception of Catalyst A, the solvent used for the reactions was 1,2-dichloroethane. For A, the solvent used was cyclohexane.

Table III.2.3(8).

CHAPTER III SECTION 3

III.3.1 Purification of reagents

Chloroform was dried over calcium hydride and distilled under nitrogen. It was then stored over molecular sieves (type 4A).

Cyclohexane was dried over calcium hydride and distilled under nitrogen. It was then stored over molecular sieves (type 4A).

1,2-dichloroethane was dried over calcium hydride and distilled under nitrogen. It was then stored over molecular sieves (type 4A).

Pet Ether (below 40) was distilled over a 50 cm Vigreux column.

Pyridine was distilled over sodium hydroxide under nitrogen. It was then stored over molecular sieves (type 4A).

Thionyl chloride was dried by distillation from 10% (w/w) triphenyl phosphite under nitrogen.

III.3.2 General Experimental Methods

All glassware was thoroughly dried overnight in an oven. In all cases, standard Quickfit glassware was used.

III.3.2.a NMR

^{19}F nmr samples in $CFCl_3$ were run on a Brüker spectrometer at 235.36 MHz.

^{1}H and ^{13}C nmr samples in $CDCl_3$ were run on a Brüker spectrometer at 400.13 MHz and 100.62 MHz respectively.

III.3.2b GC/MS

A Pye Unicam 104, interfaced to a Kratos MS25 mass spectrometer was used for analysis for all products. Electron-Impact (E.I.) mass-spectra were recorded.

General glc conditions

Column: 10% Carbowax 20M (Chromasorb WAW)

Length of column: 2.8m

Column diameter: 0.4 mm

Flow rate: 40 cm^3 min^{-1}

Solvent: $CHCl_3$

Carrier gas - Helium.

(i) Geraniol oxide

Column Temperature 190° (isothermal)

Detector Temperature 260°

Injector Temperature 240°.

(ii) 3-Methyl-2-butene-1-ol oxide

Column Temperature 160° (isothermal)

Detector Temperature 240°

Injector Temperature 220°.

(iii) 1-Methylcyclohexene oxide

Column Temperature 60° (isothermal)

Detector Temperature 160°

Injector Temperature 140°.

III.3.2c Flash Chromatography

For a reference to this technique, see the paper by Still et al.[175]

Length of column: 50 cm

Diameter of column: 25 mm

Flow rate : 5 cm min^{-1}.

Packing material Kieselgel 60 Merck 9385 (230 - 400 mesh).

Solvent Systems	Ethyl Acetate: Pet Ether (below 40)
(i) Geraniol oxide	50:50
(ii) 3-Methyl-2-butene-1-ol oxide	60:40
(iii) 1-Methylcyclohexene oxide	25:75

III.3.2d Thin layer chromatography

POLYGRAM^{R} SIL G (0.25 mm Silica Gel) plates were used.

Solvent Systems

(i) Geraniol oxide

Ethyl Acetate Pet Ether (below 40) 50:50

Detector:[176]

The tlc plate was sprayed with a solution of 0.05% Fluorescein in water and then exposed to bromine vapour.

This gives a yellow spot on a pink background.

(ii) 3-Methyl-2-butene-1-ol oxide[177]

The developing system was Petroleum Ether (20 - 40^{o}) - diethyl ether - acetic acid (75:25:1). After developing, the plate was sprayed thoroughly with 0.05M picric acid in 95% ethanol and immediately placed in a tank saturated with

the vapour of diethyl ether - 95% ethanol-acetic acid solution (80:20:1). Thirty minutes later, the plate was removed and exposed to ammonia fumes for 1–2 mins. The epoxide spot appeared as an orange spot on a yellow background.

(iii) 1 - Methylcyclohexene oxide

The same method as that used for 3-Methyl-2-butene-1-ol oxide was used for 1, Methylcyclohexene oxide.

III.3.2e Measurement of enantiomeric excess using a polarimeter

A Perkin Elmer 241 Polarimeter was used to measure enantiomeric excess. Approximately 200 mg of pure epoxide was made up to 2 cm^3 with dry $CHCl_3$. The optical rotation of the epoxide was measured in a polarimetric cell (length = 1 dm) using a sodium lamp (λ = 589 nm).

III.3.2f Measurement of enantiomeric excess using ^{19}F nmr[172]

The values obtained by ^{19}F nmr were compared with those obtained by polarimetry. Generally, good agreement was obtained from both sets of data. However, olefins could not be measured by this method.

Preparation of (-)-α-methoxy-α-trifluoromethylphenylacetyl chloride [(-)-MTPA-Cl] [172]

(-)-MTPA (5 g, 22.5 mmole), freshly distilled thionyl chloride (15 ml) and sodium chloride (60 mg) were refluxed together for 50 hrs. Excess thionyl chloride was removed under vacuum, the residue, distilled under vacuum to give 5.2 g (90%), bp 53 - 57° (1 mm).

nmr OMe, 3.4 ppm, 3 protons; Ph, 7.5 ppm, 5 protons.

Preparation of ester from (-)-MTPA-Cl and allylic alcohol oxide for ^{19}F nmr

In order to measure enantiomeric excess by ^{19}F, the allylic alcohol oxide (I) was reacted with (-)-MTPA-Cl(II) to form the diastereomeric esters (IIIA) and (IIIB).

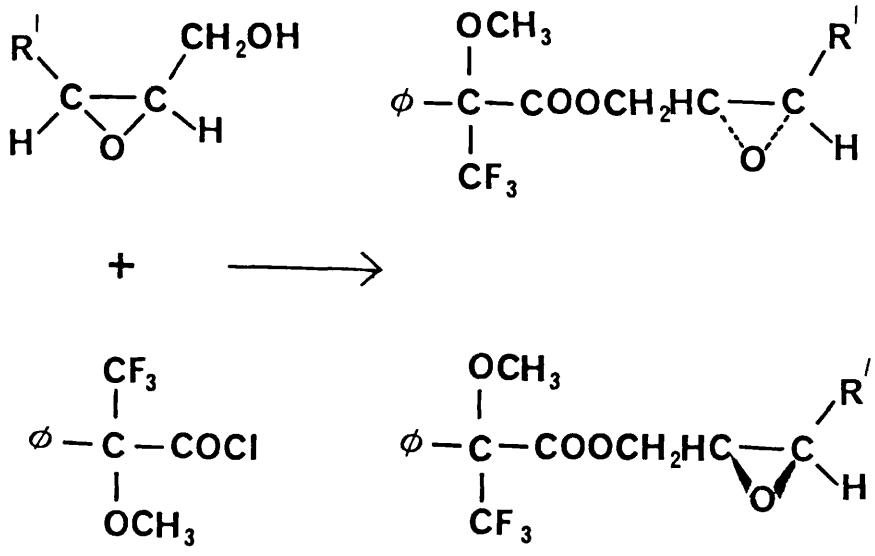

(-)-MTPA-Cl (0.045 g, 0.18 mmole) and the pure allylic alcohol oxide (0.15 mmole) obtained from the asymmetric epoxidation of the allylic alcohol were allowed to stand for 1 hr in 0.5 cm^3 of dry pyridine. Water was added to the cooled mixture which was then extracted with diethyl ether (20cm^3). The ether extract was washed successively with water, dilute sodium carbonate solution, dried ($MgSO_4$) and evaporated to give a residual oil. ^{19}F nmr showed the two enantiomers.

III.3.2g General Experimental Methods for Asymmetric Epoxidation

III.3.2g (i) Reactions carried out at 60-1°

	Geraniol	3-Methyl-2-butene-1-ol
Substrate	5 g, 32.4 mmole	5 g, 58.05 mmole
Catalyst	0.648 mmole	1.16 mmole
TBHP	32.4 mmole	58.05 mmole
Solvent	150 cm^3	150 cm^3

To a three necked 250 cm^3 round bottomed flask charged with a teflon coated magnetic stirrer and thoroughly flushed with nitrogen was added the substrate, catalyst and solvent. The reaction mixture was brought to 60°. Dropwise addition of TBHP was carried out over 5 mins - during the addition of TBHP, the source of heat was removed from the reaction vessel. On the completion of the TBHP addition, the source of heat was turned on and maintained at 60 - 1°.

5 cm^3 aliquots of the reaction mixture were taken from the reaction vessel every two hours for nine hours, chilled in ice and passed through a column packed with Florisil (Column diameter 1 cm, Florisil packed up to 10 cm). The solvent was then removed under vacuo and the residual oil purified by flash chromatography. All measured yields were carried out using the residual oil and measured by glc.

III.2.3g (ii) Reactions carried out at 28-32°, 23-24°, 5°, -20°

(Reactions carried out at 5° and -20° were performed in constant temperature rooms).

	Geraniol	3-Methyl-2-butane-1-ol	1, Methylcyclohexene
Substrate	1g,6.5 mole	1 g, 11.61 mmole	1 g, 10.4 mmole
Catalyst	0.13 mmole	0.232 mmole	0.208 mmole
TBHP	6.5 mmole	11.61 mmole	10.4 mmole
Solvent	20 cm^3	20 cm^3	20 cm^3

Length of reaction times

23-4° and 28-32° - 2 days

5° - 14 days

-20° - 30 days

To a B24 round bottomed flask charged with a teflon coated magnetic stirrer was added the substrate, catalyst, solvent and TBHP. The mixture was degassed by the 'freeze-thaw' method and kept under nitrogen. After terminating the reaction, the procedure for the work-up was the same as that described in III.3.2g (i).

III.3.3 Spectroscopic Data

III.3.3a 400.13 MHz ^{1}H nmr spectrum of Geraniol Oxide

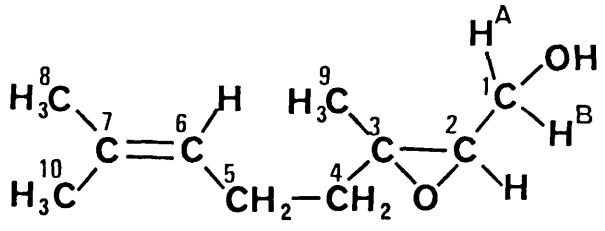

$^1CH^A$ 3.57 ppm, d.d; J_{HH^A} = 6.85 Hz, $J_{H^AH^B}$ = 12.16 Hz; 1 proton

$^1CH^B$ 3.71 ppm, d.d; J_{HH^B} = 3.98 Hz, $J_{H^AH^B}$ = 12.15 Hz; 1 proton

^2CH 2.90 ppm, d.d; J_{HH^A} = 4.12 Hz, J_{HH^B} = 6.77 Hz; 1 proton

$^4CH_2$ 1.56 ppm, m; 1 proton

1.40 ppm, m; 1 proton

$^5CH_2$ 2.01 ppm, m; 2 protons

^6CH 4.99 ppm, t; J = 7.12 Hz; 1 proton

$^8CH_3$ 1.60 ppm or 1.52 ppm, s; 3 protons

$^9CH_3$ 1.21 ppm, s; 3 protons

$^{10}CH_3$ 1.52 ppm or 1.60 ppm, s; 3 protons

-OH 3.48 ppm, s; 1 proton.

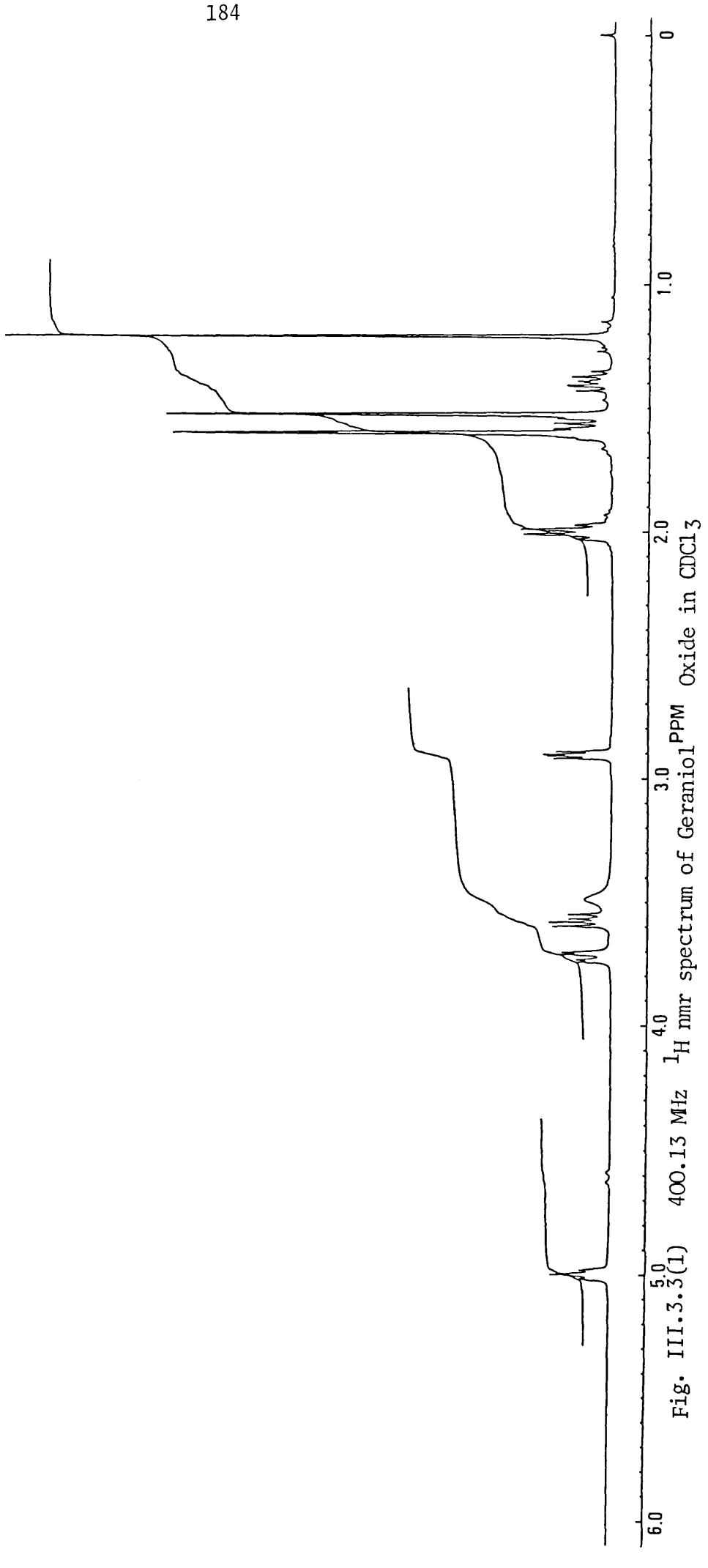

Fig. III.3.3(1) 400.13 MHz ^1H nmr spectrum of Geraniol Oxide in $CDCl_3$

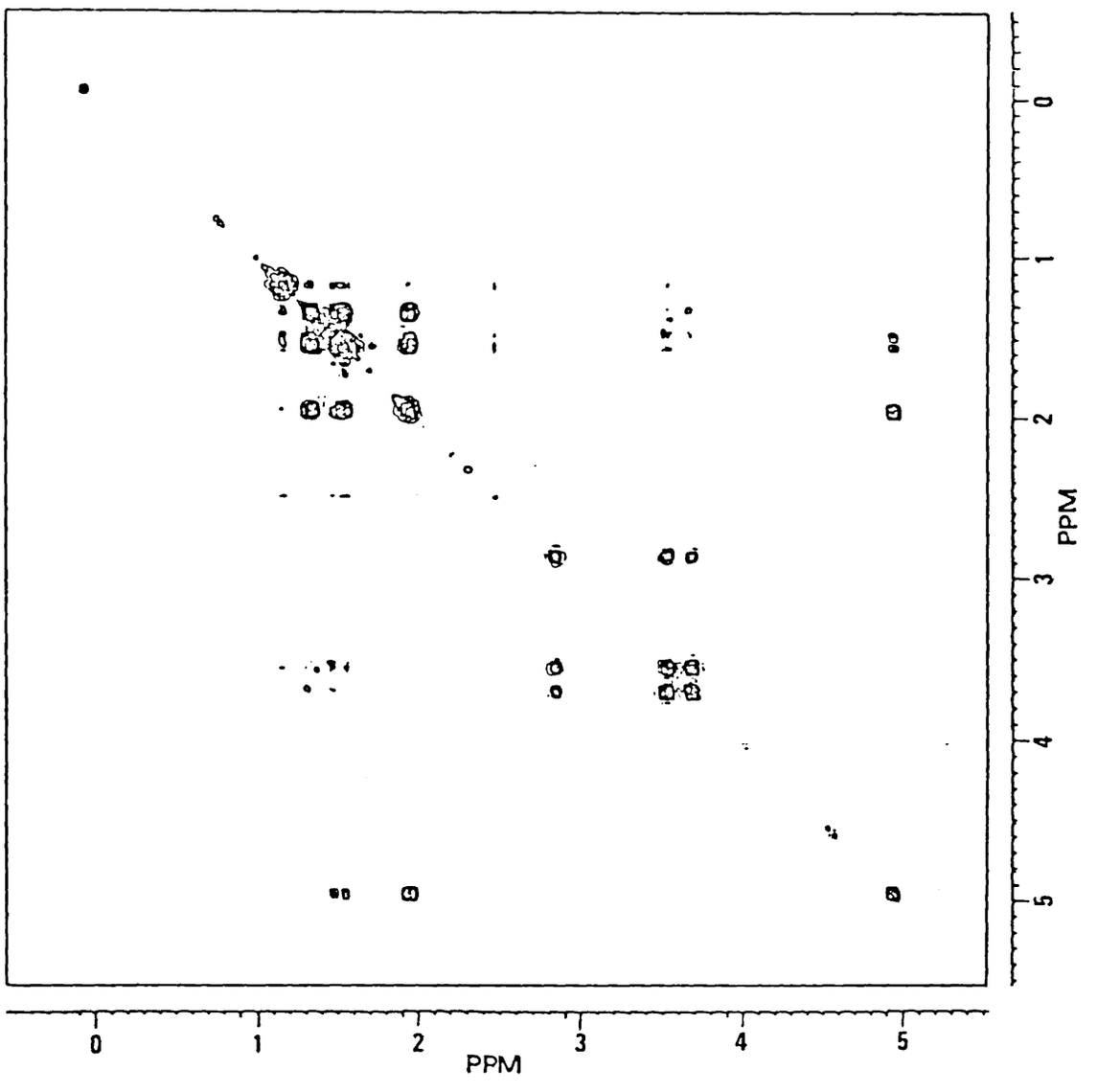

Fig. III.3.3.(2) 400.13MHz 2D ^{1}H-^{1}H correlation of Geraniol Oxide.

III.3.3b 100.62 MHz ^{13}C nmr spectrum of Geraniol Oxide

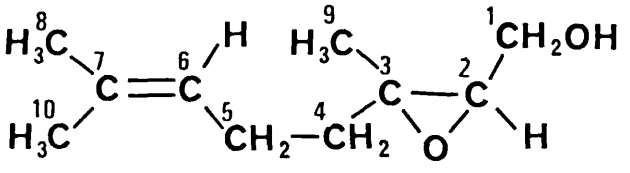

C-1	61.35 ppm
C-2	62.96 ppm
C-3	38.42 ppm
C-4	25.58 ppm
C-5	61.12 ppm
C-6	123.23 ppm
C-7	132.03 ppm
C-8	17.57 ppm or 23.60 ppm
C-9	16.68 ppm
C-10	23.60 ppm or 17.57 ppm

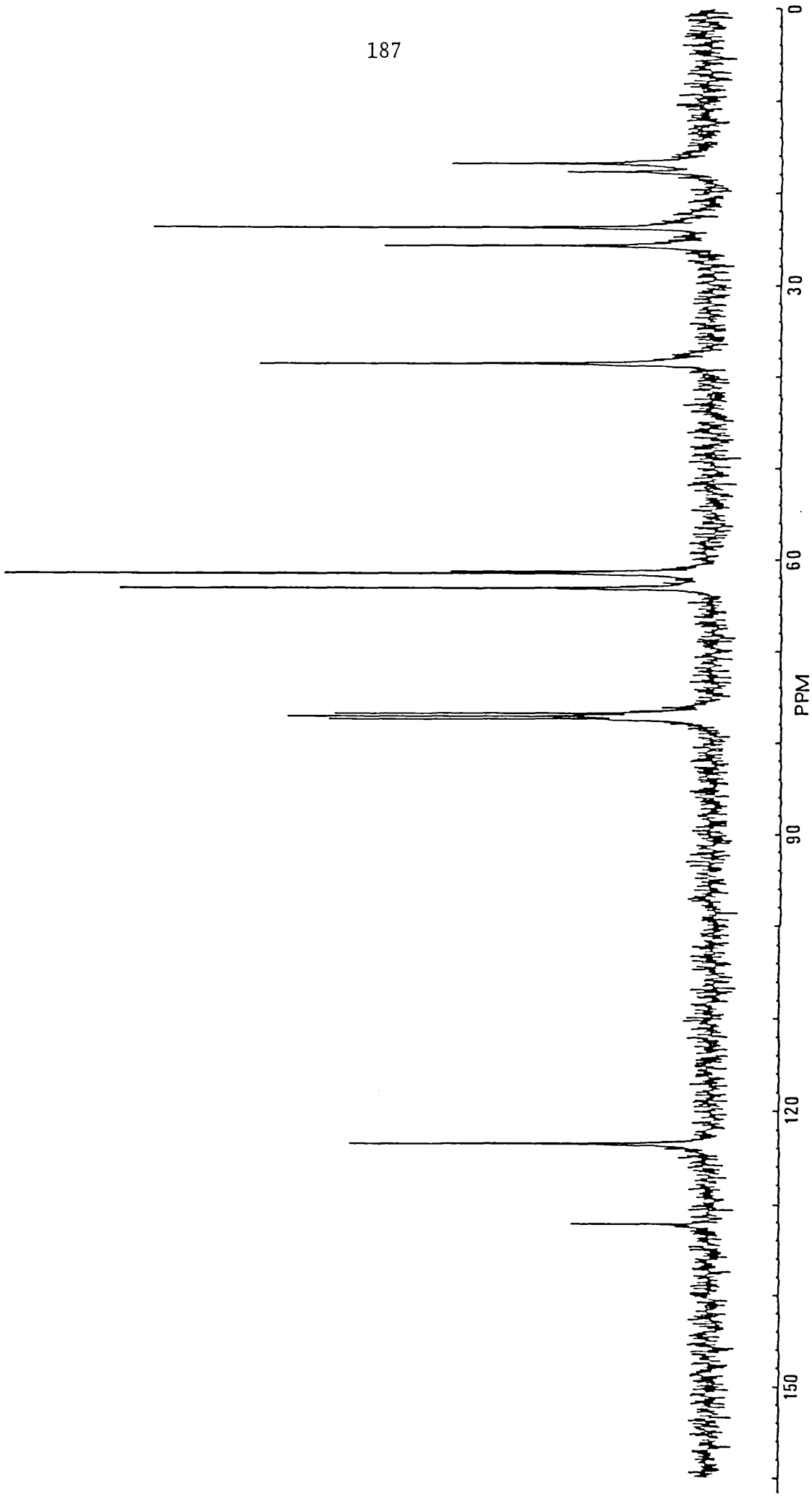

Fig. III.3.3 (3) 100.62MHz $^{13}C\{^{1}H\}$nmr spectrum of Geraniol Oxide in $CDCl_3$

III.3.3c 400.13 MHz ^{1}H nmr spectrum of 3-Methyl-2-butene-1-ol oxide

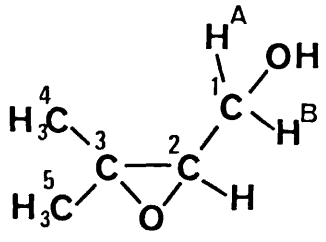

$^{1}CH^{A}$	3.64 ppm, d.d; $J_{HH}A$ = 6.80 Hz, $J_{H}A_{H}B$ = 12.19 Hz; 1 proton
$^{1}CH^{B}$	3.80 ppm, d.d; $J_{HH}B$ = 4.20 Hz, $J_{H}A_{H}B$ = 12.17 Hz; 1 proton
^{2}CH	2.97 ppm, d.d; $J_{HH}A$ = 6.78 Hz, $J_{HH}B$ = 4.21 Hz; 1 proton
$^{4}CH_{3}$	1.29 ppm or 1.33 ppm, s; 3 protons
$^{5}CH_{3}$	1.33 ppm or 1.29 ppm, s; 3 protons
-OH	2.73 ppm, b; 1 proton.

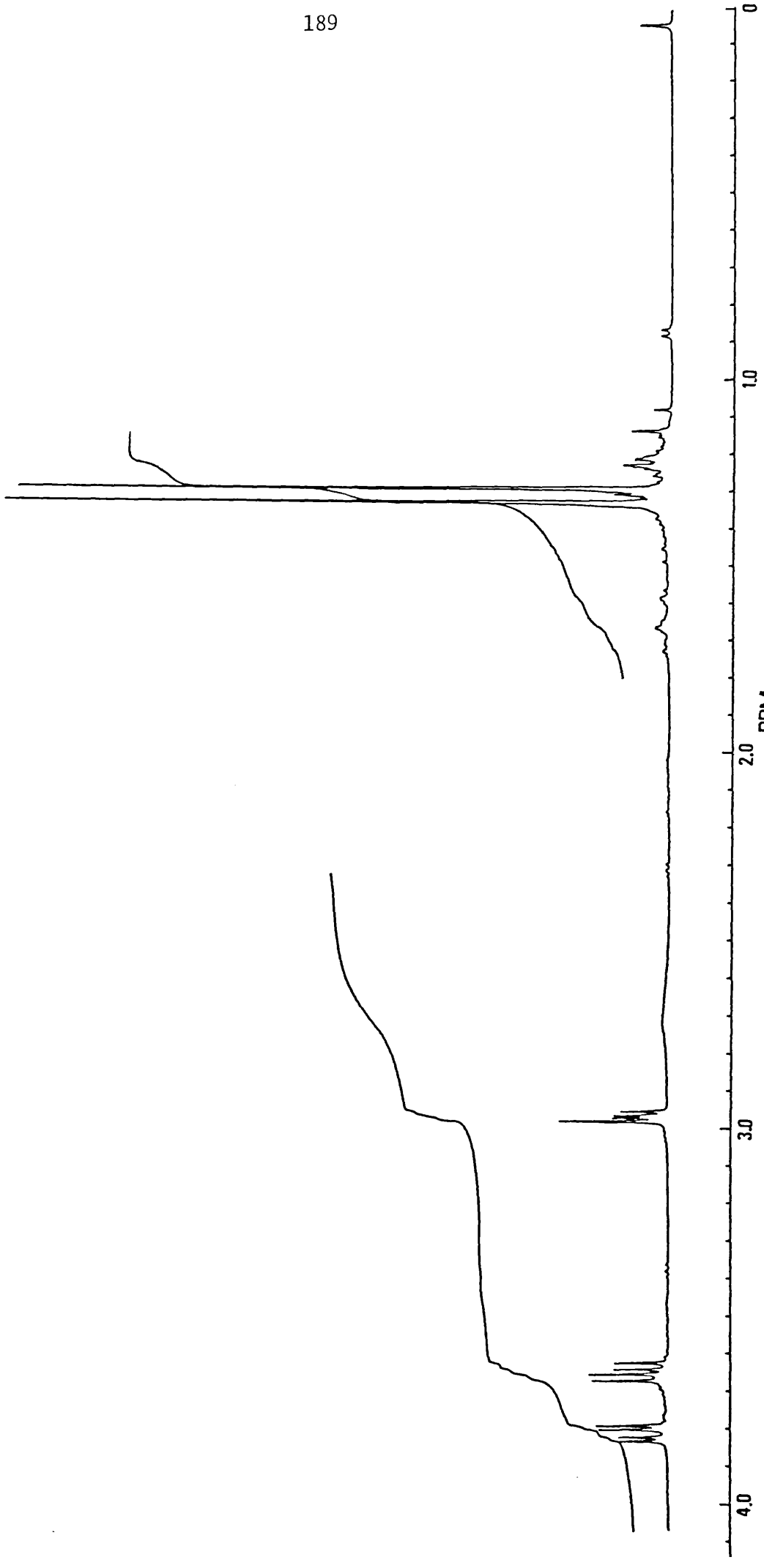

Fig. III.3.3(4) 400.13MHz ^1H nmr spectrum of 3-Methyl-2-butene-1-ol oxide in $CDCl_3$.

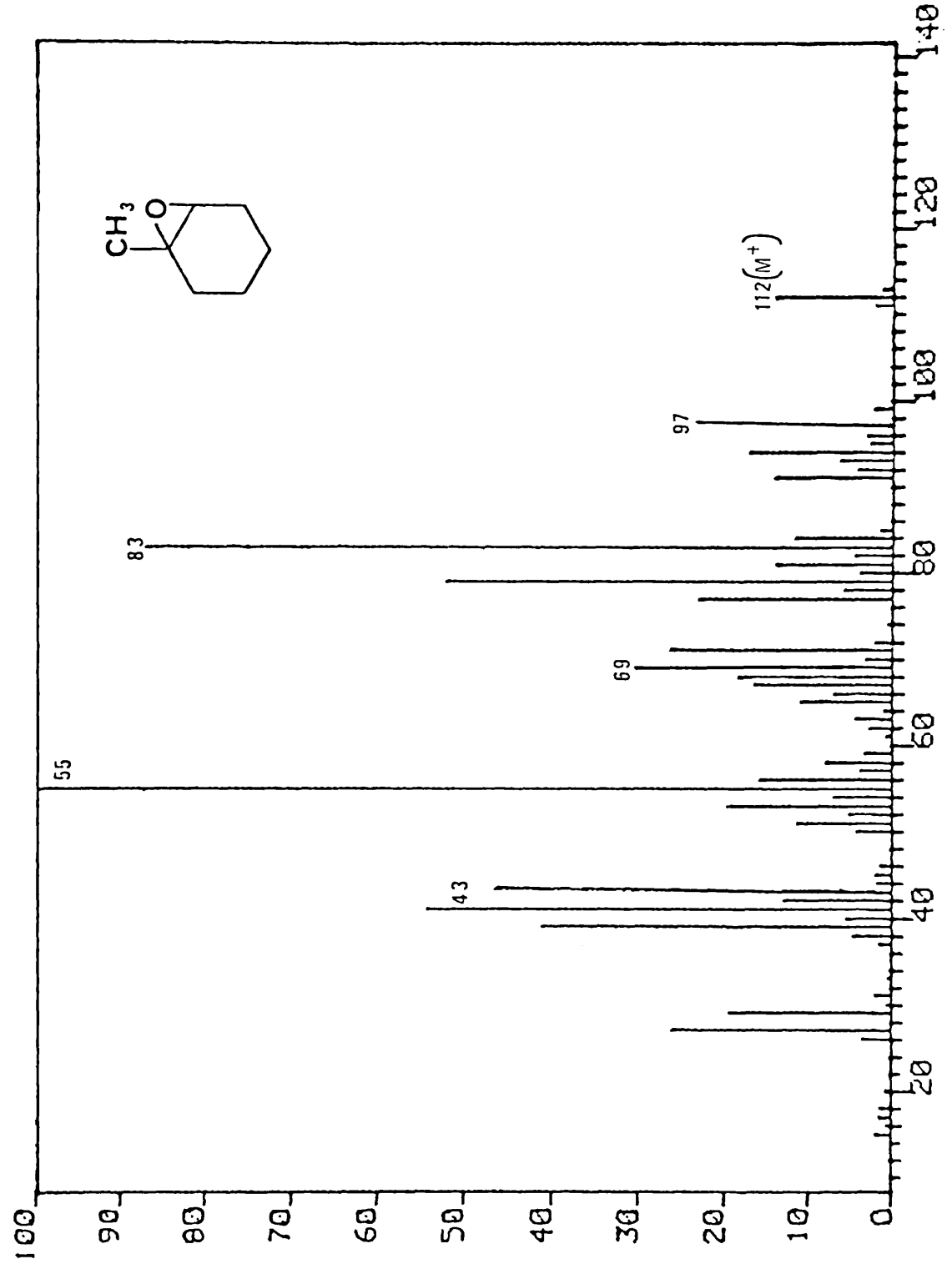

Table III.3.3(5) E.I./MS of 1-Methylcyclohexene oxide.

REFERENCES

1. E.I. Stiefel, Prog.Inorg.Chem., 22, 1 (1977).
2. 'Molybdenum Chemistry of Biological Significance' (Eds. W.E. Newton and S. Otsuka), Plenum Press : New York (1980).
3. 'Molybdenum and Molybdenum Containing Enzymes' (Ed. M.P. Coughlan.) Pergamon Press : New York (1980).
4. C.D. Garner, Coord.Chem.Rev., 37, 117 (1981).
5. C.D. Garner, Coord.Chem.Rev., 45, 153 (1982).
6. A. Muller, W. Jaegermann and J.H. Enemark, Coord.Chem.Rev., 46, 245 (1982).
7. J. Kollar, Belgian Patent 657838 (1964).
8. M.N. Sheng and J.G. Zajacek, Advan.Chem.Ser. 76, 418 (1968).
9. N.V. Sidgwick in 'Chemical Elements and Their Compounds', Oxford University Press, Vol. 2, p.1032-1053, (1950).
10. F.A. Cotton and G. Wilkinson in 'Advanced Inorganic Chemistry', p.867, Pub. Wiley-Interscience, 4th edition (1980).
11. P.C.H. Mitchell, Quart.Rev., 20, 103 (1966).
12. R.J. Butcher, H. Kipton, J. Powell, C.J. Wilkins and S.H. Yong, JCS (Dalton), 356 (1976).
13. F.A. Schroder, Acta Cryst., B31, 2294 (1975).
14. F.A. Schroder, J. Scherle and R.G. Hazell, Acta Cryst., B31, 531 (1975).
15. R.J. Butcher, B.R. Penfold and E. Sinn, JCS (Dalton), 668 (1979).
16. A.J. Matheson and B.R. Penfold, Acta Cryst., B31, 2707 (1979).
17. B.M. Craven, K.C. Ramsey and W.B. Wise, Inorg.Chem., 10, 2626 (1971).
18. S. Yamada, T. Mashiko and S. Terashima, J.Amer.Chem.Soc., 99, 1988 (1977).

19. T. Mashiko, S. Terashima and S. Yamada, Yakugaku Zasshi, 100, 319 (1980).

20. I. Buchanan, M. Minelli, M.T. Ashby, T.J. King, J.H. Enemark and C.D. Garner, Inorg.Chem., 23, 495 (1984).

21. I. Buchanan, C.D. Garner and W. Clegg, JCS (Dalton), 1333 (1984).

22. C. Knobler, B.R. Penfold, W.T. Robinson, C.J. Wilkins and S.H. Yong, JCS (Dalton) 248 (1980).

23. M. Karplus, J.Chem.Phys., 30, 11 (1959).

24. H. Conroy, 'Nuclear Magnetic Resonance in Organic Structural Elucidation' in 'Advances in Organic Chemistry', (Ed. R.A. Raphael, E.C. Taylor and H. Wynberg), Vol. 2, p.265, Interscience, New York (1960).

25. F.W. Wehrli and T. Wirthlin, 'Interpretation of ^{13}C NMR spectra' p.47, Pub. Heyden.

26. W. Beck, W. Petri and J. Meder, J.Organomet.Chem., 191, 73 (1980).

27. R. Benn and H. Gunther, Angewandte Chemie, 22, 350 (1983).

28. S.R. Hartmann and E.L. Hahn, Phys.Rev., 128, 2042 (1962).

29. A. Pines, M.G. Gibby and J.S. Waugh, J.Chem.Phys., 59, 569 (1973).

30. D.E. Demco, J. Tegenfeldt and J.S. Waugh, Phys.Rev., B11, 4133 (1975).

31. J. Schaefer, E.O. Stejskal and R. Buchdahl, Macromolecules, 10, 384 (1977).

32. J. Gombes, E. Haslinger, U. Schmidt, Chem.Ber., 109, 2645 (1976).

33. R.A. Sheldon, Recueil Trav.Chim.Pay.Bas., 92, 367 (1973).

34. N. Prilezhaev, J.Russ.Phys.Chem.Soc., 44, 613 (1912).

35. D. Swern, Chem.Rev., 45, 1 (1949).

36. D. Swern, in 'Organic Reactions', New York, Wiley, 7, Ch. 7 (1953).

37. D. Swern, Ed., 'Organic Peroxides', New York, Wiley, Vol. II, 86 (1971).

38. V.G. Dryuk, Tetrahedron, 32, 2855 (1976).

39. D.I. Metelitsa, Russ.Chem.Rev., 41, 807 (1972).

40. E.G.E. Hawkins, J.Chem.Soc., 2169 (1950).

41. W.F. Brill, J.Amer.Chem.Soc., 85, 141 (1963).

42. W.F. Brill and N. Indictor, J.Org.Chem., 29, 710 (1964).

43. G. Sosnovsky and D.J. Rawlinson in 'Organic Peroxides' (D. Swern, Ed.) Vol. II, 153 (1971).

44. A.G. Davies, 'Organic Peroxides', London, Butterworth (1961).

45. N. Indictor and W.F. Brill, J.Org.Chem., 30, 2074 (1965).

46. E.S. Gould, R.R. Hiatt and K.C. Irwin, J.Amer.Chem.Soc., 90, 4573 (1968).

47. F. Mashio and S. Kato, Mem.Fac.Indus.Arts, Scien.Technol., 16, 79 (1967).

48. R.A. Sheldon, Recl.Trav.Chim.Pays-Bas, 92, 253 (1973).

49. R.A. Sheldon and J.A. Van Doorn, J.Catal., 31, 427 (1973).

50. G.R. Howe and R.R. Hiatt, J.Org.Chem., 35, 1839 (1970).

51. C.C. Su, J.W. Reed and E.S. Gould,Inorg.Chem., 12, 337 (1973).

52. G.R. Howe and R.R. Hiatt, J.Org.Chem., 36, 2493 (1971).

53. M.I. Farberov, G.A. Stozhkova, A.V. Bondarenko and T.M. Kirik, Kinet.Katal., 13, 291, (1972).

54. T.N. Baker III, G.J. Mains, M.N. Sheng and J.G. Zajacek, J.Org.Chem., 38, 1145 (1973).

55. R.A. Sheldon and J.A. Van Doorn, J.Catal., 31, 438 (1973).

56. R.A. Sheldon and J.A. Van Doorn, J.Catal., 34, 242 (1974).

57. R.A. Sheldon in 'Aspects of Homogeneous Catalysis', (R. Ugo, Ed), Vol. 4, D. Reidel, Dordrecht p.3 (1981).

58. T.N. Baker III, G.J. Mains, M.N. Sheng and J.G. Zajacek, J.Org.Chem., 38, 1145 (1973).

59. M.I. Farberov, G.A. Stozhkova, A.V. Bondarenko and T.M. Kirik, Int.Chem.Eng., 12, 634 (1972); Kinet.Katal (Eng.Trans.), 13, 263 (1972).

60. F. Trifiro, P. Forzatti, S. Priete and J. Pasquon, J.Less Common Mets., 36, 319 (1974).

61. M.N. Sheng, J.G. Zajacek and T.N. Baker III, 'Symposium on new olefin chemistry', Amer.Chem.Soc., Div.Petrol.Chem., 15, E19 (1970).

62. S.W. Benson, 'The Foundations of Chemical Kinetics', New York, McGraw Hill (1960).

63. M.N. Sheng and J.G. Zajacek, J.Org.Chem., 35, 1839 (1970).

64. A.O. Chong and K.B. Sharpless, J.Org.Chem., 42, 1587 (1977).

65. J. Mimoun, I. Seree de Roch and L. Sajus, Tetrahedron, 26, 37 (1970) (Fr.).

66. I.P. Skibida and P. Kok, Bull.Akad.Sci. (USSR), 23, 2599 (1974).

67. J. Mimoun, J.Mol.Catal., 7, 1 (1980).

68. G. Descotes and P. Legrand, Bull.Soc.Chim.Fr., 7, 2947 (1972) (Fr.).

69. M.I. Farberov, G.A. Stozhkova, A.V. Bondarenko and A.L. Glusker, Neftekhimiya, 10, 218 (1970) (Russ.); (Chem.Abstr., 73, 44620).

70. P. Koelewyn, British Patent, 1 303 403 (1973); Chem.Abstr., 78, 124428.

71. F. Mashio and S. Kato, Yuki Gosei Kayaku Shi., 26, 367 (1968) (Jap.); (Chem.Abstr., 69, 18476).

72. M.N. Sheng and J.G. Zajacek, Canadian Patents, 799,502-4, (1968).

73. K.A. Allison, P. Johnson, G. Foster and M. Sprake, Ind.Eng.Chem. Prod.Res.Develop., 5, 166 (1966).

74. P. Forzatti and F. Trifiro, React.Kinet.Catal.Lett., 1, 367 (1974).

75. P. Forzatti, F. Trifiro and I. Pasquon, Chimica e l'Industria, 56, 259 (1974) (Ital.).

76. M. Mudgen and D.P. Young, J.Chem.Soc., 2899 (1949).

77. J.M. Church and R. Blumberg, Ind.Eng.Chem., 43, 1780 (1951).

78. R. Hiatt in 'Oxidation techniques and applications in organic synthesis' (R.L. Augustine, Ed.), New York, Dekker, 2, 113 (1971).

79. Table of Periodic Properties of Elements', Sargent Welch Scientific Co., Chicago (1968).

80. W.M. Latimer, 'Oxidation Potentials' 2nd Edn., New York, Prentice Hall (1952).

81. P.F. Wolf and R.K. Barnes, J.Org.Chem., 34, 3441 (1969).

82. H. Steinberg, 'Organoboron Chemistry', New York, Wiley, 1, (1964).

83. J.B. Lee and B.C. Uff, Quart.Rev.Chem.Soc., 21, 429 (1967).

84. J. Kollar and co-workers to Halcon International, US Patent, 3,350,422,(1967); (Chem.Abstr., 68, 2922).

85. Ibid., US Patent, 3,351,635,(1967); (Chem.Abstr., 68, 21821).

86. S. Kato, T. Ishihara and F. Mashio, Bull.Jap.Petrol.Inst., 12, 117 (1970).

87. Kh.E. Khcheyan, V.M. Platonov, K.B. Klebanova, I.K. Alferova, G.L. Bitman, A.F. Paulichev and O.S. Ermakova, Khim.Prom. (Moscow), 48, 810 (1972) (Russ.); (Chem.Abstr. 78, 43158).

88. F. List and L. Kuhnen, Erdole und Kohle, 20, 192 (1967) (Ger.).

89. C.Y. Wu and H.E. Swift, J.Catal., 43, 380 (1976).

90. I. Seree de Roch, R. Malmaison and P. Menguy, US Patent, 2,489,775,(1970).

91. V.M. Obekhov, M.I. Farberov, A.V. Bondarenko and V.A. Lysomov, Neftekhimiya, 11, 410 (1970) (Russ.).

92. V.P. Yur'ev, I.A. Gailyunas, L.V. Spirikhin and G.A. Tolstikov, J.Gen.Chem.USSR, 45, 2269 (1975).

93. T. Itoh, K. Kaneda and S. Teranishi, J.C.S.Chem.Commun., 421 (1976).

94. S. Tanaka, H. Yamamoto, H. Nozaki, K.B. Sharpless, R.C. Michaelson and J.D. Cutting, J.Amer.Chem.Soc., 96, 5254 (1974).

95. K.B. Sharpless and R.C. Michaelson, J.Amer.Chem.Soc., 95, 6136 (1973).

96. K.B. Sharpless, J.M. Townsend and D.R. Williams, J.Amer.Chem.Soc., 94, 295 (1972).

97. N.A. Milas, Chem.Rev., 10, 295 (1932).

98. N.M. Emanuel, E.T. Denisov and Z.K. Maizus 'Liquid phase oxidation of hydrocarbons', New York, Plenum Press (1967).

99. E.S. Gould and M. Rado, J.Catal., 13, 238 (1969).

100. G.A. Russell, J.Amer.Chem.Soc., 79, 3871 (1957).

101. P.D. Bartlett and T.G. Traylor, J.Amer.Chem.Soc., 85, 2407 (1963).

102. J.A. Howard, Adv.Free Radical Chem., 4, 55 (1972).

103. K.U. Ingold, Accts.Chem.Rsch., 2, 1 (1969).

104. K.U. Ingold, Pure Appl.Chem., 15, 49 (1969).

105. G. Sosnovsky and D.J. Rawlinson in 'Organic Peroxides' (D. Swern, Ed.), New York, Wiley, Vol. II, 153 (1971).

106. F.R. Mayo, Accts.Chem.Rsch., 1, 193 (1968).

107. D.E. Van Sickle, F.R. Mayo and R.M. Arluck, J.Amer.Chem.Soc., 87, 4824 (1965).

108. D.E. Van Sickle, F.R. Mayo, E.S. Gould and R.M. Arluck, J.Amer.Chem.Soc., 89, 977 (1967).

109. D.E. Van Sickle, F.R. Mayo, R.M. Arluck and M.G. Syz, J.Amer.Chem.Soc., 89, 967 (1967).

110. W.F. Brill and B.J. Barone, J.Org.Chem., 29, 140 (1964).

111. M. Koelewijn, Recl.Trav.Chim.Pays-Bas, 91, 759 (1972).

112. I. Seree de Roch and P. Menguy, French Patent, 1,505,332,(1967); (Chem.Abstr., 69, 96439); French Patent, 1,505,337,(1967); (Chem.Abstr., 69, 96440).

113. K. Takehira and T. Ishikawa, Bull.Chem.Soc.Japan, 49, 2351 (1976).

114. J. Rouchaud and P. Nsumba, Bull.Soc.Chim.Fr., 1, 75 (1969) (Fr.).

115. J. Rouchaud and J. Mawanka, Bull.Soc.Chim.Fr., 1, 85 (1969) (Fr.).

116. J. Rouchaud and J. Tripiat, Bull.Soc.Chim.Fr., 1, 78 (1969) (Fr.).

117. J. Rouchaud and M.De Pauw, Bull.Soc.Chim.Fr., 8-9, 2905 (1970) (Fr.).

118. J. Rouchaud and A. Mumbieni, Bull.Soc.Chim.Fr., 8-9, 2907 (1970) (Fr.).

119. J. Rouchaud and F. Mingedi, Bull.Soc.Chim.Fr., 8-9, 2902 (1970) (Fr.).

120. J. Rouchaud and F. Mingedi, Bull.Soc.Chim.Fr., 8-9, 2912 (1970) (Fr.).

121. J. Rouchaud and M.De Pauw, Bull.Soc.Chim.Fr., 8-9, 2914 (1970) (Fr.).

122. J. Rouchaud and M.De Pauw, Bull.Soc.Chim.Belg., 77, 543, (1968) (Fr.).

123. J. Rouchaud and I. Seree de Roch, British Patent, 1,216,645, (1970).

124. J. Rouchaud and I. Seree de Roch, British Patent, 1,217,649, (1970).

125. A. Rusi, R. Ugo and G.M. Zanderighi, J. Catal., 34. 175 (1974).

126. L. Vaska, Science, 140, 809 (1963).

127. L. Vaska and D.L. Caton, J.Amer.Chem.Soc., 88, 5324 (1966).

128. K. Takao, Y. Fumiwara, T. Imanaka and S. Teranishi, Bull.Chem. Soc.Japan, 43, 1153 (1970).

129. K. Takao, M. Wayaku, Y. Fumiwara, T. Imanaka and S. Teranishi, Bull.Chem.Soc.Japan, 43, 3898 (1970).

130. K. Kadeda, T. Itoh, Y. Fujiwara and S. Teranishi, Bull.Chem. Soc.Japan, 46(12), 3810 (1973).

131. B.R. James and E. Ochiai, Canad.J.Chem., 49, 975 (1971).

132. H. Van Gaal, H.G.A.M. Cuppers and A. Van der Ent, J.C.S.Chem. Commun., 1964 (1970).

133. A. Fusi, R. Ugo, F. Fox, A. Pasini and S. Cenini, J. Organometal.Chem., 26, 417 (1971).

134. J.E. Lyons and J.O. Turner, Tetrahedron Lett., 29, 2903 (1972).

135. J.E. Lyons and J.O. Turner, J.Org.Chem., 37, 2881 (1972).

136. R.J.P. Williams, in 'Advances in the Chemistry of Coordination Compounds, a Conference held in Detroit, 1961' (Ed. S. Kirschner), McMillian, New York, p. 279 (1961).

137. K.B. Sharpless and T.R. Verhoeven, Aldrichimica Acta, 12, 63 (1979).

138. E. Fischer, Ber., 27, 3231 (1981).

139. J.D. Morrison and H.S. Mosher, 'Asymmetric Organic Reactions', American Chemical Society, Washington, D.C. (1976).

140. Y. Izumi and A. Tai, 'Stereodifferentiation Reactions', Academic Press, New York (1977).

141. G. Bredig and P.S. Fiske, Biochem.Z., 46, 7 (1912).

142. A. Rosowsky in 'The Chemistry of Heterocyclic Compounds', (Ed. A. Weissberger), Wiley, New York (1964).

143. R.E. Parker and N.C. Isaacs, Chem.Rev., 59, 7373 (1959).

144. H.B. Henbest, Chem.Soc.Special Pub., 19, 83 (1965).

145. R.C. Ewins, H.B. Henbest and M.A. Mckervey, J.Chem.Soc.Chem. Commun., 1085 (1967).

146. R.M. Bowman, J.F. Collins and M.F. Grundon, J.Chem.Soc.Chem. Commun., 1131 (1967).

147. R.M. Bowman and M.F. Grundon, J.Chem.Soc.(C), 2368 (1967).

148. D.R. Boyd, D.M. Jerina and J.W. Daly, J.Org.Chem., 35, 3170 (1970).

149. R.M. Bowman, J.F. Collins and M.F. Grundon, J.Chem.Soc., Perkins Trans., 1, 626 (1973).

150. M.F. Grundon and I.S. McColl, Phytochemistry, 14, 143 (1975).

151. F. Montanari, I. Moretti and G. Torre, Bull.Sci.Fac.Chim.Ind. Bologna, 26 , 113 (1968).

152. F. Montanari, I. Moretti and G. Torre, J.Chem.Soc.Chem.Commun., 135 (1969).

153. F. Montanari, I. Moretti and G. Torre, Gazz.Chim.Ital., 104, 7 (1974).

154. W.H. Pirkle and P.L. Rinaldi, J.Org.Chem., 42, 2080 (1977).

155. M. Igarashi and H. Midorikawa, Bull.Chem.Soc.Jpn., 40, 2624 (1967).

156. K. Nanjo, K. Suzuki and M. Sekiya,Chem.Lett., 1143 (1978).

157. R. Helder, J.C. Hummelen, R.W.P.M. Laane, J.S. Wiering and H. Wynberg, Tetrahedron Lett., 1831 (1976).

158. R.C. Michaelson, R.E. Palermo and K.B. Sharpless, J.Amer.Chem. Soc., 99, 1990 (1977).

159. S. Yamada, S. Tetrashima and T. Mashiko, Japan Kokai, 78, 50, 111 (Cl C070303/14); (Chem.Abstr. 89, 109035).

160. H.B. Kagan, H. Mimoun, C. Mark and V. Schurig, Angew.Chem. (Ed. Eng.), 18, 485 (1979); (Ger. version, Angew.Chem., 91, 511 (1979)).

161. K. Tani, M. Hanafusa and S. Otsuka, Tetrahedron Lett., 3017 (1979).

162. K. Takai, K. Oshima and H. Nozaki, Tetrahedron Lett., 1657 (1980).

163. J. Rebek Jr. and R. McCready, J.Amer.Chem.Soc., 102, 5602 (1980).

164. T. Katsuki and K.B. Sharpless, J.Amer.Chem.Soc., 102, 5974 (1980).

165. V.S. Martin, S.S. Woodard, T. Katsuki, Y. Yamada, M. Ikeda and K.B. Sharpless, J.Amer.Chem.Soc., 103, 6237 (1981).

166. K.B. Sharpless, C.H. Behrens, T. Katsuki, A.W.M. Lee, V.S. Martin, M. Takatani, S.M. Viti, F.J. Walker and S.S. Woodard, Pure and Appl.Chem., 55, 589 (1983).

167. C.H. Behrens and K.B. Sharpless, Aldrichimica Acta 16, 67 (1983).

168. G.B. Payne, J.Org.Chem., 27, 3819 (1962).

169. S. Coleman-Kammula and E.Th. Duim-Koolstra, J.Organomet.Chem., 246, 53 (1983).

170. F.A. Davis, R.H. Jenkins Jr., S.B. Awad, O.D. Stringer, W.H. Watson and J. Galloy, J.Amer.Chem.Soc., 104, 5412 (1982).

171. F.A. Davis, M.E. Harakal and S.B. Awad, J.Amer.Chem.Soc., 105, 3123 (1983).

172. J.A. Dale, D.L. Dull and H.S. Mosher, J.Org.Chem., 34, 2543 (1969).

173. K.B. Sharpless, Proceedings of the Robert A. Welch Foundation Conferences on Chemical Research, 27, 59 (1984).

174. K.B. Sharpless, Chem. in Brit., 38 (1986).

175. W.C. Still, M. Kahn and A. Mitra, J.Org.Chem., 43, 2923 (1978).

176. J.M. Miller and J.G. Kirchner, Anal.Chem., 25, 1107 (1953).

177. J.A. Fioriti and R.J. Sims, J. Chromatog., 32, 761 (1968).